CHAPTER TWENTY SEVEN

IDENTIFICATION AND SPECIATION OF ACTINIDES IN THE ENVIRONMENT

Claude Degueldre

27.1 BACKGROUND

All actinide isotopes are radioactive. Since the middle of the last century, new actinide and transactinide isotopes have been artificially produced and the use of several of the naturally occurring actinide isotopes has increased. This production is due to the nuclear power industry and the military fabrication and use of nuclear weapons. These activities have created anxiety about the introduction of actinide elements into the environment. Consequently, environmental systems that contain or are exploited for natural actinides, or, are potentially contaminated by anthropogenic actinides, must be investigated. The analytical techniques introduced in this chapter are used, after sampling when required, to identify and quantify the actinide isotopes and to determine the species in which they are present.

The amounts or concentrations of actinide elements or isotopes in the environmental samples need to be identified and quantified. Moreover, since transport properties and bioavailability are closely linked to species and atomic environment of the actinide elements, both radiotoxicity and speciation of actinides in the studied phases must be determined to understand the behavior of these elements in the environment (Livens, 2001). In this chapter, analysis of a broad range of environmental systems are considered such as fluid phases from air or waters from surface to subsurface, samples from terrestrial

to oceanic, and samples from rocks to organic or bio-related phases. These samples range from depleted to rich in actinides and from inorganic to organic or bioorganic. The actinides are either dissolved in solid or liquid solutions, or associated with particles dispersed in the sample phase: in air or water, or in heterogeneous solids. Actinide species may also be located at phase boundaries such as rock–water or dispersed *in vivo*, associated with biofunctional environments. The phases of interest range from the nanometer to the kilometer in size, in surface or in volume.

In all cases, accurate or quantifiable sampling is required, together with identification, quantification, and determination of the redox states or of the complexes in the phases or at the interfaces, as well as characterization of the molecular environment, or emphasis on the crystalline or the amorphous phases that contain actinide isotopes, elements, or species. This information is required to understand how actinide species will behave in the environment and the way in which actinides can migrate or be retained. However, contamination may concentrate via bioaccumulation mechanisms (Holm and Fukai, 1986; Skwarzec *et al.*, 2001) or a geochemical process specific to a local hydrogeochemical environment (Bundt *et al.*, 2000). Spatial information is needed, ranging from the subnanometer to the micrometer size to understand migration behavior from the microscopic to the geographic scale, and temporal information is needed, ranging from second fractions to millions of years.

Figure 27.1 schematizes the source, location, or occurrence of natural actinides and of present or potential contamination including man-made actinide elements in the environment. The actinide elements and isotopes considered are the natural ones, with Th and U (primordial nuclides formed in the buildup of the terrestrial matter and still present today) being the major elements at the 10^{13} ton level in the Earth's crust (Wasserburg *et al.*, 1964) and with Ac and Pa being the trace elements formed by decay of the major natural actinide isotopes. Naturally occurring Np and Pu are present at the ultratrace level generated by nuclear reactions in the environment, and are also residual traces of primordial actinides, or produced man-made, as discussed below.

Natural actinide isotopes are present in rocks or minerals, e.g. phosphates containing uranium or thorium (^{232}Th and ^{235}U, ^{238}U) (Heier and Rogers, 1963; Khater *et al.*, 2001). The minor components (^{227}Ac, ^{228}Ac, ^{227}Th, ^{228}Th, ^{230}Th, ^{231}Th, ^{234}Th, ^{231}Pa, ^{234m}Pa, ^{234}U) are produced by decay of the major actinide isotopes (e.g. Murray *et al.*, 1987; Arslanov *et al.*, 1989). Natural ^{236}U has been detected at an atomic ratio, ^{236}U/^{238}U, of 6×10^{-10} in uranium deposits such as at the Cigar Lake, Saskatchewan, Canada (Zhao *et al.*, 1994). It may be generated by neutron capture on ^{235}U. Similarly, a long-lived actinide such as ^{237}Np was found in ultratrace levels (^{237}Np/^{238}U: 2×10^{-12}) in uranium ores from Katanga (Myers and Lindner, 1971). Ultratrace components such as ^{239}Np or ^{239}Pu are also generated by neutron capture (Curtis *et al.*, 1987; Barth *et al.*, 1994), with typical concentrations in the order of 10^{-12} g Pu per gram sample

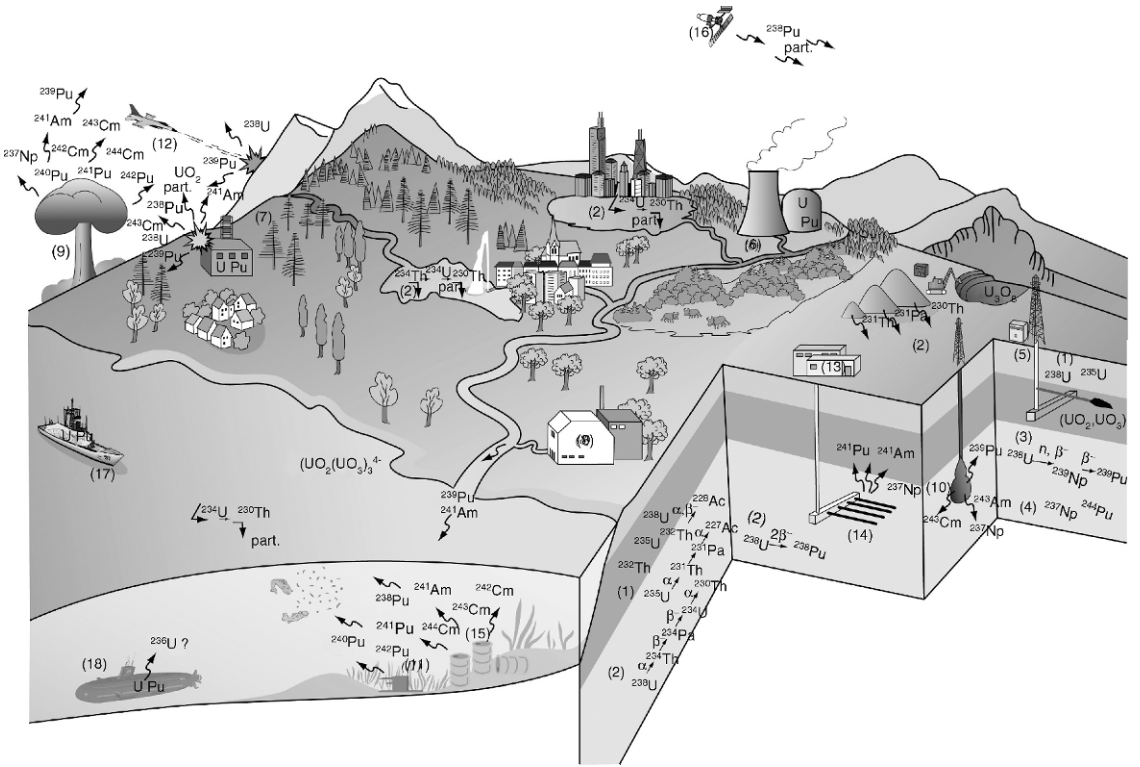

Fig. 27.1 *Natural and anthropogenic actinide species in the environment.* (1) *Natural major actinides,* (2) *minor actinides,* (3) *actinides at the ultratrace level generated from the majors by neutron capture in environment,* (4) *actinides of primordial origin,* (5) *natural actinide contamination around uranium mining and milling plants. Anthropogenic actinides:* (6) *released intentionally below legal norms from nuclear power plants,* (7) *by accident, or* (8) *reprocessing facilities. Actinides released from military activities, e.g. weapons production:* (9) *atmospheric tests,* (10) *underground detonations, or* (11) *objects from nuclear naval vessels, or* (12) *depleted uranium warheads. Waste management activities:* (13) *intermediate or* (14) *geologic and* (15) *oceanic disposal. Unexpected events from nuclear power sources, e.g.* (16) *satellite reentry in atmosphere,* (17) *nuclear icebreaker, or* (18) *nuclear submarine sinking; 'part' stands for colloidal particles.*

in pitchblende, 10^{-14} g Pu per gram U ore, and maximum concentrations in the order of 5×10^{-15} g Pu per gram lava (Hawaiian), 10^{-15} to $3 \times 10^{—17}$ g Pu per gram granite (Kontinentales Tiefbohrprogramm). ^{244}Pu, which was found in a rare earth mineral to the extent of 1 part per 10^{18}, is likely to have been produced during Earth formation (Hoffman *et al.*, 1971). As identification techniques become increasingly sensitive, it may be possible that specific isotopes such as heavy curium isotopes may be found at the ultratrace level as natural components as it was targeted in a study about supernova producing long-living radionuclides in terrestrial archives (Wallner *et al.*, 2000).

The specific case of the natural fossil reactors in the Oklo region (e.g. Oklo, Oklobonde, Bagombe), which underwent spontaneous chain neutronic reaction some 2×10^9 years ago, was studied extensively and revealed the buildup of large quantities of transuranium elements during chain reactions. However, most of them have now decayed. Natural plutonium has been produced and has remained in the environment even before it was produced artificially. It remains the heaviest natural element found in the environment at the level of milligrams per 100 tons of uranium ore residues (Peppard *et al.*, 1951).

Artificial or anthropogenic actinides are those generated by civilian and military activities. Actinide isotopes that have been artificially produced in significant amounts are ^{233}Pa, ^{233}U, ^{236}U, ^{237}Np, ^{238}Pu, ^{239}Pu, ^{240}Pu, ^{241}Pu, ^{242}Pu, ^{241}Am, ^{243}Am, ^{242}Cm, ^{243}Cm, and ^{244}Cm (Mitchell *et al.*, 1995b; Lujaniene *et al.*, 1999), with about 2000 tons Pu produced until now, which some groups would like to reuse in a very pragmatic way (Degueldre and Paratte, 1999). The amount of artificially produced actinides is larger than that occurring naturally. Actinide isotopes such as ^{239}Np and ^{239}Pu belong to both classes and are qualified as natural or anthropogenic according to their origin. Recently, attention has also been drawn to depleted uranium and its use in projectiles. Its dispersal in the environment has been the subject of investigations with regard to its toxic potential.

Natural processes typically disperse, transport, and dilute contaminants. Some local geophysical, hydrochemical, or bioorganic processes can concentrate them. Usually, however, atmospheric flow transports particulate contaminants through the atmosphere or the stratosphere. Water flows allow contaminants to migrate to the geosphere or at its surface. In these systems, naturally occurring actinides may be used as tracers to estimate element residence time in particulate form in air or in water systems. For example, ^{234}Th is used as a natural marker to study particles in Lake Michigan (Nelson and Metta, 1983) or Lake Geneva (Dominik *et al.*, 1989). Similarly, Th isotopes may be used to investigate their scavenging by colloidal mechanisms in seawater (Baskaran *et al.*, 1992). Similar studies may be applied to study actinides in particulate phases, or aerosols, in the atmosphere (Salbu, 2001). The naturally occurring actinides U and Th, as well as Ra, may be utilized in studies of paleoclimate, dating old groundwaters, rock–water interaction processes (Ivanovich, 1994), and geochronology systems (Balescu *et al.*, 1997), using

$^{234}U/^{238}U$ or $^{230}Th/^{234}U$ ratios. Anthropogenic actinides may also be used as markers; for example, the use of $^{239+240}Pu$ to replace ^{137}Cs as an erosion tracer in agricultural landscapes contaminated with the Chernobyl fallout (Schimmack *et al.*, 2001) was recently suggested.

Actinides from human activities have also been occasionally released into the environment. The potential of contamination begins at the uranium mine with tailings and the problems associated with, for example, the release of U and Th, and their daughter products (e.g. Winkelmann *et al.*, 2001); hazards continue all along the nuclear fuel cycle with research, commercial, or military activities and the potential for real spread and contaminations of the environment, as for example, the Irish Sea, Semipalatinsk, and Maralinga (Kim *et al.*, 1992; Cooper *et al.*, 1994; Kazachevskiy *et al.*, 1998), due to commercial or military activities or accidental events. Actinides may be dispersed, at restricted levels and below legal limits, from electric power utilities during operations (Mátel *et al.*, 1993), or may be instantaneously dispersed in large doses, for example, as a consequence of an accident involving a reactor (Holm *et al.*, 1992), an aircraft carrying nuclear weapons (Mitchell *et al.*, 1995a; Rubio Montero and Martin Sánchez, 2001a,b), or during nuclear bomb testing (Wolf *et al.*, 1997; Kudo, 1998). These actinide releases contaminate the environment, such as desert (Church *et al.*, 2000) or forest soil, but contaminate flora specimens such as mushrooms insignificantly (Mietelski *et al.*, 1993). However, diluted in water, actinides undergo bioaccumulation, e.g. in a marine environment (Baxter *et al.*, 1995), within phytoplankton and macro algae (Holm and Fukai, 1986), crustacean (Swift and Nicholson, 2001a,b), and fish (Skwarzec *et al.*, 2001). The reentry of a satellite equipped with a ^{238}Pu power source in the atmosphere and its disintegration through the stratosphere has been a source of contamination. In the ocean the leakage of objects from naval reactor pressure vessels in submarines (Mount *et al.*, 1995) or waste dumping on the seabed (Rastogi and Sjoeblom, 1999) are also potential sources of actinide contamination. In the geosphere, contaminants may affect the saturated or the unsaturated zones (Penrose *et al.*, 1990). All these cases schematized in Fig. 27.1 depict situations for which actinides are present as a main or a diluted phase. They also may be in a 'dissolved' state or present as colloidal particles in the liquid or gas environment. Consequently, the analytical techniques used range from major component quantitative analysis to detection at the ultratrace level. The analytical methods used to identify and characterize, i.e. provide speciation information for the actinides, must be efficient, accurate, very sensitive, and able to provide information on the chemical characterization of the environment of the actinide. This allows the reconstruction of the history of the actinide-loaded phases and consequently the prediction of actinide behavior in the environment to be made. For example, an oxide phase produced at low temperature will dissolve faster in water than a high-temperature oxide phase. Size distribution of these particles is a relevant parameter to estimate dissolution or transport behavior.

Before analysis, sampling and/or sample treatment, with separation if needed, must be utilized when the analytical technique is not applied *in situ*.The investigated analytical techniques are classified according to the interaction (if any) between irradiation particles or reagent and the analyzed sample, and for the signal detected or recorded (see Table 27.1). For passive techniques, excitations are absent. For interactive techniques, irradiations or reagent additions are made with phonons, photons, electrons, neutrons, or ions with a known energy, flux, chemical affinity, or mass. The irradiation or injection is done locally while the reception may be carried out in a given space at a given angle from the stimuli direction or the incident beam, instantaneously or after a certain time after irradiation. The detection tools are spectroscopy (S), microscopy (M), or radiography (RAD) instruments. The reaction takes place within or without a specific field such as electrical and magnetic flow or mechanical acceleration. The detected signal may be the same in nature as the incident one, with the same energy, or a signal with lower energy, with particles being phonons, photons, electrons, neutrons, or ions. In addition to these analytical tools or techniques, neutral species such as atoms or molecules may also be used to interrogate the material. They are treated in this chapter as ions (from a mass point of view). The techniques are classified according to increasing energy of reagents or incident particles. The combination of all excitation or reagent addition and reception or product detections makes the analytic potential very rich for identification of elements or isotopes, quantitative determination, and spatial speciation in a broad way.

The sensitivity κ (units of $M \cdot au^{-1}$, with M: $mol \cdot L^{-1}$, and au: arbitrary unit), and detection limit DL of the concentration C(M) of isotope, element, or species, or their amount N(mol) must be discussed at both theoretical and experimental levels. From the experimental side these concentration and amount limits are given by:

$$C_{DL} = 3\sigma\kappa \tag{27.1}$$

$$N_{DL} = V_{min} C_{DL} \tag{27.2}$$

where σ(au) is the standard deviation of the limiting noise and V_{min}(L) is the minimum volume that can be analyzed (e.g. 1 mL). From the theoretical side, a detection limit may be evaluated from the physical–chemical process and from the performance of the analytical unit, while it remains usually an experimental limit.

For all analyses, sample volume, mass, or amount, the flux of the reagent, the size of the analyzed part of the sample, and the acquisition time or time of analysis are key parameters linked to the detection limit. The nature and origin of the environmental sample dictate the size of the sample. However, the size of the sample is also coupled with the analytical technique for which time and detection limits (DLs) are key parameters for its application. DL is a function of the number

Table 27.1 *Analytical techniques including excitation (if any) and detection for isotope, element, or species characterization (see list of abbreviations in the glossary). Note: excitation or detection is performed with phonons, photons, electrons, neutrons, ions (or atoms or molecules) considering the particles (plain, solvated, or cluster) or their associated waves.*

Detection / *Excitation*	*Phonon*	*Photon*	*Electron*	*Neutron*	*Ion*
–	–	XS, γS, MBES	EHE, RAD, LSC, βS	NS	GRAV, ISE RAD, LSC, αS
Phonon	SR, aAFM	–	–	–	–
Photon	LIPAS, (LIPDS), LIBD	IRFT, DRS, AAS NIR-VIS-UVS, COL, RAMS TRLITS, PHOS, PCS, XAS, XRF, TOM, PHOTA	UPS, XPS, SEXAS	NPHOT	TIMS, RIMS, LAMMA, LAICPMS
Electron	SEAM	EDS, EMPA	eAFM, SEM, TEM, AES, EELS	–	DPP, DPV, COUL, ESMS, SSMS
Neutron	–	NAA	NAA	DNAA	NAA, RAD
Ion	–	ICPOES, PIXE, PIGE	–	NRA	VOL, AFM ICPMS, SIMS, AMS, RBS, ERDA, NRA

of actinide atoms, the volume of the sample, the subsample excitation conditions (see Section 27.2), and the acquisition quality of the detector, and interferences such as quenching or peak overlapping. It may, however, be desirable to split the speciation range according to 'macro concentration' $> 10^{-6}$ M $>$ 'trace concentration'. Analysis may be performed in-line, on-line, on a flow bypass with direct detection of activity, for example, or at-line with intermediate samples, or off-line with the transfer of the sample in the laboratory. The analysis may be carried out *in situ*, for example using an atmospheric balloon, or in an underground rock laboratory in the considered phase, or *ex situ* with transfer of the sample and separation. To complete the picture it must be mentioned that separation techniques such as filtration, centrifugation, diffusion, electrodiffusion, electroplating, partitioning (liquid–liquid or solid–liquid) may also be applied, making the analysis more specific or efficient.

Information required such as activity (chemical, radioisotopic), amount (mass), concentration (fraction), and structures of the actinides in the studied phases have to be determined at the nuclear (pm), atomic, molecular (nm), microscopic (μm), macroscopic structural (mm), bulk scale (cm), at the component or system scale (m), or at environmental or geographic scale (km) according to the requirements of the study. Identification concerns the actinide elements and isotopes, but speciation may be understood not only at the molecular scale but also in a broader sense such as at the environmental scale. Understanding in the macroscopic scale by plain washing, leaching, or extraction tests would be a step for remediation investigations. In many types of soil the mitigation approach could be some type of soil washing to remove selectively the contaminating species (Burnett *et al.*, 1995). The selective extraction tests are also discussed in this chapter; the phases are, however, analyzed using the techniques discussed below.

Passive and active analytical methods will be reviewed (Table 27.1) through Sections 27.2 and 27.3, with examples of their utilization in transmission, injection diffusion, or reflective modes. The sampling area, beam size, and reagent quantities are macroscopic, microscopic, or nanoscopic in nature, while spatial–temporal conditions make excitation vs detection direction through solid angle, with synchronous detection or with temporal delay, possible. In Section 27.4, combinations of techniques are discussed. For example, seismic reflection (SR), which cannot be used by itself for identifying thorium or uranium, can be used in combination with other techniques as a prospecting tool. Atomic force microscopy (AFM) morphological studies also provide useful information; however, they must be complemented with other technique results to provide the required identification result (e.g. Walther, 2003). Similarly, *Eh* electrode (EHE) measurements may contribute to the speciation of redox-sensitive actinides such as U, Np, or Pu in waters. They are, however, generally completed by spectroscopic investigations. Chromatography, which is basically a separation technique, must be combined with detectors and is also studied in this chapter.

Separation of elements of interest, which are later analyzed by different analytical techniques, is an important prerequisite of any analytical method, as discussed in Section 27.2. The analytical procedure typically includes sampling or sample preparation (e.g. decomposition), separation, and/or enrichment before analysis in either a passive or an interactive way.

27.2 SAMPLING, HANDLING, TREATMENT, AND SEPARATION

In environmental systems, actinides may sometimes be analyzed on site. This requires a probe or detector installation *in situ* and direct detection or measurement of actinide concentration, activity, or amount. This is an ideal case. Because of interferences, low levels of concentrations, or difficulties in transporting the analytical unit, sampling is generally the best solution, with transfer of samples or subsamples to the laboratory for further analysis. The sampling and sample handling are performed taking into account (Salbu, 2000):

- representative samples and fractionation of samples,
- treatment *in situ*, at-site, or shortly after sampling, and
- dilution or pre-concentration, and chemical yield (efficiency of handling).

Sampling, pretreatment, shipment to laboratory, and analysis are areas where contaminations, losses, or speciation changes can occur (Harvey *et al.*, 1987). Corrections for these artifacts must be applied by using isotopic tracers or specific handling conditions.

27.2.1 Sample and data collection of compounds

The two main strategies are either to make measurements on site without sampling and adapting the probe *in situ* or to collect samples and then perform the analysis *ex situ*, as discussed below.

Sample amounts and collection techniques are dependent on the nature of the sample and on its actinide content. Samples with high actinide contents do not generally need enrichment phases, while very dilute actinide samples may require treatment, enrichment, and other time-consuming protocols. The strategy may be very different for fluids (such as air or water) than for solids (such as rock or biospecimen).

In air samples, actinides are usually present as liquid aerosols or particles since their partial pressure as gaseous species is insignificant. A particulate phase must be characterized in terms of size distribution and nature, because its behavior in the environment may be function of production mode and history, which have a direct impact on composition, nature, specific size distribution, and actinide-release properties.

In water samples, the actinides may be present as truly dissolved species, as separate particulate, and/or as colloidal phases. Here again the particle structure and size distribution must be determined to understand the actinide migration potential.

In solid samples, actinides are either present as constituents of solid solutions or as phases that are heterogeneously dispersed within the matrix phases. This is also valid for biospecimens. The sample in all cases must be preserved from degradation, contamination, or other physicochemical changes. Specific protocols such as collection under a controlled atmosphere, a preservative reagent, and storage in the dark and at a reduced temperature may be required. The larger the sample volume and the corresponding contact area of the vessel, the smaller will be the loss by sorption on the vessel wall and the shorter the storage time, and the less will be degradation of the sample by contamination or particle aggregation.

As an example, typical air sample volumes range over several hundred meters (Iwatschenko-Borho *et al.*, 1992). Rainwaters, for example, require collectors of $\sim$1 m^2 active surface, and water samples of the order of 100 L (Rubio Montero and Martin Sánchez, 2001b). Analysis of river water may also require some 100 L (Garcia *et al.*, 1996) for Pu and Am determination. Seawater sampling also requires very large volumes, processed up to 6000 L (Livingston and Cochran, 1987; Robertson, 1985), in order to achieve concentration measurements of trace level of Th, Pu, and Am isotopes. Rock samples may be as large as the 100 kg amount that was required for the detection of ^{244}Pu (Hoffmann *et al.*, 1971) in nature.

27.2.2 Sample treatment and separation

Sample preparation and separation of ions or other species of interest, which are later analyzed by different analytical techniques, are usually important prerequisite steps of any analytical method. Radiotracer techniques may be applied for each step of the separation: sample decomposition, trace–matrix separation (precipitation, ion exchanger, solvent extraction), volatilization, and other treatment without any restriction on the chemical and physical forms of sample. All these techniques may be quantitatively applied using isotope dilution, e.g. with ^{235}Np, ^{236}Pu (Bellido *et al.*, 1994), or ^{244}Pu spikes according to the specific requirements.

Air samples are generally treated in a way such that their particulate content may be collected on filters or impactors (Iwatschenko-Borho *et al.*, 1992). Aerosol analysis generally requires treatment of a very large volume of air.

Aqueous solutions are generally filtered, typically through a 0.45 μm pore membrane, followed by a series of ultrafiltration (Orlandi *et al.*, 1990; Francis *et al.*, 1998) or centrifugation (Kim *et al.*, 1997; Dominik *et al.*, 1989; Itagaki *et al.*, 1991) steps. Centrifugation requires larger instrumentation compared to filtration. This limits the use of centrifugation on site and

furthermore *in situ*. The two new samples produced are: (1) single particle or colloid cake on the collector surface, or colloid concentrate; and (2) the filtered liquid phase with its soluble content. Treatments of restricted volumes of water are required, depending on the level of contamination of the water. For example, observation of chemical speciation of plutonium was carried out after filtration of Irish Sea and western Mediterranean Sea waters (Mitchell *et al.*, 1995). The redox state distribution of ^{239,240}Pu and ^{238}Pu in these waters shows little variation with 87% as Pu(V). Pu(IV) is mostly associated with particles.

In situ dialysis has also been applied to concentrate the colloid phase associated with actinides. Extraction of an actinide from the particulate phase or from a rock sample may be carried out by applying a successive leaching technique (e.g. Szabó *et al.*, 1997; Nagao *et al.*, 1999), with reagents successively more and more aggressive such as, for example, the following:

1. water at 25°C to desorb exchangeable actinides;
2. sodium acetate at pH 5 and 25°C to dissolve carbonate phases;
3. ammonium oxalate at pH 3 and 25°C to separate reducible phases, i.e. (Fe, Mn);
4. sodium hydroxide 0.3 M at 60°C to leach actinide associated with organics;
5. hydrogen peroxide at pH 1 and 60°C to dissolve sulfide phases;
6. nitric acid 8 M at 80°C to leach mineralized phases including actinide oxides.

Each step must be characterized by a reagent, a pH value, a temperature, a sample/reagent volume or mass ratio, and a given time. Each extraction step may be repeated several times before the next extraction step in order to follow the reversibility of the desorption or leaching process (Salbu, 2000). Sequential leaching has been applied to perform speciation of uranium associated with particulates in seawater (Hirose, 1994). The major species consists of an insoluble complex that dissolves by leach test at pH 1.

Co-precipitation is usually applied as an enrichment technique of an actinide from an aqueous solution with $Fe(OH)_3$ (Morello *et al.*, 1986), LaF_3 (Nelson and Lovett, 1978), or $Ba(SO_4)$ for Ac assay on Ra (Niese, 1994), as a carrier phase, followed by dissolution and separation.

Electroplated sources are very useful for alpha spectroscopy (αS). Electroplating is the preparation of very thin and uniform actinide films obtained by electrodeposition onto stainless steel disks. The literature on electrodeposition describes the procedure (see Chapter 30), which remains empirical, perhaps because electrodeposition is a multiparametric process that includes the electrolyte solution (concentration, *pH*), the hydrodynamic profile in the cell, the nature and geometry of the electrodes, the deposition current and potential, and the electrodeposition time. The electrodeposition of americium was reviewed with emphasis on the physicochemical behavior of the solution (Becerril-Vilchis *et al.*, 1994). The use of a tracer may be required to evaluate losses by adsorption of the studied actinides, or a quantitative method is

followed such as the use of a hydrogen sulfate–sodium sulfate buffer (Bajo and Eikenberg, 1999). The effect of a counter-ion was also studied in detail (Zarki *et al.*, 2001). Recently, however, specific microprecipitation followed by ultrafiltration has been used as an alternative for source preparation.

The separation and/or concentration of elements or species as soluble entities may be performed by applying partitioning between two phases such as:

- liquid–liquid, with specific complexes soluble in an organic phase: e.g. 2,4-pentanedione (Haa) in toluene (Engkvist and Albinsson, 1992), thenoyltrifluoroacetone (TTA) in xylene for Np extraction (Dupleissis *et al.*, 1974), tri-*n*-octylphosphine oxide (TOPO) in toluene for Pu, Am, and Cm extraction (Kosyakov *et al.*, 1994), and solvent liquid extraction can be used for the analytical determination of actinides in urine (Harduin *et al.*, 1993);
- liquid–solid, with specific polymers: anionic or cationic, organic (Qu *et al.*, 1998) or inorganic (Kobashi *et al.*, 1988). For example, actinides from contaminated soil samples can be separated by use of anion-exchanger columns for Am, Cm, and Pu spectroscopy (Michel *et al.*, 1999), and uranium from waters may be pre-concentrated using an ion exchanger and filtered off before desorption in small aliquot acidic solution and analyzed using inductively coupled plasma optical emission spectroscopy (ICPOES) (Van Britsom *et al.*, 1995).

Chromatography is discussed in combination with detections in Section 27.4.

The separation of colloidal species may be performed by applying specific techniques such as:

- field-free techniques: ultrafiltration, gel permeation, or size exclusion chromatography (Taylor and Farrow, 1987; Hafez and Hafez, 1992), or
- within a controlled field: flow-field fractionation (Bouby *et al.*, 2002), density gradient fractionation (Mohan *et al.*, 1991), or capillary or gel electrophoresis.

The latter technique has been performed for actinide separation by applying an electrical field during liquid–solid distribution. Speciation and solubility of neptunium has been studied in an underground environment by paper electrophoresis, ion exchange, and ultrafiltration (Nagasaki *et al.*, 1988). Gradient gel electrophoresis was used to characterize 13 kDa polysaccharide ligands complexing ^{234}Th from marine organic matter (Quigley *et al.*, 2002). Capillary electrophoresis is growing in importance as a versatile assay for speciation; however, there are still major challenges that limit the practical acceptance of the technique. The potential problems are inadequate attention to sample preparation (species stability, matrix effect), ignoring possible change in speciation during electrophoresis, inappropriate treatment on method validation and system suitability, and no sample enrichment methodology. Recommendations have recently been suggested (Timerbaev, 2001).

27.3 IDENTIFICATION AND SPECIATION

27.3.1 Passive techniques

Radiometric techniques dominate the analyses of short- and medium-lived actinide nuclides. The passive techniques currently used for actinide detection are summarized in Table 27.2. They include spectroscopy (S) or RAD of X-rays or gamma photons, along with Mössbauer emission spectroscopy (MBES), conversion electrons or β^-, neutrons, and ions such as alpha or spontaneous fission products that are emitted during decay of actinide nuclides. The investigated systems range from geographic to microscopic in size and the detection tool may also be adapted to these scales. The actinide isotopes considered in the environmental studies are not β^+ emitters; they may be neutron emitters that can consequently be detected by neutron spectroscopy (NS). Nothing is reported so far for the detection of the phonons generated by the actinide decays. Ion-selective electrodes (ISEs) may be used to detect actinide elements in a passive way, while gravimetry (GRAV) may be applied for concentrated phases.

The passive techniques and more especially the radiometric techniques remain widely used for the analysis of actinides because they utilize low-cost instrumentation, are simple to operate, achieve low-cost of analysis per sample, and have the possibility to perform non-destructive sample analysis.

In X-ray spectroscopy (XS) and γ-ray spectroscopy (γS), the most important developments include the production of high-efficiency coaxial and well-type detectors operating with anti-cosmic ray or anti-Compton shielding. Detection is currently carried out using a semiconductor crystal or by scintillation. Typical analytes include natural actinides such as ^{234}Th or anthropogenic actinides with detection limits of the order of 1 mBq. Based on this activity limit, the detection limits for actinide isotope amounts are calculated for relevant isotopes in Table 27.2. Sample preparation may require classical specific treatments before radioanalysis, such as separation or enrichment, as treated in Section 27.2.

Measurements of transuranics, in particular several isotopes of plutonium, are especially difficult to carry out due to the low-penetrating nature of their radiations (α- and X-rays). Direct alpha detection is difficult; therefore thin scintillators that rely on the detection of L-shell X-rays (13–21 keV) are used for survey work (Miller, 1994). These instruments may be used for environmental detection and for X-ray astronomical measurements in space. Theoretical detection limits for thin-layer samples are given in Table 27.2. Determination of actinides in solution may also be carried out by using a high-purity germanium crystal detector, allowing for plutonium a detection limit near 10^{-10} mol (Gatti *et al.*, 1994).

Classically, ^{227}Ac may be determined in environmental samples from the beta or gamma activity of its daughter products (Khokhrin and Denisov, 1995). Gamma-ray spectroscopy was used *in situ* and in the laboratory to determine

Table 27.2 *Passive analytical techniques used for actinide isotope, element, or species identification. Detection limit (DL) in mol recalculated from DL in Bq.*

Detection	*Goal*	*Sample*	*$^{A}An(Y)$*	*Detection limit*	*Remarks*
Photon					
XS, γS, MBES, RAD	determination of isotope activity and identification of isotope	solid or liquid bulk or film	^{227}Ac	2×10^{-14}	γS, *DL*: 1 mBq
			^{230}Th, ^{232}Th	1×10^{-11}, 5×10^{-7}	
			^{231}Pa	2×10^{-14}	
			^{234} U, ^{238}U	2×10^{-11}, 2×10^{-8}	
			^{237}Np	2×10^{-12}	
			^{239} Pu, ^{240}Pu	7×10^{-12}, 1×10^{-12}	(Bojanoswki, 1987)
			^{241}Am	1×10^{-16}	(Guillot, 2001)
			^{242}Cm, ^{244}Cm	5×10^{-15}, 1×10^{-16}	
Electron					
βS, LSC, RAD	concentration or activity determination	solid film electroplated or liquid bulk scintillation	^{228}Ac	5×10^{-22}	β LSC, *DL*: 10 mBq, in 1 mL
			^{234}Th	5×10^{-20}	
			^{233}Pa	5×10^{-20}	
			U	–	
			Np	–	
			^{241}Pu	1×10^{-17}	(Yu-fu, 1990)
			Am	–	
			Cm	–	
Ion					
GRAV, ISE, αS, LSC, RAD	determination of mass or of isotope activity and identification of isotope	solid film electroplated or liquid bulk scintillation	^{227}Ac	4×10^{-18}	αS, *DL*: 10 μBq
			^{228}Th, ^{230}Th, ^{232}Th	1×10^{-21}, 6×10^{-17}, 1×10^{-11}.	
			^{231}Pa	2×10^{-17}	
			^{234}U, ^{235}U, ^{238}U	2×10^{-21}, 4×10^{-17}, 3×10^{-11}	
			^{237}Np	2×10^{-15}	(Bojanoswki, 1987)
			^{238}Pu, ^{239}Pu, ^{240}Pu	7×10^{-20}, 2×10^{-17}, 5×10^{-18}	(Yu-fu, 1990)
			^{241}Am	3×10^{-19}	(Degueldre, 1994)
			^{242}Cm, ^{248}Cm	3×10^{-22}, 10^{-20}	

^{228}Ac activities in eight sites around the proposed Yucca Mountain repository in Nevada (Benke and Kearfott, 1997). The *in situ* determined specific activities were consistently within the ±15% of the laboratory soil sample results. Despite the good correlation between field and laboratory results, *in situ* counting with calibrated detector was recommended.

Gamma-ray spectroscopy has been systematically used to detect ^{232}Th or ^{238}U from environmental samples. The detection of these isotopes may be done using gamma photons from daughter nuclides. *In situ* determination of uranium in surface soil was performed by gamma spectroscopy measuring ^{234}Th and ^{234m}Pa using a high-resolution γ-ray spectrometer and assuming secular equilibrium (Miller *et al.*, 1994). On the other hand, uranium and thorium were also detected in soil samples by measuring ^{208}Tl and ^{214}Bi (LaBreque, 1994), respectively, which were as well assumed to be in secular equilibrium with their respective parents. The determination of the specific activity of these major natural actinides may be carried out by airborne gamma spectroscopy using the above key nuclides, or other nuclides, e.g. U by Ra (Kerbelov and Rangelov, 1997). This method enables analysis during fixed-wing aircraft or helicopter flight (Guillot, 2001). The sensitivity of the spectral analysis of windows at 2615 and 1764 keV for ^{232}Th (by ^{208}Tl) and ^{238}U (by ^{214}Bi), respectively, was optimized by subtraction of the Compton continuum in the detection window. The detection of ^{232}Th and ^{238}U is possible in their natural background of 33 Bq kg^{-1} in a large-volume NaI detector (16 L) and a short sampling time (1–5 s) at 40 m ground clearance. The calculation of the concentrations is then simple and reliable. A quantitative estimate of radioactive anomalies can also be obtained easily. The spectral profile analysis is of great interest and has been applied within the framework of environmental monitoring studies. Fig. 27.2(a) shows a map obtained for ^{232}Th during a mapping exercise. Similarly, aerial measurements above uranium mining and milling area have also been reported (Winkelmann *et al.*, 2001).

A gamma-logging (γS) probe has been used to monitor thorium and uranium as a function of depth in a borehole (Nagra, 1991; Mwenifumbo and Kjarsgaard, 1999), as presented in Fig. 27.2(b). The technique is used for uranium exploration; it discriminates between valuable uranium ore and other radioactive material of little value. Here again, lateral resolution is linked to detector geometry and improvements, e.g. coaxial logging cables are suggested (Conaway *et al.*, 1980). Gamma logging has been used recently in a well contaminated with plutonium (Hartman and Dresel, 1998). In addition, the use of gamma spectroscopy for identifying and measuring plutonium isotopes in contaminated soil samples has been reported (Kadyrzhonov *et al.*, 2000).

The application of marine γ-ray measurements follows similar principles. The difference from the aerial technique is that water absorbs γ-rays rather strongly and that the detector must move at the surface of the seabed while being towed. The emitters are detectable if they are present in sufficient quantities and have energies above 100 keV. Consequently, if ^{238}U and ^{232}Th are

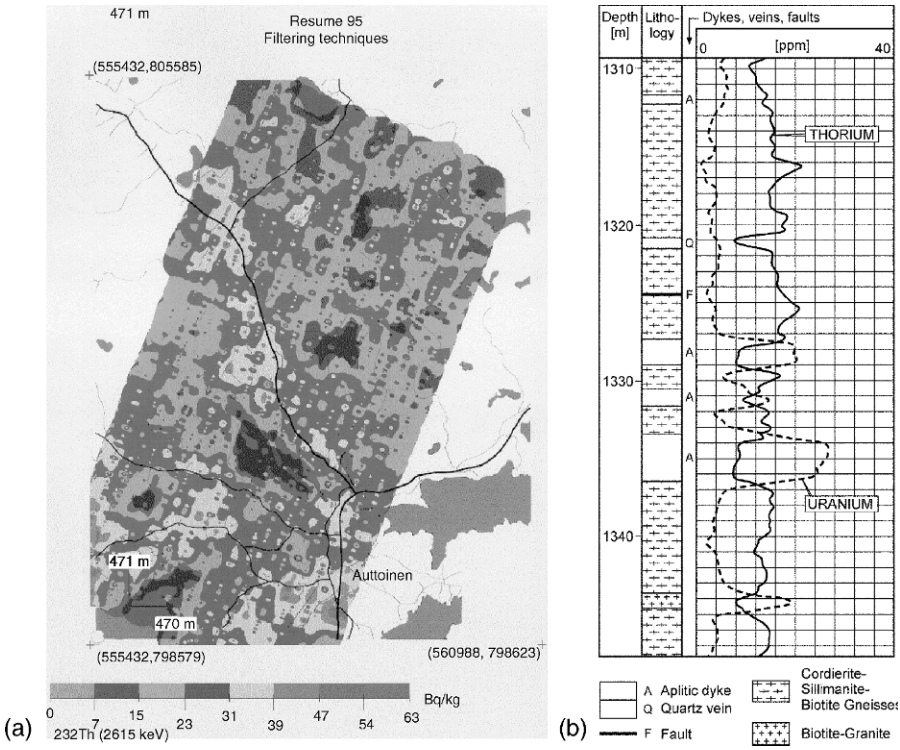

Fig. 27.2 (*a*) ^{232}*Th maps* (*from exercise in Finland, Area* 2) *processed by the filtering and window methods* (*Guillot,* 2001). (*b*) *Th and U profiles from gamma spectroscopic* (*γS*) *instrumental analysis in Leuggern borehole* (*north Switzerland*). *Note the uranium* (*opposite scale*) *depletion through defined faults in formation* (*Nagra,* 1991).

detectable with daughter isotopes, low-energy γ emitters such as ^{241}Am and the plutonium isotopes are very difficult to measure by applying this *in situ* technique (Jones, 2001).

The radiometric technique alone is not effective for speciation. Only MBES, a resonant emission of gamma photons, can provide information. Among the actinide isotopes, ^{231}Pa, ^{232}Th, ^{238}U, ^{237}Np, and ^{243}Am are active as the Mössbauer nucleus. While ^{237}Np is an excellent Mössbauer nuclide, little speciation has been done for environmental samples, perhaps because Mössbauer spectroscopy requires macroconcentrations.

In the field of beta spectroscopy (βS), introduction of a very low background liquid scintillation counting (LSC) spectrometer enables the analysis of soft β emitters such as ^{241}Pu with detection limits of the order of 10 mBq (Yu-fu *et al.*, 1990). This makes it possible to estimate the detection limit for beta

spectroscopy in Table 27.2. However, since the beta spectrum is continuous, application of beta spectroscopy cannot be directly used for the identification of actinides in environmental samples without the use of specific separation techniques. The counting yield of beta scintillation counting is always smaller than 100%.

NS can be applied in a plain counting mode to detect spontaneously fissile actinides in the environment and in the framework of trafficking. Plutonium-239 is hard to detect by means of its α-, x-, or γ-rays, but neutrons are more penetrating and can be specifically detected. Recently, sensitive neutron detectors including ^{3}He proportional counter tubes moderator and integrated electronic have been developed to detect ^{239}Pu down to the gram (5×10^{-3} mol) level at 20 cm in 5 s (Klett, 1999).

GRAV belongs to the last class of passive techniques. Actinide GRAV, e.g. from ore samples, may be carried out after dissolution and separation with, for example, oxalate or oxinates at pH 5–9. Uranium in neutral conditions gives a red precipitate with oxine, $UO_2(C_9H_6NO)_2{\cdot}(C_9H_7NO)$ (Hecht and Reich-Rohrwig, 1929), which should be washed with oxine solution (Claassen and Vissen, 1946). However, this technique suffers from a lack of specificity.

ISEs belong to the class of electron detection passive tools for species analysis, and while the hydrated electrons themselves are not detected, the electronic exchange remains the driving force. Poly(vinyl chloride) matrix membrane uranyl ion-sensitive electrodes based on organophosphorous sensors were successfully tested (Moody *et al.*, 1988). Recently, multi-sensors were developed for the determination of Fe(II), Fe(III), U(VI), and U(IV) in complex solutions (Legin *et al.*, 1999). Twenty-nine different sensors (selective electrodes) with various solid-state crystalline and vitreous materials with enhanced electronic conductivity and redox and ionic cross-sensitivity have been incorporated into the sensor array. The system was tested for Fe(II) and Fe(III) concentrations in the range 10^{-7} to 10^{-4} M, as well as for U(VI) and U(IV), the latter being determined with a precision of 10–40%, depending on the concentration. The developed multi-sensor system could be applied in the future for the analysis of mining and borehole waters, and other contaminated natural media; it can include on-site measurements.

For alpha spectroscopy, the high-resolution silicon detectors have proved to be sensitive down to 10 μBq levels for analysis of both natural Th and U isotopes and daughter nuclides, as well as for the anthropogenic actinides. The isotope ^{227}Ac was quantitatively determined in environmental samples after sample treatment and electrodeposition: a first alpha count at 4.85–4.95 MeV for the 1.38% alpha decay of ^{227}Ac and a second at 5.5–6.1 MeV after ^{227}Th buildup to equilibrium (Bojanowski *et al.*, 1987) were obtained. After sample treatment ^{232}Th and ^{238}U from environmental samples are better characterized by alpha spectroscopy than by gamma spectroscopy as, for example, in urine analysis (Eikenberg *et al.*, 1999) (Fig. 27.3(a)). Natural (U, Th) and anthropogenic (Pu, Am) actinides were, for example, determined and their

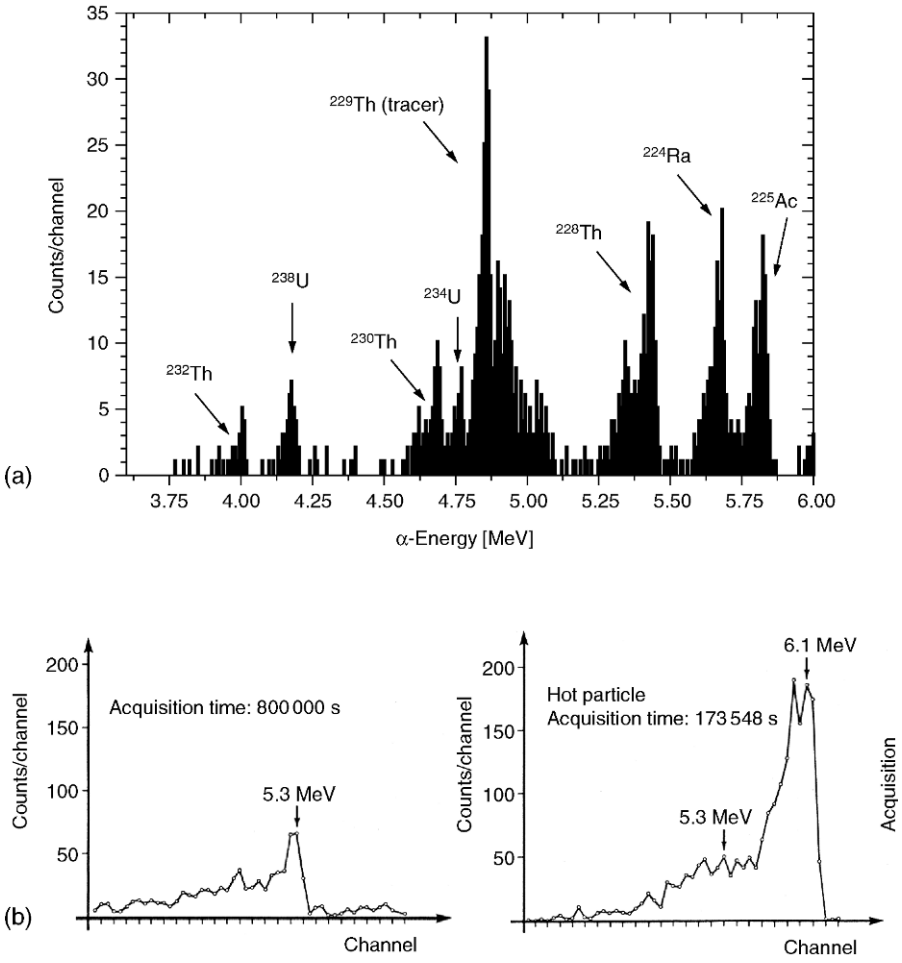

Fig. 27.3 (*a*) *An alpha spectrum of naturally occurring nuclides in urine with an added* ^{229}*Th spike for determination of the chemical recovery of Th. At high energy, the peaks of* ^{224}*Ra and* ^{225}*Ac are daughter products of* ^{228}*Th and* ^{229}*Th, respectively. Isotopes of U are also present because the fast procedure for actinide extraction does not separate between Th and U* (*Eikenberg* et al., 1999). (*b*) *Alpha spectrum obtained for an air filter;* ^{242}*Cm is identified at* 6.1 MeV*; the sampling was* 960 m^3 *air through a* 154 cm^2 *filter, without hot spot and with a hot spot* (0.03 Bq α, ~10^{-21} mol ^{242}*Cm*), *note the* 5.3 MeV *peak is due to natural* ^{210}*Po* (*Gäggeler* et al.,1986).

speciation determined in Venice canal sediment samples (Testa *et al.*, 1999). Here sequential extraction was applied before extraction chromatography, followed by electroplating and alpha spectroscopy. Pu and Am were found at the 1.0 and 0.3 Bq kg^{-1} level, respectively, with a ^{241}Am/$^{239+240}$Pu ratio of 0.3,

while Th and U were at the 20 and 30 Bq kg^{-1} levels. These isotopic analyses show that the sediments were not affected by the Chernobyl fallout but have been contaminated by nuclear weapon test fallout.

An activity may be measured after separation of the sample on a membrane after filtration or ultrafiltration. This may be applied for electrolytic fluids, solutions, or gas. Activity measurements on size-fractionated aerosols indicate different transport mechanisms for I and Ru, Cs (gaseous), or actinides (particulate) released during the Chernobyl accident. A hot particle found by autoradiography on an air filter sample was measured with a surface barrier detector (Gäggeler *et al.*, 1986). Its alpha activity was identified to be mainly due to ^{242}Cm (Fig. 27.3(b)).

Alpha LSC is attractive because it offers a nearly 4π geometry and because the counting yield for an actinide α emitter is about 100%, but with a lower energy resolution than for alpha spectroscopy. Improvements for alpha energy resolution and background reduction are key needs. An improvement of alpha energy resolution for determining low-level plutonium has been achieved using combined solvent extraction low-level liquid scintillation counter (Yu-fu *et al.*, 1990) and can also be applied for $^{239+40}$Pu and ^{241}Pu activity measurements in seawater (Irish Sea and North Sea) and soils (Cumbria and Belorussia) (Yu-fu *et al.*, 1990). Resolution of the order of 275 keV for liquid scintillation spectra can be achieved, which allows low-level determination of plutonium (see Fig. 27.4(a)).

Autoradiography (RAD) consists of using a photographic film or an organic-sensitive polymer to record tracks induced by the decay products from hot spots or contaminated phases in seawater, sediments, or marine organisms (Wong, 1971; Baxter *et al.*, 1995) (e.g. Fig. 27.4(b)) or, for example, natural rock samples sorbed with uranium and americium (Smyth *et al.*, 1980). After development, quantification of the tracks can be performed by counting the tracks or using a densitometer. Extensive work has also been performed with rock samples contacted with actinide solutions or simply contaminated (e.g. Fig. 27.4(c)). ^{241}Am and ^{233}U sorbed onto the rock cause tracks in the autoradiographic emulsions, which may be revealed and observed with an optical microscope. Direct detection with a grid detector and an image reconstruction of the source can also be carried out (Ward *et al.*, 1998).

In all passive techniques, geometrical parameters such as size of the system analyzed, size of the detector, and object–detector distance are key parameters, which, together with acquisition time, rule the detection limit for actinide identification.

Radon and helium contents in groundwater, rock, or soil may be analyzed as actinide by-products to identify uranium- or thorium-rich phase locations. Radon and uranium contents may be correlated (Virk, 1997). However, radon data need to be correlated with helium to yield more accurate results (Virk *et al.*, 1998). It must be noted that radon emanations and helium data are controlled not only by the uranium content of the rock and soil but also by structural zones (thrust, fault, etc.) that help in the easy migration of helium and radon from

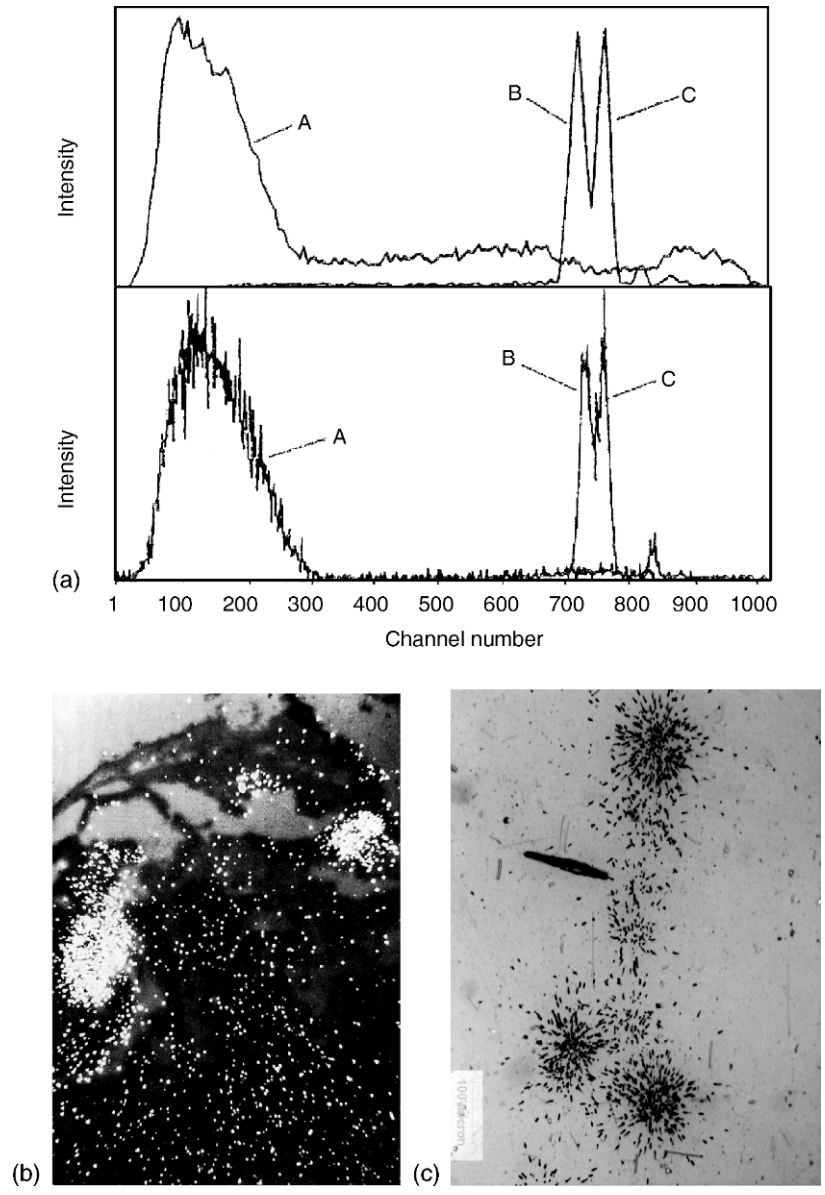

Fig. 27.4 (*a*) *Liquid scintillation counting spectrum from a soil layer, showing* (*A*) ^{241}Pu (β) *and alpha activities including both* $^{239}Pu + {}^{240}Pu$ (*B*) *and the* ^{236}Pu *tracer* (*C*) (*Yu-fu* et al., 1990). *Note that compared to alpha spectrometry, LSC resolution is lower.* (*b*) *Heterogeneous alpha-track distribution in the digestive gland of the winkle following* 13 day *uptake of* ^{239}Pu *from labeled food. A 19* day *exposure* (3 cm = 500 μm) (*Baxter* et al., 1995). (*c*) *Alpha tracks of a hot spot from the analysis of the humus layer, exposure time* 46 days*, total number of alpha tracks about* 600*, corresponding to an activity of* ~0.5 mBq (*Carbol* et al., 2003).

deeper parts of the Earth's crust. Consequently, for uranium prospection, the use of helium and radon data must be verified by combining other techniques, as discussed in Section 27.4.

27.3.2 Interactive photon–photon techniques

The techniques derived from the interaction of photons with a sample and subsequent detection and spectral analysis of photons are numerous, taking advantage of the potential of the large energy spectrum available. They are listed by increasing energy of the incident photon beam as follows: nuclear magnetic resonance (NMR), electron paramagnetic resonance (EPR), infrared Fourier transform spectroscopy (IRFT), diffuse reflection spectroscopy (DRS), near-infrared and visible spectroscopy (NIR-VIS), or spectrophotometry, or colorimetry (COL), Raman spectroscopy (RAMS), atomic absorption spectroscopy (AAS), laser ablation inductively coupled plasma optical emission spectroscopy (LAICPOES), time-resolved laser-induced fluorescence spectroscopy (TRLIFS), phosphometry (PHOS), ultraviolet spectroscopy (UVS), X-ray absorption spectroscopy (XAS), X-ray fluorescence spectroscopy (XRF), X-ray tomography (TOM), Mössbauer absorption spectroscopy (MBAS), and photoactivation (PHOTA). Table 27.3 depicts the way in which these techniques may be used in spatial (transmission, reflection) and temporal (with or without delay) modes when applied to actinide identification or speciation.

In transmission mode, single- or double-beam techniques are applied, the second technique subtracting automatically the blank. In reflection or scattering mode the axis along the detection probe forms an angle with the incident beam. In the delayed mode, detection is carried out at a specific time after excitation of the sample.

NMR is a radiofrequency spectroscopy method that utilizes the interaction of a nuclear magnetic dipole or an electric quadrupole moment with an external or internal magnetic field. Information collected from these investigations characterizes chemical atomic environments. Actinide isotopic species such as ^{229}Th(IV), ^{233}U(VI), and ^{235}U(VI) are active in NMR (Fisher, 1973) at concentration above 10^{-2} M, and for ^{231}Pa(V) and ^{237}Np(VII) above 10^{-4} M. However, very little NMR is done in actinide environmental science except using the NMR signals of actinide neighbor nuclides (^{1}H, ^{17}O,...). EPR is a spectroscopy involving the interaction of electrons in magnetic field, allowing magnetic characterization and indirectly speciation. This technique has been mostly used to study the effect of actinide decay on the magnetic properties dictated by the paramagnetic center concentration of the sample, e.g. soil matrix (Rink and Odom, 1991; Li and Li, 1997; Kadyrzhanov *et al*., 2000).

Infrared spectroscopy (IRS) has occasionally been used for the study of actinides under environmental conditions. It has been used in the transmission mode as well as in the diffuse reflectance mode, both with and without the

Table 27.3 *Interactive analytical techniques including photon–photon for actinide isotope, element, or species characterization.*

Detection	*Goal*	*Sample*	*^{A}An (Y)*	*Detection limit*	*Remarks*
Transmitted photon					
IRS, IRFT, NIR-VIS, PCS, COL, AAS, UVS, XAS, TOM, MBAS	identification and determination of species	solid or liquid bulk, or interphases	Ac(III)	–	VIS or COL
			Th(IV)	3×10^{-8} M COL	
			Pa(V)	–	
			U(VI)	4×10^{-8} M COL	(Keil, 1981)
			Np(V)	1×10^{-7} M VIS	(Keil, 1979)
			Pu(IV–VI)	–	(Gauthier *et al.*, 1983)
			Am(III–VI)	–	
			Cm(III)	–	
Reflected scattered photon					
NMR, EPR, DRS, RAMS, PHOS, UVF, XRF	determination of species	solid bulk or liquid bulk	Ac(III)	–	XRF
			Th(IV)	–	
			Pa(IV,V)	–	
			U(IV–VI)	6×10^{-10} mol	
			Np(IV–VI)	2×10^{-9} mol	(Civici, 1997)
			Pu(IV–VI)	1×10^{-9} mol	(Akopov *et al.*, 1988)
			Am(III–V)	1×10^{-9} mol	
			Cm(III)	–	
Delayed photon					
LAICPOES, TRLIFS, PHOTA	determination of elements species or isotopes	liquid bulk or solid bulk	Ac(III)	–	TRLIFS
			$^{227–232}$Th(IV)	–	
			$^{2331–234}$Pa(V)	–	
			$^{234–238}$U(VI)	1×10^{-12} M	(Moulin *et al.*, 1991)
			^{237,239}Np(IV–VI)	1×10^{-9} M	(Stepanov, 1990)
			$^{238–244}$Pu(IV–VI)	4×10^{-8} M	(Moulin, 1995)
			^{241,243}Am(III)	4×10^{-9} M	(Beitz, 1980, 1988)
			$^{242–250}$Cm(III)	4×10^{-11} M	

application of the Fourier transform. IRS may provide useful information on the speciation of an actinide when present in relatively large concentrations. For example the complexation and reduction of uranium by lignite was determined with site-specific material (Nakashima, 1992). An alternative way to determine actinide speciation may be obtained applying RAMS. The vibrational frequencies concerned are assigned to AnO_2^{i+}, which yields a peak near 870 nm for U(VI) to 860 nm for Np(VI), 767 nm for Np(V), and 835 for Pu(VI) and for actinide concentrations above 10^{-3} M (Basile *et al.*, 1978; Maya and Begun, 1981). The speciation of uranyl in water and sorbed on a smectite (see Fig. 27.5 (a) and (b)) was investigated by Raman vibrational spectroscopy (Morris *et al.*, 1994). The uranium loading was from 0.1 to about 50% of the cation-exchange capacity. The spectral peaks varied in shape and morphology, suggesting speciation changes during the loading. RAMS may be applied at the macroscale (cubic millimeter) as well as at the microscale (cubic micrometer).

NIR-VIS of the 5f elements is a powerful technique for the characterization of oxidation state (e.g. Gauthier *et al.*, 1983) for Np and complexes (e.g. Runde *et al.*, 1997) of actinides. Molar absorptivities (ε) of actinide ions are however smaller than 500 M^{-1} cm^{-1}, limiting the detection limit of the actinide solutions to ~10^{-5} M. Consequently, for actinide ion speciation in natural waters ((An) $<10^{-6}$ M), classical NIR-VIS is not sufficiently sensitive. Addition of a specific complexing dye is required, as described in the next paragraph.

COL, which is a specific application of absorption spectroscopy, has been applied to analyze actinide ions. This technique remains a powerful one despite the emergence of new techniques. This method requires in principle addition of an absorbent specific complex before spectrochemical analysis in the domain 300–1000 nm. Arsenazo-III has been used in the past for the determination of Th and U after extraction (Keil, 1979, 1981) with DL = 7 ng·mL^{-1} (3×10^{-11} mol·mL^{-1}) and 10 ng·mL^{-1} (4×10^{-11} mol·mL^{-1}), respectively. Pyrocatechol violet (3,3′,4′-trihydroxyfuchson–2″-sulfonic acid) has been used recently in a competitive complexation to derive speciation data of uranyl with respect to orthosilicic acid (Jensen and Choppin, 1998). Silicate complexes of uranyl are derived from these tests, allowing estimate of uranyl in silica-rich groundwaters such as those found in the tuff formations in Nevada. (Hydroxy-2-disulfo-3-6-naphtylazo-1)-2 benzene arsonic acid (Thoron) was used at 540 nm for Th quantification in various waters and rocks, e.g. sand (Bhilare and Shinde, 1994). Recently, the use of coumarine azo dyes was suggested for the determination of thorium by spectrophotometry (El-Ansary *et al.*, 1998). DRS has been used to detect uranium down to 35 ng (1.5×10^{-11} mol) on gel by specific complex with 2-(5-bromo-2-pyridylazo)-5-(diethylamino)phenol (5Br-PADAP) in a 10 mL volume of solution (Ivanov *et al.*, 1995).

Actinide colloids may be characterized by photon correlation spectroscopy (PCS). This technique makes use of the light scattered from a laser beam in a colloidal suspension and of dynamic analysis of the scattered light by

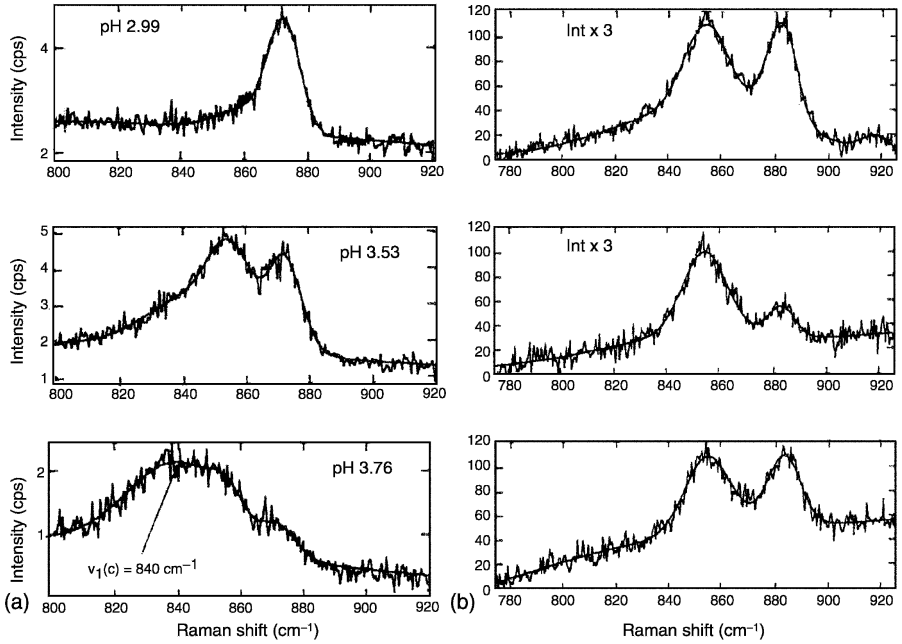

Fig. 27.5 (*a*) *Raman spectrum of U*(*vi*) *in water as function of pH, and* (*b*) *spectra of air-dried smectite samples loaded with U*(*vi*) *form uranyl solutions from alpha. Conditions: intensities are in arbitrary units, fits were obtained from combinations of Gaussian and linear terms, and spectra were generated with* 363.8 nm *Ar laser excitation* (*Morris* et al., 1994).

deconvolution. Little has been done with actinide colloids apart from analysis of their size as reported for thorium colloids (Walther, 2003) or for plutonium colloids (Triay *et al.*, 1991).

AAS is based on the metal-ion absorption of light in a flame or furnace atmosphere. AAS has occasionally been applied for uranium analysis but the detection limit is relatively high, e.g. 7 ppm in flame or 31 ppb in furnace (Goltz *et al.*, 1995).

LAICPOES applies the combination of sample vaporization by a laser ablation process followed by ICPOES (see Section 27.3.5). LAICPOES has been applied in the field in a mobile laboratory for the *in situ* determination of uranium in soil from sites suspected to contain uranium (Zamzow *et al.*, 1994). The optical emission spectroscopy (OES) detection uses the U line at 409.014 nm, with a detection limit for uranium around 5 ppm. Concentration of uranium determined for 15 sites ranged from <20 to 285 ppm. For these concentrations, uncertainty is very large (2σ: 85 ppm). It is, however, reduced

when performing the analysis in the laboratory (2σ: 10 ppm). For 10 ppm C (DL) and a 10 μm^3 crater the N(DL) is around 10^{-18} mol.

UVS may occasionally be used for actinide analysis, but has poor detection limits. It has however been used for speciation studies with Np(V) in carbonate solutions (Neck *et al.*, 1994) and with Am(III) in the micrometer range (Kim *et al.*, 1993).

Detection in a fluorescence mode improves the speciation method and allows trace analysis in liquid or solid samples. Classically, the excitation is carried out in the UV domain, around 340 nm, e.g. with a mercury lamp or with a laser, and the detection performed in the visible region, e.g. from 490 to 570 nm for U(VI), and near 600 nm for Cm(III). Although this technique may be applied to aqueous solutions, it was developed for pellet samples of fluorite salt solid solutions. Salt mixtures, e.g. NaF–LiF, as fluxes with the sample (an aliquot containing U) are melted, e.g. at 1000°C, and examined with a fluorimeter (fluorometer) after cooling at room temperature (Price *et al.*, 1953; Veselsky and Ratsimandresy, 1979). This technique, which is not limited by the interference effect of organics, is however limited by the quenching effect due to the presence of absorbing elements (e.g. Veselsky and Ratsimandresy, 1979; Veselsky and Degueldre, 1986). Structural characterization of Cm(III) on phosphate mineral surfaces was carried out using laser spectrofluorimetry (Cavellec *et al.*, 1998). This technique also allows characterizing the surface complexes of Cm on the mineral surface. Future improvements may include the use of microchip lasers and *in situ* measurements.

TRLIFS, like kinetic PHOS, applies detection temporal windows during fluorescence decay after decrease of organic impurities fluorescence. Pioneering studies demonstrated the powerfulness of this technique for actinide analysis in aqueous solutions (Beitz and Hessler, 1980; Beitz *et al.*, 1988). It is a very versatile tool to achieve speciation of actinides such as uranium and curium (see Fig. 27.6). It has been used successfully to characterize U(IV) hydroxide complexes in environmental conditions (Moulin *et al.*, 1995), occasionally doped with phosphates (Eliet *et al.*, 1995), and for uranium speciation in waters from different mining areas (Bernard *et al.*, 1998). Direct speciation of Cm(III) in natural aquatic system shows that the method is applicable at concentrations down to 7×10^{-9} M (Wimmer *et al.*, 1992) (see Fig. 27.6). The technique can also be applied to gain surface speciation information.

XAS today takes advantage of third-generation high-brilliance synchrotron radiation sources fitted with insertion devices such as wigglers and undulators. This technique has revived interest in the field of hard X-rays in macro- and microprobes. Recent developments are based on the use of Fresnel zone plates and containment techniques such as taped glass capillaries and plastic films, which allow microanalysis to be performed. Typical performance of synchrotron microprobes corresponds to a photon flux of 10^{10} $s^{-1} \cdot \mu m^{-2}$, with minimum

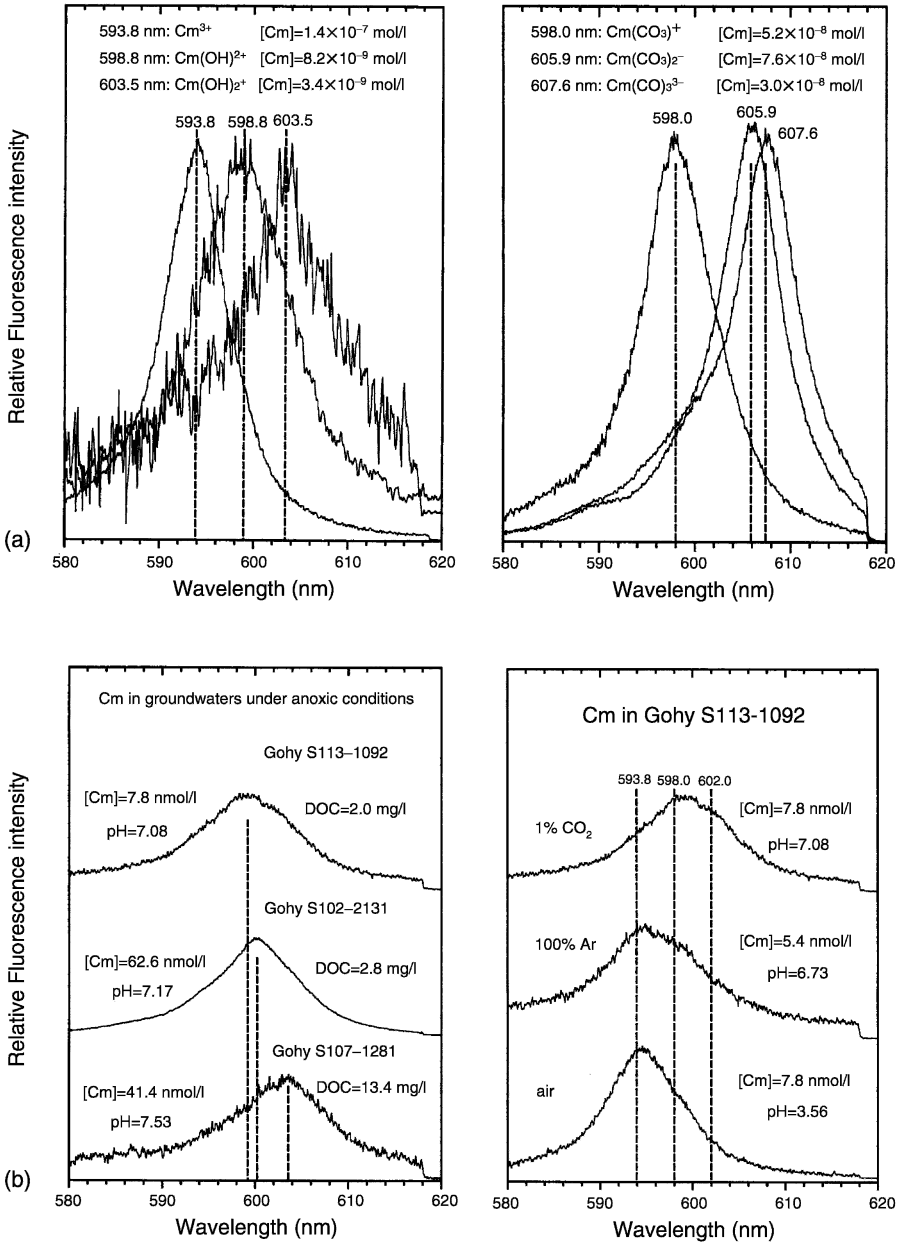

Fig. 27.6 *Time-resolved fluorescence spectrum of Cm(III) in water samples.* (*a*) *Cm in solution to identify the hydroxo and carbonato species and* (*b*) *Cm in groundwater with various dissolved organic carbon DOC concentration and pH. Conditions: the intensities are scaled to be the same height* (*Wimmer* et al., 1992).

detection limits ~10^{-15} g (~4×10^{-18} mol). Analyses are performed by X-ray absorption near-edge spectroscopy (XANES) methods to map elemental distribution and to determine the oxidation states, and extended X-ray absorption fine structure spectroscopy (EXAFS) method to determine the coordination environment of the atoms in question.

Several authors (Nitsche, 1995; Hess *et al.*, 1997; Antonio *et al.*, 2001) suggested recently the use of X-rays provided by synchrotron beams in absorption spectroscopy (XAS) as a new tool for actinide speciation in solids (soils) and liquid (waters) as well as at their interface. This technique is quasi non-destructive, element-specific (L edges for actinides), and very attractive for actinide speciation and for the definition of their atomic environment (Conradson, 1998; Degueldre *et al.*, 2004) and redox state (see Fig. 27.7). It makes use of monoenergetic beams in the range up to (100 keV, focusing a very intense beam over a small area. The micro X-ray absorption beam may be used to focus on local details, for example to better understand the sorption of uranium in soil sediments (Bertsch *et al.*, 1994). In addition, comparison of fine structure for various valence state of uranium (IV) and (VI) was for example recently reported (Hunter and Bertsch, 1998).

XRF is based on the measurement of the fluorescent characteristic radiation emitted by an element when its inner shell electrons are excited. Technically the method is applied in two different spectroscopy modes called wavelength-dispersive spectrometry (WDS) and energy-dispersive X-ray spectroscopy (EDS) modes. The energy-dispersive system is a multielemental technique that can determine the elements in a wide range of concentration from 10^{-6} to 1 $g \cdot g^{-1}$ (ppm). It is non-destructive, with minimum spectral interference. The analysis is very fast and in many cases the sample preparation requires only grinding and pelletizing. The recent use of detectors with better energy resolution down to 10 eV (superconducting tunnel junction) makes this technique even more promising. XRF is also a technique that can be applied in the field with portable units. It may be applied for mineral exploration, mining, monitoring of polluted areas, and other environmental studies.

Aerosol deposits on a filter create homogeneous and thin layers, which result in negligible matrix effects during XRF analysis. The most recent advances are the application of synchrotron-induced XRF. In water, suspended matter can be separated on a filter and analyzed by XRF. Actinides in samples like soils, sediments, rocks, minerals, fly ash, and solid waste are often detected at the 10^{-6} $g \cdot g^{-1}$ level when applying an XRF method. This technique has been applied for analysis of particles from waters, sediments, and waste phases. (see Fig. 27.8) and may also be applied for determination in biological tissues, analysis of airborne particles, and foodstuffs (Akopov *et al.*, 1988; Misaelides *et al.*, 1995; Hunter and Bertsch, 1998). Uranium can be determined in water by precipitation with a non-specific chelating reagent and collection on a filter, which is analyzed by XRF (Civici, 1997). The detection limit is 0.15 μg U (6×10^{-10} mol) or 10^{-9} mol for a 500 mL sample. It can be improved with a microbeam.

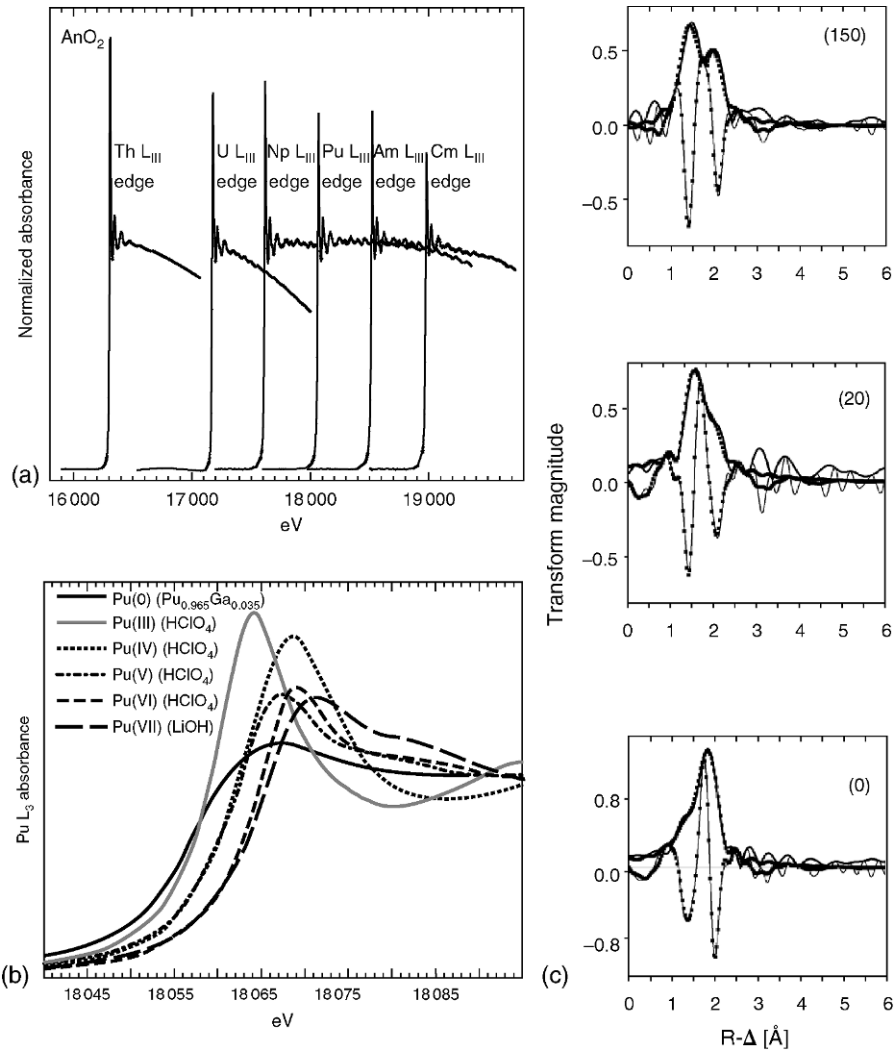

Fig. 27.7 (*a*) *Normalized L3 edge XAS spectrum of Th, U, Np, Pu, Am, and Cm from their dioxides,* (*b*) *XANES of Pu*(0), *Pu*(III), *Pu*(IV), *Pu*(V), *Pu*(VI), *and Pu*(VII) (*derived from* (*Conradson,* 1998)) *showing the shift induced by the oxidation, and* (*c*) *Np L3EXAFS magnitudes and imaginary part of the Fourier transform recorded for a Np*(IV) *acidic solution during* in situ *photooxidation of Np*(IV), *initial result compared after* 20 *and* 150 min, *note the presence of Np*(V) *formation* (*Denecke* et al., 2004).

X-ray TOM investigations have been carried out to identify and locate the spatial extension of phases. When used with dichromatic or dual-energy mode for the element discrimination, the irradiation is first performed below the element edge and then above the edge. This mode of TOM allows analyzing a specific

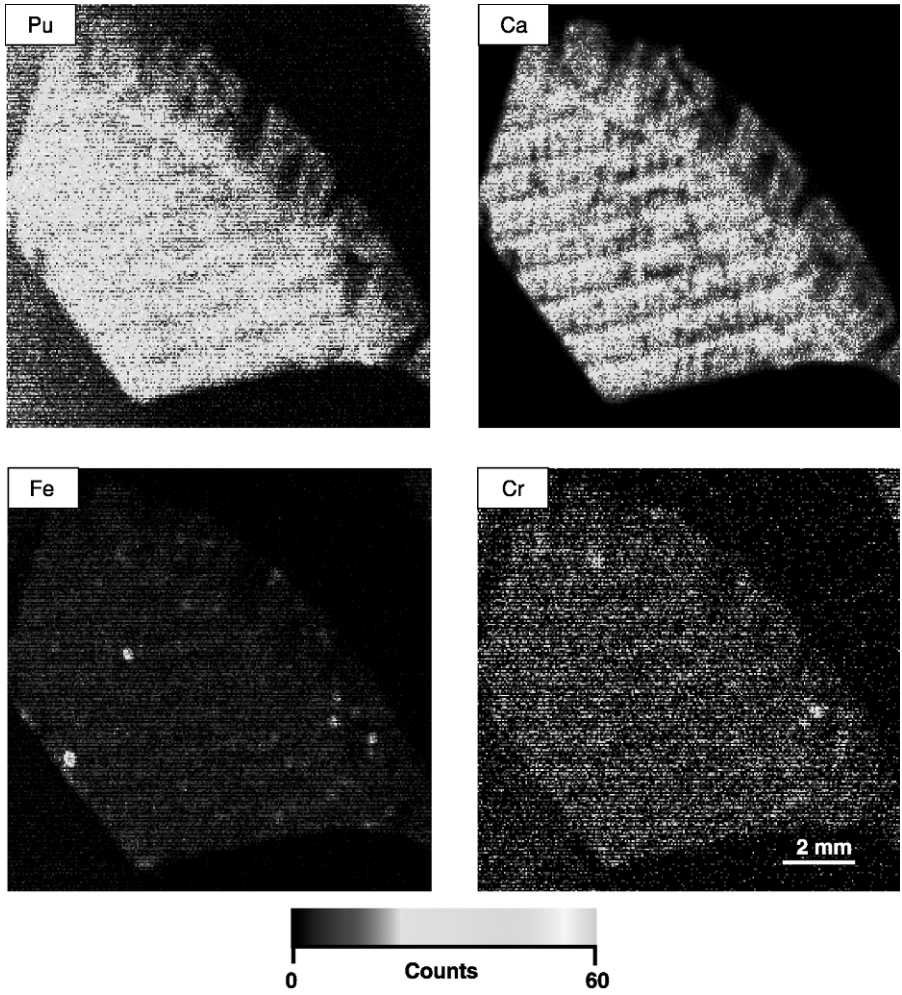

Fig. 27.8 *Micro X-ray fluorescence maps for a precipitate sample filtered from a test container showing Pu- and Sr-enriched phases. Conditions: the thermal scale represents higher concentration of the particular elements; a* 100 μm *aperture that restricts the output beam is used* (*Schoonover and Havrilla,* 1999).

element by comparing the intensity of X-ray absorption below and above the edge. Since the actinide atomic number is high, the energy of the X-ray absorption K edge is rather high too. The sample is placed on a rotation table; the beam is several millimeters in size, with photon intensity of the order of 10^8 mm^{-2} s^{-1}. The detector is a charge-coupled device (ccd) camera that records the image obtained on an X-ray converter screen. Images collected are translated into a 3D tomogram of the element considered, visualizing the element densities. Fig. 27.9 presents

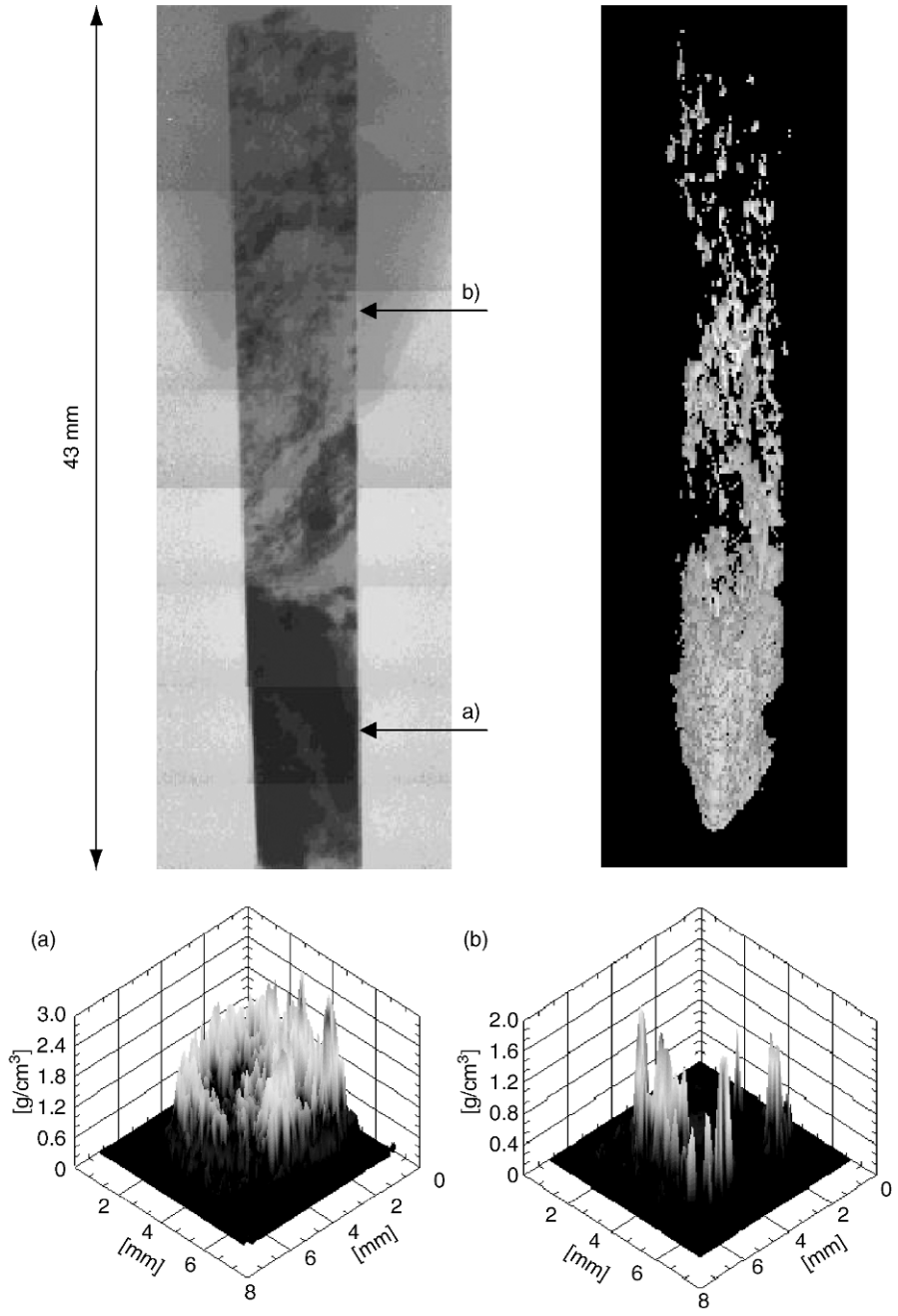

Fig. 27.9 *Single radiograph of Okelobondo* (*top left*) *sample with synchrotron radiation at* 87 keV *and iso-density surfaces* (*top right*) *showing the uranium distribution in the sample; tomograms* (*a*) *and* (*b*) *of the U phase recorded with two light energies* 114.6 *and* 116.6 keV (*Baechler* et al., 2001).

typical radiograms and tomograms obtained for a sample from Okelobondo, Oklo, Gabon (Baechler *et al.*, 2001).

MBAS is a resonant absorption of gamma photons that may be applied to provide information on several actinide isotopes: ^{231}Pa, ^{232}Th, ^{238}U, ^{237}Np, and ^{243}Am. Recently, preparation details of source and sealed absorption holders for ^{237}Np and ^{238}U Mössbauer measurements were reported (Nakada *et al.*, 1998). However, little has been done for actinide speciation of environmental samples, perhaps because this technique requires macro quantities. However, the study of the interaction of Pu(IV) and Np(IV,V,VI) with iron hydroxides has been performed by Fe Mössbauer spectroscopy in order to predict the behavior of actinides in environmental media (Grigoriev *et al.*, 2001).

PHOTA, which involves γ-ray absorption by nuclides, has not yet been used for actinide characterization so far.

27.3.3 Interactive photon–phonon, –electron, –neutron, –ion techniques

Interactive techniques implying photon irradiation and detection of other signals such as phonons, electrons, neutrons, and ions are also used to identify or analyze the actinides. The techniques described below are laser-induced photoacoustic spectroscopy (LIPAS), laser-induced thermal lensing, laser-induced photothermal displacement spectroscopy (LIPDS), laser-induced breakdown detection (LIBD), ultraviolet photoelectron spectroscopy (UPS), X-ray photoelectron spectroscopy (XPS), secondary electron X-ray absorption spectroscopy (SEXAS), laser ablation micro mass analysis (LAMMA), laser ablation inductively coupled plasma mass spectroscopy (LAICPMS), resonance-induced mass spectroscopy (RIMS), and neutron photoactivation (NPHOT), the latter being only occasionally used. They are listed in Table 27.4 on the basis of the particle detected.

Photoacoustic spectroscopy (PAS) is based on the detection of the acoustic signal during photon absorption in the system. PAS has been applied for speciation studies of uranium and transuranium species in aqueous solution as well as in precipitates. LIPAS has been adapted for the UV–VIS and NIR photon energy, as well as for the infrared, domain. The technique applies the absorption of light that creates locally a thermal shock wave, which is detected through a piezoelectric crystal using a dual-beam system (Pollard *et al.*, 1988; Klenze *et al.*, 1991). LIPAS permits identification of U, and its speciation may be performed down to 10^{-6} M. It may be used to achieve speciation of uranium ions in mill tailing water (Geispel *et al.*, 1998). This technique may be used for the speciation of uranium in solution or in precipitates (Kimura *et al.*, 1992). LIPAS has also been used to characterize plutonium species as Pu(VI) in slightly acidic solutions (Okajima *et al.*, 1991) and in neutral solutions (Neu *et al.*, 1994), as well as to generate americium colloids (Buckau *et al.*, 1986). This was carried out for various actinide speciation tests in solution that simulate environmental conditions (see Fig. 27.10). Using an optical heterodyne interferometer, the

Table 27.4 *Interactive analytical techniques including photon–phonon, –electron, or –ion for actinide isotope element or species characterization.*

Detection	*Goal*	*Sample*	*$^{A}An(Y)$*	*Detection limit*	*Remarks*
Phonon					
LIPAS, LIPDS, LIBD	speciation complexes or redox and determination	liquid bulk	Ac(III)	–	LIPAS
			Th(IV)	–	
			Pa(V)	–	(Geipel *et al.*, 1998)
			U(VI)	5×10^{-6} M	(Pollard, 1988)
			Np(V)	1×10^{-7} M	(Okajima, 1991)
			Pu(VI)	2×10^{-5} M	(Klenze and Kim, 1988)
			Am(III)	1×10^{-8} M	
			Cm(III)	–	
Electron					
UPS, XPS, SEXAS	speciation at interfaces	solid surface film	Ac(III)	–	estimated for XPS
			Th(IV)	4×10^{-11} mol	with 10 nm × 1 cm × 1 cm
			Pa(IV,V)	–	sample of density 1 g cm^{-3}
			U(IV–VI)	4×10^{-11} mol	and 1% An weight fraction
			Np(IV–VI)	–	
			Pu(IV–VI)	–	
			Am(III–V)		
			Cm(III)		
Ion					
TIMS, RIMS, LAICPMS, LAMMA	analysis of isotopes elements, chemical species	solid film or bulk nano-micro	Ac	–	RIMS, DL
			$^{227–232}$Th(IV)	3×10^{-18} mol	
			$^{2331–234}$Pa(IV,V)	–	
			$^{234–238}$U(IV–VI)	3×10^{-18} mol	
			^{237,239}Np(IV–VI)	3×10^{-18} mol	(Trautmann, 1992)
			$^{238–244}$Pu(IV–VI)	3×10^{-18} mol	(Trautmann *et al.*, 1986)
			^{241,243}Am(III–V)	3×10^{-18} mol	
			$^{242–250}$Cm(I–II)	3×10^{-18} mol	

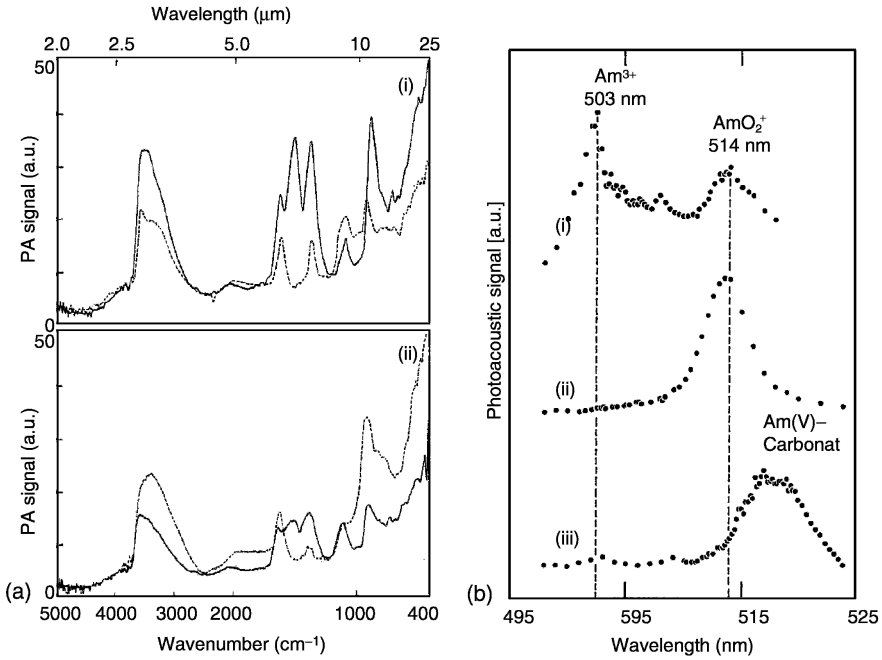

Fig. 27.10 (*a*) *IR-LIPAS spectrum of uranium precipitate* (*i*) *in* 1 M $NaHCO_3$ (*bold line*) *and* 1 M $NaClO_4$ (*broken line*) *solutions, and* (*ii*) *in* 0.05 M (*bold line*) *and* 0.02 M (*broken line*) $NaHCO_3/NaClO_4$ *solutions from* (*Kimura* et al., 1992). *Note solutions simulating groundwaters; absorption bands: OH:* 3521 *and* 1632 cm^{-1}, CO_3: 1098, 1383, *and* 1524 cm^{-1}, *OUO:* 907 cm^{-1}. (*b*) *Speciation of autoradiolytic oxidation process of Am*(III) *during the dissolution of* $Am(OH)_3(s)$ *in* 5 M *NaCl, spectrum after* (*i*) 3.6×10^{-6} M *after* 1 day *dissolution at* $pH = 8.3$, (*ii*) 10^{-4} M *after* 7 days *at* $pH = 8.3$ (*iii*) 10^{-5} M *after* 7 days *at* $pH = 10.7$ *from* (*Klenze and Kim,* 1988). *Note solutions simulating salt dome brine.*

LIPAS unit can be modified in a photothermal displacement instrument (LIPDS), which can be used for the speciation of lanthanides and actinides (Kimura *et al.*, 1998).

When the laser intensity is increased, phase breakdown occurs. Instead of a simple thermal shock, the material is atomized (breaks down). Laser-induced breakdown spectroscopy (LIBS) is used to detect colloidal particles (Gutmacher *et al.*, 1987) and allows the detection of actinide colloids or actinide-associated particles. LIBS was applied to determine the solubility product of Th(IV) colloids (Bundschuh *et al.*, 2000; Bitea *et al.*, 2003).

UPS and XPS applies to spectroscopy of electrons excited by UV or X-ray photons from samples under vacuum. UPS was not applied to environmental samples but to thin-layer actinide research only (Gouder, 1998).

XPS techniques have occasionally been used to characterize actinides associated with environmental samples. They help to understand how uranium is sorbed onto phosphate (Drot *et al.*, 1998) or calcite (Geipel *et al.*, 1997) surfaces, as well as how actinides behave in contaminated soil (Dodge *et al.*, 1995) in the presence of microbes (Francis *et al.*, 1994). In all cases XPS allows redox and spatial speciation of the actinides by the use of energy shifts. For XPS, the detection limit may be estimated as 4×10^{-11} mol for a sample of 1 cm^2 with a 10 nm thickness and a density of 1 g cm^{-3} and 1% actinide mass. This detection limit can be upgraded for microbeam units.

SEXAS could be used to study particles on filters, but nothing has been reported on actinide investigations with this technique. In this case a layer of the order of 100 nm is analyzed and the DL for a 1 to a 10 μm size XAS would be 10^{-11} to 10^{-19} mol, respectively.

Other photon–particle interactive techniques include production of neutrons or ions. Photoneutron logging (PHOTN) was discussed for uranium detection in boreholes in the frame of rock and ore analysis in their occurrence site (Burmistenko, 1986).

Thermal ionization mass spectroscopy (TIMS) applies thermal ionization by evaporating a sample from a heated metal surface and simultaneous measurement of all isotopes of an actinide, using up to nine Faraday detectors. These conditions lead to high precision of isotope ratio measurements ($\leq$0.01%). Due to isobaric interferences, a chemical separation of the interfering elements must be performed before analysis. Therefore, isotopic dilution analysis mass spectroscopy coupled with TIMS represents one of the most accurate methods for the determination of the content of actinides and their isotopic composition. TIMS is currently applied to analyze actinide isotopic composition. The analysis of ^{230}Th distribution in the waters of a North Atlantic site (Vogler *et al.*, 1998), as well as the study of the origin of initial Th from Lake Lahontan, Nevada (Lin *et al.*, 1996), was performed by TIMS. The isotopic measurements of rock samples from the Oklo uranium ore deposit (Ohnuki *et al.*, 1996), as well as a wide variety of environmental samples (Buesseler, 1989), were analyzed by TIMS. Isotope dilution can provide for concentration determination down to the 10^{-15} to 10^{-18} g (4×10^{-18} to 4×10^{-21} mol) range.

LAMMA could be used to study particles on filters or directly on solid samples, but very little has been reported on actinide investigations with this technique. As an example, LAMMA has been applied to fingerprinting coal constituents in bituminous coal. Uranium phases were detected (Lyons *et al.*, 1987). Laser desorption ionization mode of matrix-assisted laser desorption ionization (MALDI) time-of-flight mass spectrometry (TFMS) analysis of U(VI) leads to the formation of uranium oxide clusters (Soto-Guerrero *et al.*, 2001). The formation of clusters can be eliminated using selected matrices, and a more sensitive uranium determination with a detection limit down to 10^{-12} M is possible.

LAICPMS has been used for determination of elemental concentration (in ppm range) and their isotopic composition in solid samples (conducting or not

conducting). It can be done without time-consuming sample preparations. The beam diameter can vary from ~10 to 300 μm. The method allows a depth profile analysis in the range from about 10 μm to several millimeters. The inductively coupled plasma mass spectroscopy (ICPMS) technique is described and illustrated in Section 27.3.5. LAICPMS has been applied for the *in situ* determination of thorium and uranium in silicate rocks and soils (Perkins *et al.*, 1993). Powdered geological materials have been prepared both as pressed powder disks and as fused glasses. Detection limits are better than routine XRF, but comparable with instrumental neutron activation analysis (NAA). For a 10 μm^3 crater and a 1 ppm C(DL) the N(DL) would be 10^{-19} mol. Uranium was analyzed successfully by LAICPMS in various geological samples such as in Neo-Proterozoic or older zircons or baddeleyite with U contents $\geq$65–270 ppm (Horn *et al.*, 2000), in a coral colony (*Porites lobata*) (Fallon *et al.*, 1999) and in the chalcopyrite wall of a black smoker chimney (Butler and Nesbitt, 1999). Dating of the normal faulting along the Indus Suture in the Pakistan Himalayas has also been performed by analyzing ^{231}Pa–^{235}U disequilibrium by LAICPMS (Anczkiewicz *et al.*, 2001).

In resonance ionization spectroscopy (RIS), atoms or molecules are excited stepwise from a defined state, normally the ground state, to highly excited states by resonant absorption of photons followed by an ionization process. An additional mass separation step completes the method of resonance ionization mass spectroscopy (RIMS). Spectroscopic study of thorium using continuous-wave RIMS with ultraviolet ionization provided sufficient signal for isotopic analysis of volcanic-like samples containing as little as 1–5 ng of thorium. The ability to determine accurately and precisely the ^{230}Th/^{232}Th isotopic ratios for 1 ng samples represented an improvement over TIMS (Johnson and Feary, 1993). Detection and speciation of trace amounts of neptunium and plutonium is possible by RIMS, with a three-step photoionization in combination with TFMS (Trautmann, 1992). The detection efficiency allows analysis of 10^7 atoms (2×10^{-17} mol) of an actinide, allowing identification at very low concentrations (see Fig. 27.11). RIMS has been applied to plutonium and transplutonium elements and should allow detection down to 10^6 atoms (3×10^{-18} mol) (Trautmann *et al.*, 1986; Erdmann *et al.*, 1998).

27.3.4 Interactive electron–photon, –electron, –ion techniques

Several techniques using electrons as incident beam or reagent are also applied to identify or characterize actinides. They are summarized in Table 27.5: electron–photon, such as EDS or wavelength-dispersed spectroscopy (electron microprobe analysis, EMPA); electron–electron, such as scanning electron microscopy (SEM) or transmission electron microscopy (TEM), Auger electron spectroscopy (AES), and electron energy loss spectroscopy (EELS); electron–ion, such as electrospray ionization mass spectroscopy (ESMS), and spark

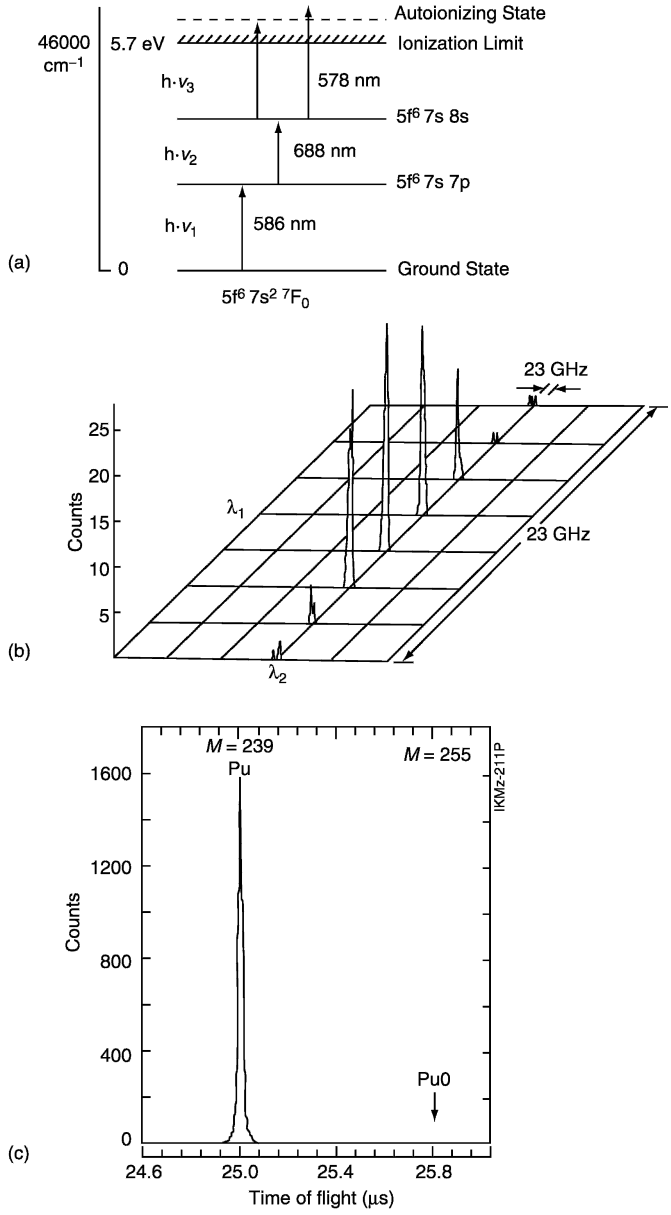

Fig. 27.11 *RIMS of plutonium.* (*a*) *Excitation scheme used for resonance ionization of plutonium.* (*b*) *Plutonium resonance measured by scanning the dye lasers for the first two steps with* λ_3 *fixed.* (*c*) *Time-of-flight mass spectrum of* ^{239}*Pu with two wavelengths in resonance, from* (*Trautmann* et al., 1986).

Table 27.5 *Interactive analytical techniques including electron–photon, –electron, or –ion for actinide isotope element or species characterization.*

Detection	*Goal*	*Sample*	*$^{A}An(Y)$*	*Detection limit*	*Remarks*
Photon					
EDS, EMPA	identification and composition of microphases determination	solid bulk subsurface	Ac(III)	5×10^{-16} mol	estimated for EDS and EMPA with $1 \times 1 \times 1$ μm sample of density 3 g cm^{-3} and 5% An weight fraction
			Th(IV)	5×10^{-16} mol	
			Pa(IV,V)	5×10^{-16} mol	
			U(IV–VI)	5×10^{-16} mol	
			Np(IV–VI)	5×10^{-16} mol	
			Pu(IV–VI)	5×10^{-16} mol	
			Am(III–V)	5×10^{-16} mol	
			Cm(III)	5×10^{-16} mol	
Electron					
SEM, TEM, AES, EELS	morphologic investigations and nanophase speciation	solid, film, or bulk subsurface	Ac(III)	1×10^{-22} mol	estimated for EELS with $2 \times 2 \times 50$ nm sample of density 3 g cm^{-3} and 10% An weight fraction
			Th(IV)	1×10^{-22} mol	
			Pa(IV,V)	1×10^{-22} mol	
			U(IV–VI)	1×10^{-22} mol	
			Np(IV–VI)	1×10^{-22} mol	
			Pu(IV–VI)	1×10^{-22} mol	
			Am(III–V)	1×10^{-22} mol	
			Cm(III)	1×10^{-22} mol	
Ion					
ESMS, SSMS DPV, DPP, COUL	molecular speciation element-isotope speciation and quantitative analysis	solid and solutions solutions	Ac(III)	–	DPV, DPP in solution
			Th(IV)	–	
			Pa(IV,V)	–	
			U(IV–VI)	4×10^{-9} M	(Keil, 1978)
			Np(IV–VI)	2×10^{-8} M	(Kuperman *et al.*, 1989)
			Pu(IV–VI)	2×10^{-8} M	
			Am(III)	–	
			Cm(III)	–	

source mass spectroscopy (SSMS). Electron–phonon methods such as scanning electron acoustic microscopy (SEAM) have not been reported for the identification of actinides. Electroanalytical techniques such as differential pulse voltammetry (DPV) or differential pulse polarography (DPP) may also be applied to characterize the actinides and are treated below.

In the field of structural analysis, microscopic techniques such as TEM, SEM, and high-resolution electron microscopy (HREM) are powerful imaging techniques with nano-scale resolution as well as microprobe capabilities using electron excitation and XS, electron loss spectroscopy, or time-of-flight atom probing. With EDS, high-resolution semiconductor detectors capable of spectral resolution of X-ray lines of neighboring elements made possible the construction of energy-disperse systems. SEAM studies of actinide-doped samples are not reported so far in the literature.

EMPA applies a WDS of the X-rays produced by interaction in the sample. Radiation from the sample is resolved by crystal diffraction, and the monochromatic photons are measured at different angles, assuming a very good resolution of the lines. EMPA is well established and used mainly for elemental analysis in industrial and environmental fields. This technique is used for actinide characterization in environmental samples with a lateral resolution better than 1 μm (Berry *et al.*, 1989, 1994).

Inhalation of respirable particles of uranium is a radiological concern. An investigation of some exposures to low enriched uranium indicated that intakes occurred from the inhalation of surface oxide (UO_x) particles, for example, above low enriched uranium metal plates. Measurements of the size distributions of these particles were made by SEM image analysis (Linauskas *et al.*, 1996). The size distribution analysis from 0.05 to 50 μm allowed a better understanding of the inhalation properties of these uranium oxide particles. As is known, inhaled particles with size <1 μm may be retained in the lungs. SEM allows excellent morphological analysis, which can be completed by backscattered electron analysis to complement the phase study, such as the actinide-doped phase (uranpyrochlore) vs the actinide-depleted phase (baddeleyite), as presented in Fig. 27.12.

X-ray analyses by EDS associated with SEM or TEM enable the investigation at the subcellular level. Since actinides have been introduced in marine environments, their bioavailability to marine organisms is of economic and ecological interest. Cellular and subcellular distributions of ^{238}U, ^{239}Pu, and ^{241}Am have been examined by means of microanalytical techniques, i.e. EDS in organisms: oysters, mussels, shrimps, crabs, and sea spiders (Chassard-Bouchaud and Galle, 1988). Actinide bioaccumulation was detected in target organs, cells, and organelles for every species. The process of the physiological strategies involved in the uptake, storage, and elimination of these actinides was elucidated. The concentration factors range from 10 to 2×10^3. If detection is performed in a cubic micrometer phase with 2% actinide doping, the detection limit DL calculated is reported in Table 27.5. This detection limit is reduced by

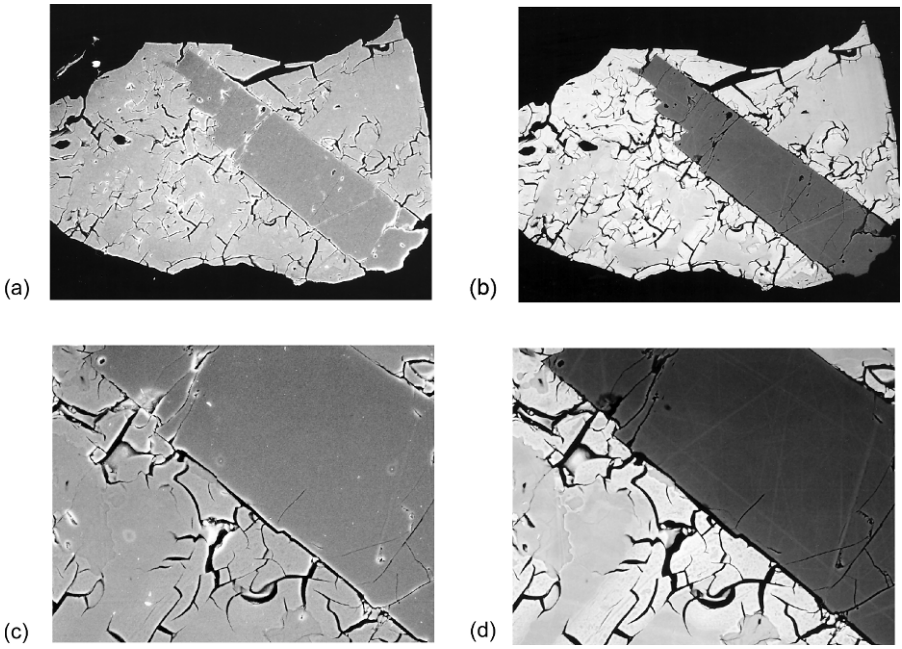

Fig. 27.12 *SEM comparison of secondary* (*a,c*) *and backscattered* (*b,d*) *electron images* (*Lumpkin,* 1999). *Conditions: pairs of intergrowth between uranpyrochlore and baddeleyite from Jacupiranga carbonatite complex, Brazil. Micrograph widths* (*a*) & (*b*) 500 μm; (*c*) & (*d*) 200 μm. *Images taken at low magnification* (*a,b*) *show the general features, including microfracturing and alteration in the uranpyrochlore* (*lighter gray,* $(U,Ca,Ce)_2(Nb,Ta)_2O_6(OH,F)$) *and the platy habit of the baddeleyite* (*darker gray,* ZrO_2).

a factor of 10^3 in a 10^6–10^7 nm^3 phase for an EDS adapted to a TEM unit. However, overlapping of peaks from L and K edges of elements may reduce the accuracy of the analysis.

AES is a technique yielding results similar to XPS. However, AES makes use of the electron as an excitation tool. AES has not been utilized for characterizing actinides in environmental samples. The only AES studies in this field concern the oxygen states in the oxides of uranium and their Auger spectra (Teterin *et al.*, 1997; Gouder, 1998).

EELS may be coupled to TEM or to scanning transmission electron microscopy (STEM) analysis. It is based on spectroscopy of the electron energy after passing through the microscopic specimen. EELS allows study of the oxidation state and the chemical coordination of lanthanides and actinides to be performed in host materials. The speciation may be derived from the M4/M5 edges position and structure. Low levels of transuranics may be characterized with a lateral resolution of the order of 1 nm and concentrations of <200 ppm (Buck and Fortner, 1997). This was applied to redox studies in glasses for plutonium

immobilization (Fortner *et al.*, 1997), in uranium pyrochlore and uraninite as natural analogs of Pu- and U-bearing waste forms (Xu and Wang, 1999), as well as to test the role of alveolar macrophages in the dissolution of different industrial uranium oxide phases (Henge Napoli *et al.*, 1996). The characterization of zirconia–thoria–urania ceramics by X-ray and electron interaction has recently been performed, bridging for actinides EELS and X-ray absorption fine structure spectroscopy (XAFS) potential (Curran *et al.*, 2003). The comparison of EELS spectra collected for these ceramics with spectra recorded for UO_2 and U_3O_8 reference materials also allows assessing U oxidation state at the nanometer-size level in these samples.

Because of its excellent lateral resolution ($2 \times 2 \times 10$ nm) and high sensitivity (1–0.1%), EELS has a demonstrated superior detection limit vs EDS for elements with absorption edges <1000 eV (see Table 27.5).

DPV and DPP are based on electron exchanges between polarizable electrodes and a solution containing redox-sensitive actinides such as U, Np, and Pu (Fig. 27.13). Uranium can be analyzed in U–Fe mixtures by DPV routinely at the 20 μg mL^{-1} (10^{-4} M) level in phosphate solution (Sreenivasan and Srinivasan, 1995) and down to 0.3 μg mL^{-1} (10^{-6} M) level without a preconcentration step in the processing and waste streams of a uranium plant (Sawant *et al.*, 1996). Submicrogram quantities of neptunium and plutonium may be determined by potentiometric voltammetry down to 2×10^{-8} M (Kuperman *et al.*, 1989). Investigations of the redox behavior and the speciation of plutonium in concentrated NaCl solutions with respect to an intermediate-level waste repository were carried out with a rotating disk electrode (Marx *et al.*, 1992). Concentrations of Pu(IV) may be determined quantitatively from the peak height while the shifts in potential are due to speciation changes (complexation) within the solution. In addition, simultaneous determination of U(VI), Pu(VI), and Pu(V) in 0.5–4.0 M NaOH was reported by DPV (Abuzwida *et al.*, 1991). U(VI) is detected at the dropping mercury electrode in the range 10^{-7} to 3×10^{-3} M. Pu(VI) and Pu(V) at the platinum electrode were analyzed at concentrations from 4×10^{-6} to 10^{-3} M even in the presence of various potential interfering ions such as Mo(VI), W(VI), V(V), and Cu(II) in salts such as $NaNO_3$, $NaNO_2$, and NaI.

On non-polarizable electrodes, quantitative electroanalytical methods can also be applied, taking advantage of the rich redox chemistry of the actinide elements. Numerous controlled potential coulometry (COUL) studies have been reported in the literature. For example, neptunium determination is possible at as low as the 2 mg level with a precision of 0.2% (Kasar *et al.*, 1991), even in the presence of interfering elements such as Pu, U, Ce, Cr, Fe, or Mn (1000-fold) (Karelin *et al.*, 1991).

ESMS is a recently developed analytical technique that seems promising for speciation studies. This technique applies a spray of electrons on a material surface followed by mass spectrometry of the cluster ions formed in 'soft conditions'. First developed for biological samples, it is now used for direct

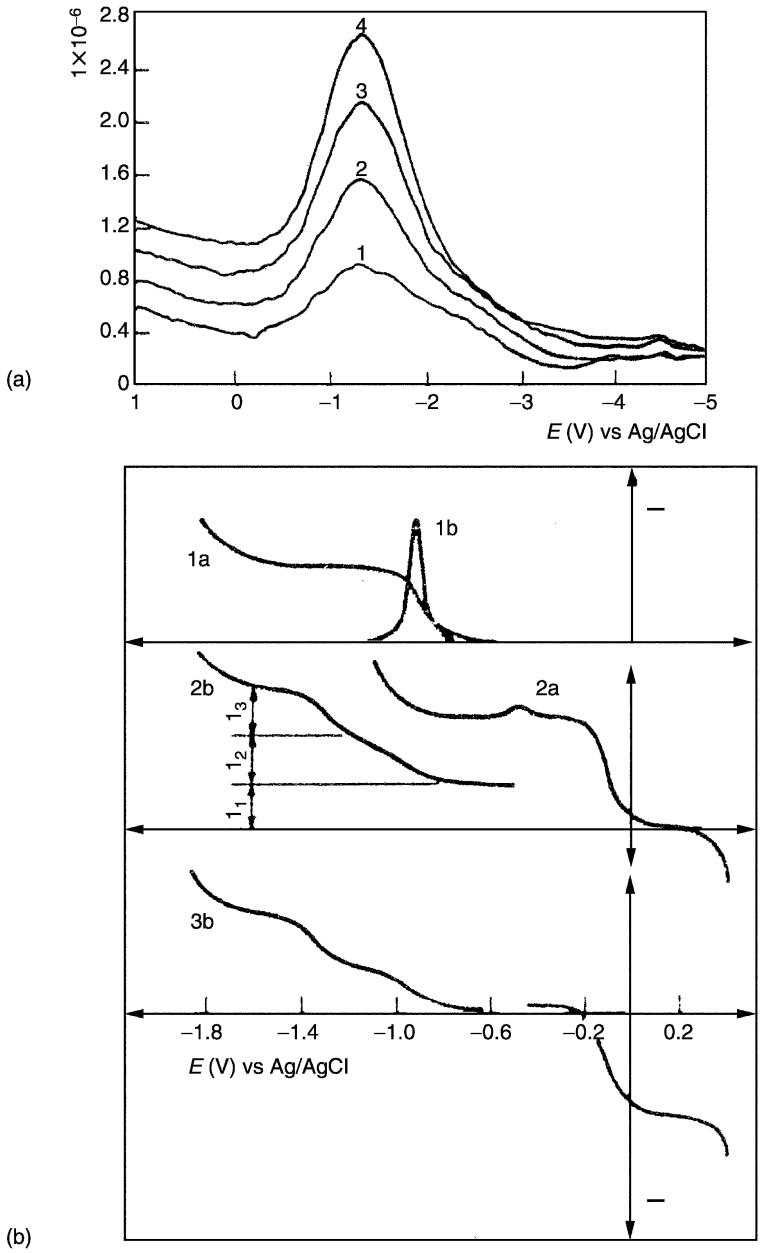

Fig. 27.13 (*a*) *Differential pulse polarogram* (*DPP*) *of U* 1.5 *to* 6×10^{-5} M *at dropping mercury electrode* (*Sawant* et al., 1996)*, possible down to* 10^{-6} M *level without a pre-concentration step in the processing and waste streams of a uranium plant, and* (*b*) *DPV of U and Pu* 10^{-4} M *on Pt electrode* (*Abuzwida* et al., 1991) *in* 1 M *NaOH.*

speciation studies in solution. It is now possible to directly couple a liquid at atmospheric pressure to mass detection at reduced pressure, even if the mechanisms taking place are rather complex. ESMS investigations were adapted for the speciation of Th(IV) hydrolysis species (Moulin *et al.*, 2001) and U(VI) in neutral solutions (Moulin *et al.*, 2000). Fig. 27.14 shows a typical spectrum obtained

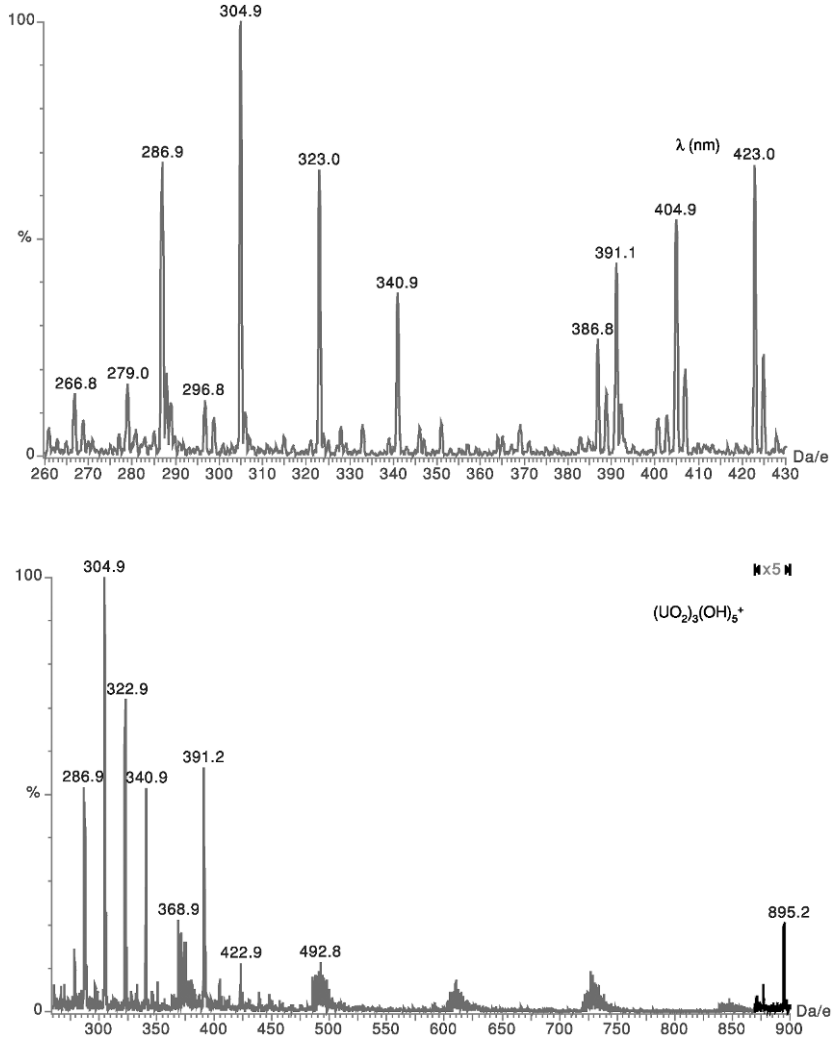

Fig. 27.14 *Electrospray mass spectrum of uranium at* 10 mg L^{-1} *at pH* 3.5 *and at pH* 6.5 (*Moulin* et al., 2000). *Note the presence of species such as* (*a*) $(UO_2OH(H_2O)_n)^+$ *with masses* 286.9 + n·18 *at pH* 3.5 *and* (*b*) *at pH* 6.5, *where* $((UO_2)_3(OH)_5)^+$ *with mass* 895.2 *is also observed.*

for a uranyl solution at pH 3.5. Peaks can be interpreted for the species $((UO_2)_i(OH)_j\,(H_2O)_n)^{(2i-j)+}$.

Increasing the energy of the electronic stimuli permits the technique to be extended from molecular to atomic analysis. SSMS is similar to the former technique but the source of electrons is driven at higher potential. This allows direct quantitative analysis of elements and isotopes of the material. SSMS was used to determine trace elements in the U_3O_8 standard (Li *et al.*, 1991) as well as in other actinide oxides. In a complementary way SSMS may be used to analyze uranium from environmental samples.

27.3.5 Interactive neutron–photon, –electron, –neutron, –ion techniques

Neutron-interactive techniques make use of neutron scattering or absorption in the studied environmental samples. Absorption may be specific to actinide isotopes. The nuclide generated by neutron capture may be detected for its emission of gamma photon, neutron, or ion (fission products or alpha). Its detection is performed as described in Section 27.3 using spectrometric (S) or radiographic (RAD) techniques such as fission track (FT) techniques. Analytical data are given in Table 27.6.

Neutrons are ideal probes for the study of condensed matter, having important advantages over other radiation types. The outstanding feature of neutrons as probes is their high penetration (~10 cm) in materials, while the non-systematic variation of scattering length and absorption cross section from element to element makes its use versatile for actinide analysis. However, neutron RAD has not found applications for actinide speciation in environmental samples but may be used to characterize nuclear fuel pellets in segments of rods (e.g. Groeschel *et al.*, 2003).

NAA, being essentially an isotopic and not an elemental method of analysis, is capable of determining a number of actinide nuclides of radioecological interest by transformation of a nuclide into a radionuclide more quantifiable. The nuclear characteristics that favor this technique may be summarized in an advantage factor relative to radiometric analysis of the original radioanalyte. NAA can be performed by means of several kinds of sources such as nuclear reactors for cold, thermal, epithermal, and fast neutrons, portable isotopic sources such as Am–Be neutron sources, actinide (^{252}Cf) sources, and accelerator/generator or spallation sources with which originally fast neutrons can be thermalized. After activation, the nuclides that are produced are detected by gamma, beta, or alpha spectrometry. Its advantage is that NAA is a multielement, very highly sensitive, not handling intensive, efficient, instrumental, quasi non-destructive, and isotopic technique. On the other hand, it suffers from high costs, nuclear interferences, and residual radioactive wastes. NAA is a sensitive and accurate method for bulk analysis. NAA has been widely used for actinide analysis, in particular in the field of uranium prospecting. Nowadays it

Table 27.6 *Interactive analytical techniques including neutron–photon, –electron, or –ion for actinide isotope element or species characterization.*

Detection	*Goal*	*Sample*	*$^{A}An(Y)$*	*Detection limit*	*Remarks*
Photon					
NAA	isotopic analysis	liquid bulk	^{232}Th	2×10^{-15} mol	NAA *DL* for 1 h
			^{231}Pa	2×10^{-15} mol	irradiation at 4×10^{12} cm^{-2}s^{-1}
			^{238}U	2×10^{-15} mol	(May, 1987)
			^{237}Np	2×10^{-15} mol	(Byrne, 1999)
			Pu	–	
			Am	–	
			Cm	–	
Neutron					
DNAA	isotopic analysis	solid subsurface film bulk depth profiling	^{232}Th	–	
			^{231}Pa	–	DNAA
			^{235}U	–	(Jaiswal *et al.*, 1987)
			^{237}Np	–	(Alfassi, 1990)
			^{239}Pu	–	
			^{241}Am	–	
			^{244}Cm	–	
Ion					
NAA, FTRAD	elemental or isotopic analysis	solid film or bulk nano microdepth profiling	^{232}Th	–	Fission Track *DL* for 7 h
			^{231}Pa	–	irradiation in neutron
			^{235}U	4×10^{-18} mol	flux of 4×10^{12} cm^{-2}s^{-1}
			^{237}Np	2×10^{-16} mol	(Hursthouse *et al.*, 1992)
			^{239}Pu	2×10^{-18} mol	(Johanson, 1996)
			^{241}Am	–	
			^{244}Cm	–	

is applied to determine concentrations in environmental, geological, and biological samples. NAA has also the advantage of being well suited for routine analysis.

Since neutrons activate almost all elements present in the sample, it is necessary to resolve the activity generated by actinides from activities of other elements. Separations are achieved through instrumentation or chemical methods.

The application of NAA to determine ^{230}Th, ^{232}Th, ^{235}U, ^{238}U, and ^{237}Np quantitatively provides an independent quantification that complements the conventional radiometric techniques (Byrne, 1993). NAA was used to determine, in the presence of other elements, Th distribution in geological material (Castillo *et al.*, 1996), ^{231}Pa in environmental and biological samples (Byrne and Benedik, 1999), ^{235}U and ^{238}U in geological samples (Sheng *et al.*, 1985), and ^{237}Np in sediments (Byrne, 1986) (Fig. 27.15) and in biological samples (May *et al.*, 1987), the latter with detection limits down to 5×10^{-13} g Np (2×10^{-15} mol) corresponding to 2.5×10^{-9} mg kg^{-1} for a 200 mL seawater sample.

NAA is currently used for solid samples. However, it has also been successfully applied to the analysis of waters. For example, the effect of humic material on the dissolution of natural trace elements, especially of actinide homologs, and on the sorption behavior of Np, Pu, Am, and Cm has been determined (Probst *et al.*, 1995). The groundwater constituents have been analyzed by applying NAA as well as other analytical techniques. Fractions of fluid samples were obtained by ultrafiltration and by ultracentrifugation. The study showed that trace actinides were associated with the colloidal phase (Kim *et al.*, 1987).

Delayed neutron activation analysis (DNAA) applies delayed neutron detection (see Section 27.3.1) after nuclide activation by neutrons. This technique is very sensitive to the detection of fissile isotopes. It has been compared to other techniques for ^{232}Th, ^{238}U, ^{239}Pu, and ^{240}Pu analysis (Alfassi, 1990; Jaiswal *et al.*, 1994). DNAA was performed for isotopic analysis of uranium in safeguard studies (Papadopulos and Tsagas, 1994), and was applied to uranium analysis in sediments (Noller andHart, 1993), in vegetal specimens (Apps *et al.*, 1988), and in human tissues (Gonzales *et al.*, 1988).

Track-etching is a form of RAD that may also be applied for localizing phases rich in fissile actinides (Fernandez-Valverde *et al.*, 1988). This technique has been applied for ^{235}U and ^{238}U quantification. Different kinds of polycarbonates were used as fission fragment detectors. Sample solutions, with U at the ppm level, dried on the detector are neutron irradiated for a given fluence and fission fragment tracks are microscopically counted (Berry *et al.*, 1989). FT detection is appropriate for the detection of ^{239}Pu in, for example, biological and environmental samples (Johansson and Holm, 1996). The lower detection limit is a few microbecquerel ($2\ \mu\text{Bq} = 4 \times 10^{-18}$ mol), which is comparable to the detection limit of mass spectroscopy and more sensitive than the alpha spectroscopic method. It must, however, include a removal of uranium from the sample.

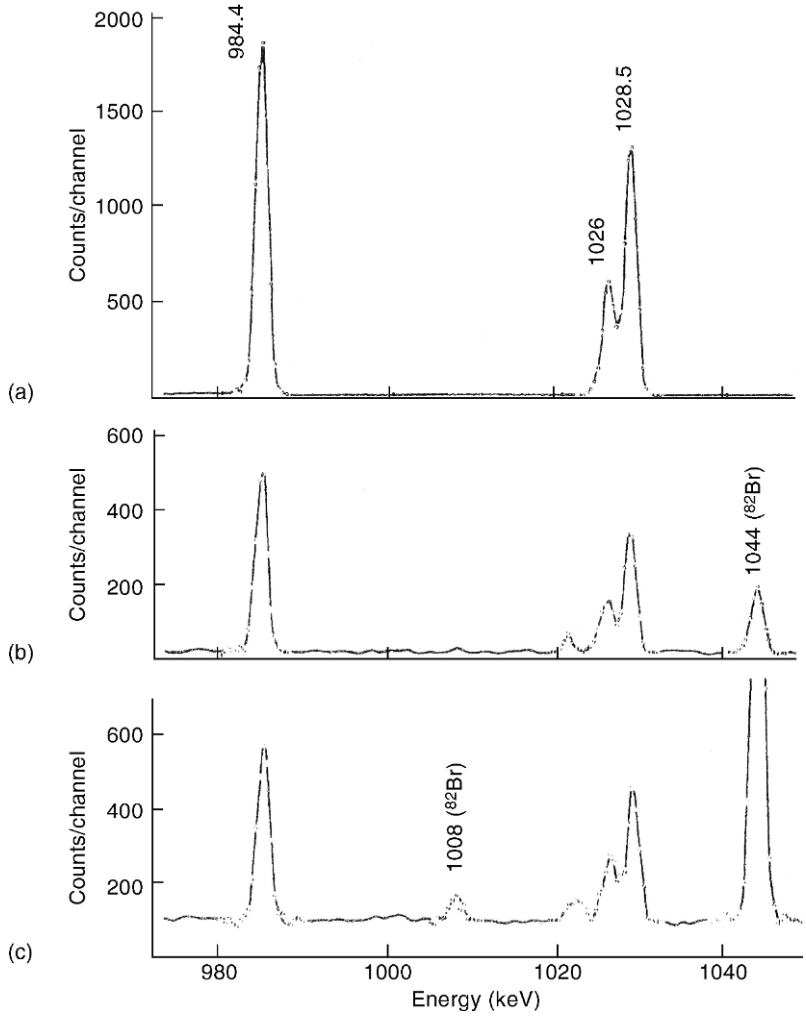

Fig. 27.15 *NAA: partial gamma spectra of* ^{238}*Np from standard and Cumbrian sediments* (*Byrne,* 1986): (*a*) 26.8 ng ^{237}*Np standard, counted* 600 s*; and* (*b*) *Ravenglass sediment* 2 g, 0.2 ng *Np* g^{-1} *counted* 10 000 s*: and* (*c*) *Grange-over-Sands sediment,* 5 g, 20 pg *Np* g^{-1} *counted* 50 000 s. *Conditions: sediment irradiation in Triga Mark II reactor at a neutron flux of* 2×10^{12} cm^{-2} s^{-1} *for about* 20 h *with Np standards.*

27.3.6 Interactive ion–photon, –electron, –neutron, –ion techniques

The techniques derived from the ion reaction/interaction with sample particle detection make use of the large potential of the spectrum of particles produced or reemitted. They are listed as follows: ion–photon, ion–phonon, ion—electron, and ion–ion (Table 27.7). The ion–photon techniques are LAICPOES,

Table 27.7 *Interactive ion–photon, –electron or –ion techniques for actinide isotope element or species characterization.*

Detection	*Goal*	*Sample*	*$^{A}An(Y)$*	*Detection limit*	*Remarks*
Photon					
ICPOES	concentration determination	liquid	^{227}Ac	–	ICPOES
			^{232}Th	4×10^{-9} M	*DL*
			$^{231–234}$Pa	–	(Miekeley *et al.*, 1987)
			^{238}U	8×10^{-9} M	
			^{237}Np	2×10^{-7} M	(Van Britsom *et al.*, 1995)
PIXE, PIGE	identification depth profile	solid subsurface	^{239}Pu	1×10^{-7} M	
			^{241}Am	8×10^{-9} M	(Huff and Bowers, 1990)
			^{248}Cm	1×10^{-8} M	
Neutron					
NRA	elemental and isotopes analysis		^{227}Ac		NRA not recommended for actinide analysis, see text
			$^{231–234}$Th	–	
			$^{231–234}$Pa	–	
			$^{234–238}$U	–	
			^{237,239}Np	–	
			$^{238–244}$Pu	–	
			^{241,243}Am	–	
			$^{242–244}$Cm		
Ion					
VOL, ICPMS	concentration determination	solid surface or bulk nano microdepth profiling	^{227}Ac(III)	4×10^{-14} M[a]	ICPMS
			$^{227–232}$Th(IV)	4×10^{-14} M[a]	*DL* estimated
SIMS, AMS, RBS, ERDA, NRA	elemental or isotopic analysis, also depth profiling		$^{2331–234}$Pa(IV,V)	4×10^{-14} M[a]	
			$^{234–238}$U(IV–VI)	4×10^{-14} M[a]	
			^{237}Np(IV–VI)		(Kim, 1989)
			$^{238–244}$Pu(IV–VI)	4×10^{-14} M[a]	(Hursthouse *et al.*, 1992)
			^{241,243}Am(III–V)		
			$^{242–250}$Cm(III)		(Agaranda, 2001)

[a]Occasionally down to 4×10^{-16} M.

proton (particle)-induced X-ray emission spectroscopy (PIXE), and particle (proton)-induced gamma radiation emission (PIGE). Both ion–phonon and ion–electron techniques have not been applied so far. However, the ion–ion analytical mode is adapted by several powerful techniques such as ICPMS, secondary ion mass spectroscopy (SIMS), accelerator mass spectroscopy (AMS), Rutherford backscattering (RBS), elastic recoil detection analysis (ERDA), and nuclear reaction analysis (NRA). Finally, volumetry (VOL) is added as representative for the ion reaction with ions in solution.

The methods that utilize low-energy ions are dominated by inductively coupled plasma (ICP) techniques. In ICP an inductively coupled argon plasma is used to ionize an aerosol from the finely dispersed matrix and an optical emission spectrometer (ICPOES) detects the emitted light intensities. ICPOES allows, in principle, analysis of actinides at ~2 to 20 ppb levels (~10^{-8} to 10^{-7} M) (Van Britsom *et al.*, 1995; Huff and Bowers, (1990)). It has been used to analyze uranium (at 385.96 nm) at low levels (<100 ppm) in raw phosphoric acid from leachate of phosphate rocks (Waqar *et al.*, 1995). High-resolution (HR) ICPOES has also been used in the nuclear field to analyze fuel burn-up and to analyze samples for major uranium isotopes. The determination of the $^{235}U/^{238}U$ isotopic ratio demonstrates the versatility of the HR-ICPOES technique (Johnson *et al.*, 1998).

Other methods that employ high-energy ions use accelerator-based techniques to generate these ions. The ion accelerators provide a variety of ion beams with energies from a few keV to a few hundred MeV, and beam size ranges from the nanometer to the millimeter scale. Ion beams are applied to trace element determination using X-rays produced in the ionization process or nuclear reactions, including elastic or inelastic scattering or Coulomb excitation to measure actinides or isotopes in the sample. Detection limits are typically of the order of 10^{-6} g g^{-1} mass ratio (~4×10^{-9} mol g^{-1}), or much lower when detection is performed by mass spectroscopy. Ion microbeam analysis uses an ion beam focused to micrometer dimensions for elemental imaging at sample surfaces. This can be performed by measuring secondary radiation induced by the primary ion beam, such as X-rays and nuclear reaction products, or by measuring the energy loss of transmitted primary ions. This technique is very powerful in combination with electron microscopy for investigations of dust and soil particles, particularly those loaded with actinides.

PIXE is typically based on the use of MeV protons and allows the quantification of trace elements ranging from Na to actinides with sensitivities in the range from 10^{-6} – to 10^{-3} $g \cdot g^{-1}$, depending on element and matrices. The μPIXE detection limit is about 5×10^{-16} mol for a $5 \times 5 \times 5$ μm phase depending on the actinide detected. PIXE was, for example, used to determine qualitatively and quantitatively the distribution of uranium and plutonium sorbed onto a variety of rocks and their constituent minerals (Berry *et al.*, 1994). Both surface and subsurface concentrations of actinides were measurable. This identified which minerals are important for the sorption of uranium and plutonium for a given

rock. U and Pu were detected by PIXE in particle grains from contaminated soils (Kadyrzhanov *et al.*, 2000).

PIGE is normally used to detect light elements but cannot be applied to detect actinides.

NRA may be applied with neutron detection, e.g. (d,n). This method is used for elements for which PIXE analysis is unfavorable (e.g. $Z < 20$) but is not applicable to actinides, perhaps because of their larger Coulomb barrier.

VOL analyses such as complexometry and redox titration are two methods in which actinide ions react with other ions in solution to determine the actinide element concentration. For example, Th(IV) can be titrated by ethylenediaminetetracetic acid (EDTA) for the estimation of thorium concentration in low-grade ores (Strelow, 1961), or thorium-rich minerals. This complexation titration is carried out at pH 9–9.5, using Eriochrome Black T as an indicator (Negi and Malhotra, 1980). EDTA complexometry for Np(IV) was reported at pH from 1.3 to 2.0 with xylenol orange as indicator (Rykov *et al.*, 1975). Plutonium and uranium may also be titrated by the same complexation reagent.

Redox titrations are only possible for U, Np, and Pu. Volumetric determination of uranium is classically carried out by reduction using titanous sulfate as reducing reagent before oxidimetric titration (Wahlberg *et al.*, 1957). Ce(IV) (Moss, 1960) or AgO (Godbole and Patil, 1979) may be used to oxidize Np(V) to Np(VI), and Fe(II) to titrate Np(VI) to Np(V). Assay of uranium and plutonium in the same aliquot is possible by potentiometric titration (Nair and Kumar, 1986). The Macdonald method, rescaled down to milligrams of plutonium, was applied using an electrochemical process for each step; the end point of the final titration was determined potentiometrically (Kuvik *et al.*, 1992). Here again, as for GRAV, chemical separation may be required in order to avoid specific complexometric or redox interferences.

In ICPMS the analysis of assayed ions generated in an argon-ion plasma torch is carried out in a quadrupole or a magnetic mass spectrometer. The low detection limits for a large number of elements and the possibility to measure isotopic ratios have established ICPMS as a powerful analytical tool. The advantages are clearly a large dynamic range, 10^{-6} to 10^{-12} g·g^{-1} (4×10^{-14} M: see Table 27.7), occasionally down to 10^{-14} g·g^{-1} (4×10^{-16} M), and the use of various sample introduction techniques with the possibility to measure liquid or solid samples. Nevertheless, the numerous molecular and isobaric overlaps restrict the direct analysis of some elements. The latter problem may be overcome by using a higher-resolution unit (sector spectrometer) or separation (see Section 27.4). Precise and accurate analysis and isotope ratio measurement of long-lived actinides at trace and ultratrace concentration levels in environmental samples can be carried out by ICPMS. This technique allows the analysis of isotopic ratio variation in environmental materials and can provide evidence of contamination from radioactive wastes. The technique is widely used today and is routinely applied for age dating, as well as characterization of samples from the environment and from nuclear reactor materials. The determination of

precise isotopic ratio of uranium, thorium, and plutonium samples with relative standard deviation of the order of 0.05% can be achieved by utilizing a quadrupole mass spectrometer, a direct-injection high-efficiency nebulizer (Becker and Dietze, 1999a), and optimal isotope analysis (Becker and Dietze, 1999b). For actinides, ICPMS has been used to analyze Th and U in soil and plants (e.g. Yukawa *et al.*, 1999), neptunium (Kim *et al.*, 1989) in contaminated soil (Igarashi *et al.*, 1990), and transuranium elements (Agarande *et al.*, 2001) up to Cm (Barrero Moreno *et al.*, 1996). In addition to the large variety of injector, nebulizer, and torch design, electrothermal vaporization (ETV) allows direct introduction of solid samples (such as in a fine suspension) in the plasma. The advantage of the ETV is that there is no need for dilution. ETV–ICPMS was used to determine $^{240}Pu/^{239}Pu$ atomic ratios and ^{237}Np concentrations in marine sediments (Sampson *et al.*, 1991). Determination of a small volume of Am solution, e.g. 20 μl, can be performed using a micronebulizer and a minicyclonic spray chamber (Becker and Dietze, 1999a). Recently ICPMS has been used to analyze colloids in a single-particle mode. This method was applied for the analysis of thorium colloids (Degueldre and Favarger, 2004) and uranium colloids (Degueldre *et al.*, 2005).

SIMS is used for isotopic analysis with high sensitivity and micron-size space resolution. It makes use of a sputter-ion source and a mass spectrometer for analysis and detection of keV secondary particles (positive, negative, or neutral) produced. SIMS may be used in a static way for ion imaging of a surface or in a dynamic way by sputtering for depth profiling. The use in a SIMS system of an accelerator mass spectrometer improves the detection limit for many elements by several orders of magnitude. This technique is sometimes referred to as super-SIMS. Super-SIMS systems that allow bulk sensitivities of 10^{13} atoms per cm^3 (2×10^{-11} mol per cm^3) have been developed, which may be used for both bulk and depth profile measurements.

Micro-SIMS was used to characterize and map actinides ingested in marine organisms, allowing isotopic measurement and cellular images (Chassard-Bouchaud and Galle, 1988) (see Fig. 27.16). Concentrations of uranium and plutonium sorbed onto minerals can be routinely determined with sensitivities down to 1 ng cm^{-2}. Data obtained have been used to identify the minerals in a rock that are relevant to actinide sorption. The age determination of Pu particles was demonstrated by SIMS images (Wallenius *et al.*, 2001). This age is highly important in view of the pending cut-off treaty for nuclear weapon materials. By collecting particles from the vicinity of or inside the nuclear facilities and determining their ages, it is possible to monitor the observance of the agreement. SIMS was also used to measure qualitatively the distribution of sorbing actinides and their penetration rates into minerals after sorption tests (Berry *et al.*, 1993). SIMS has excellent spatial resolution (less than micrometer scale) and achieves some depth profiling to a few micrometers beneath a surface.

AMS incorporates an ion accelerator and its beam transport system as elements of an ultrasensitive mass and charge spectrometer. Isotopic ratios of

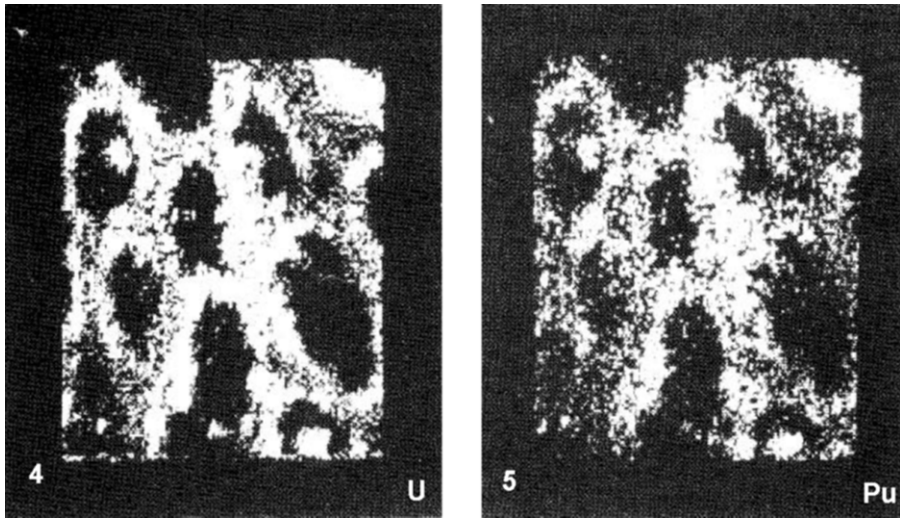

Fig. 27.16 *SIMS pictures of U and Pu from subcellular features of a mussel* Mytilus edulis *digestive gland* (*Chassard-Bouchaud and Galle,* 1988) (200 mm *full horizontal scale*).

less than 1 part in 10^{15} can be measured for some actinide isotopes. This is four or five orders of magnitude smaller than possible with conventional mass spectroscopy. Negative ions produced by a sputter-ion source (e.g. Cs or Ga) can be detected using an AMS system. AMS assay of ^{229}Th, ^{230}Th, ^{233}U, ^{236}U, ^{237}Np, ^{239}Pu, and ^{244}Pu are reported (Zhao *et al.*, 1994a,b; Purser *et al.*, 1996; Zhao *et al.*, 1997). The theoretical detection limit is determined by the overall efficiency of the system: the product of the AnO^- negative ion formation, which ranges from 0.15 for ThO^- to 1.0% for PuO^- (Fifield *et al.*, 1997), multiplied by the transmission efficiency through the accelerator to the detector. The overall efficiency is 1×10^{-6}, so that the sensitivity is 1 count for 1.7×10^4 atoms or 2.8×10^{-20} mol with an extremely small background (virtually zero). Among the lowest-level samples analyzed recently were the river waters downstream from the Mayak plant (Oughton *et al.*, 2000). A sample containing 6×10^7 atoms of ^{239}Pu yielded 63 counts in 15 min in a sample of 3 mg Fe_2O_3. The extreme case was described recently (Wallner *et al.*, 2000) for the detection of supernova-produced long-lived actinide nuclei.

RBS measures the composition profile of a material near the surface. Conventional RBS is performed using helium ions, while heavy-ion RBS has the advantage of a better mass resolution for heavy elements, being able to separate isotopes in some cases. Sensitivity increases for higher masses. Depth resolutions down to 1 nm can be obtained with Si surface barrier detectors in optimized setups, leading to quantitative studies of surface interface mixing and interdiffusion (see Fig. 27.17). The scavenging properties of inorganic particles towards heavy elements such as actinides may be studied by RBS

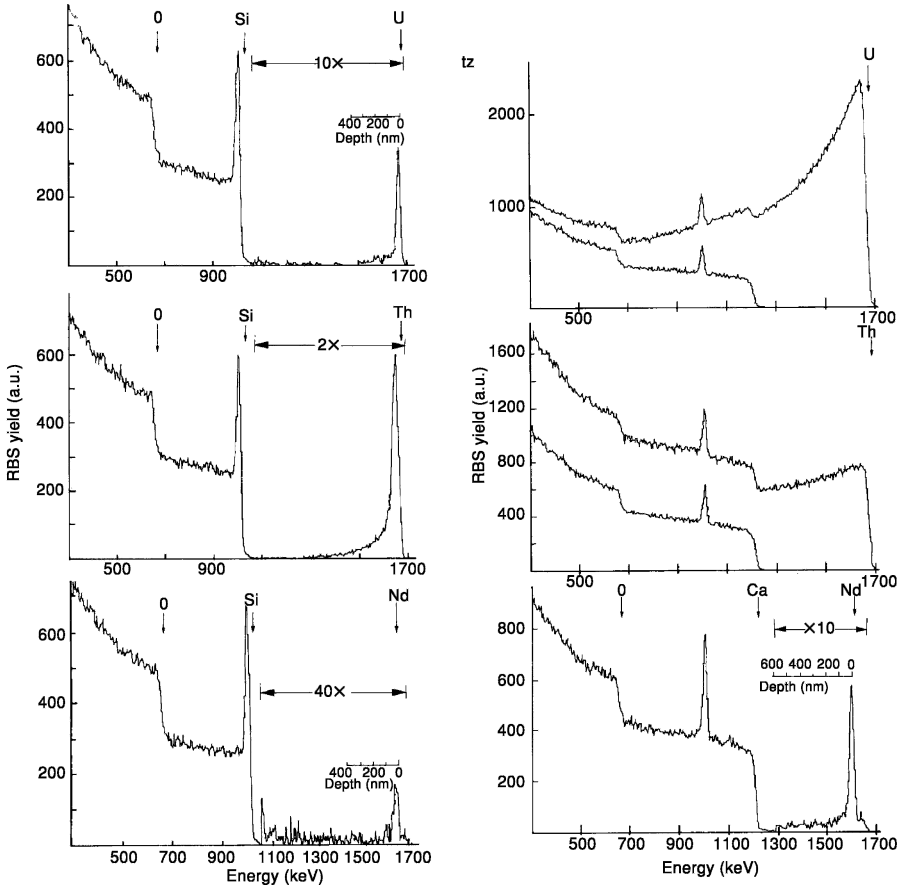

Fig. 27.17 *RBS spectra of U and Th sorbed* (*a*) *on quartz on the surface at* 100°C *and* (*b*) *on calcite at* 50°C *with diffusion in the bulk* (*below the spectra of calcite leached with DI-water*). *Conditions:* 2.2 MeV $^4He^{2+}$. *Note the thin actinide layer on quartz and the diffuse profile in calcite* (*Dran* et al., 1988).

(Della Mea *et al.*, 1992). The interactions of U(VI) and Th(IV) at the calcite–solution interface have been investigated by RBS; it was observed that uranium forms a solid solution while Th yields precipitates (Carroll *et al.*, 1992). Sorption of these actinides was also studied on silica and granite by this technique (Dran *et al.*, 1988). Further sorption work was carried out with uranium and plutonium on minerals with loadings of the order of 1 ng cm^{-2} (Berry *et al.*, 1993). This technique remains a very powerful tool for the identification of the actinides on light-element matrices (soil, bioorganic material).

ERDA makes use of glancing angle heavy-ion irradiation to extract light-element ions from a matrix. This technique is not used to identify actinides but to contribute to light element speciation studies in actinide compounds. ERDA was used to quantitatively measure hydration and hydrogen profiles in the near surface of UO_2 for spent nuclear fuel direct storage, and for a tailor-made titanium-based ceramic that was developed to incorporate radioactive waste for safe and long-term underground storage (Matzke *et al.*, 1990; Matzke and Turos, 1991). In these specimens, no hydrogen uptake was observed at temperatures below 100°C, but for higher leaching temperatures up to 200°C and for longer times, hydrogen profiles could be measured for both materials.

With NRA, specific (d,p), (d,α), (p,α), and other nuclear reactions are used to make sensitive determination of many specific isotopes. In general this method is used for elements for which PIXE analysis is unfavorable (e.g. $Z < 20$) but is not applied for actinides, perhaps because of their larger Coulomb barrier.

27.4 COMBINING AND COMPARING ANALYTICAL TECHNIQUES

The sequential and comparative use of analytical techniques is an important way to improve the quality of any analytical investigations. This has been widely applied to actinide characterization. Combination of techniques is a useful strategy to optimize and confirm information on species. Physical or chemical separation followed by applying one or several identification or speciation techniques is a key route for performing specific and accurate analysis.

SR has become a valuable tool for uranium ore body prospecting. SR is applied in a high-resolution mode, by the action of vibroseis (acoustic source emitters) at a low frequency (10–80 Hz) that are separated by, for example, 10 m, and an array of receivers (geophones) (Phelps and Davis, 1981). Seismic waves can respond specifically to uranium-bearing ore deposits (Liu *et al.*, 1985). SR data incorporate the mapping of geophysical features with radon/helium detection, transient electromagnetic (EM) sounding (Rozenberg and Hoektra, 1982), gravity anomalies, airborne gamma spectroscopy, and gamma logging, to identify high-grade uranium deposits (Dong, 1990; Poty and Roux, 1998). Often the confidential aspect of seismic studies does not allow their use to be made public. Uranium deposit exploration requires, consequently, extensive studies of empirical regional parameters including relationship to geophysical and geochemical records. X-ray diffraction (XRD) and IRS in a reflective mode provide useful lithogeochemical data. These need also to be combined with an EM survey that can be obtained by airborne scanning. Conductive zones that could be key indicators and uranium-rich features may be detected in these bodies. Radiometric survey, gravity mapping, and resistivity measurements complete the later studies. Geochemical and geophysical signatures are correlated in a semiempirical way to guide exploration before uranium ore body identification (Matthews *et al.*, 1997).

AFM has been used to characterize thorium oxyhydroxide colloids (Walther, 2003). This technique, being non-specific for an element, must be combined with others such as SEM/EDS and TEM/EDS to identify the actinide colloidal species. However, AFM is very powerful for determining the morphology and the size of these actinide colloids. The derived techniques such as acoustic AFM (aAFM) and electrochemical AFM (eAFM) allow characterization of specific properties. The latter was recently applied for nanoscopic observation of U(IV) oxide surface dissolution and remineralization (Römer *et al.*, 2003).

EHE may be used for speciation of redox-sensitive actinides such as U, Np, or Pu in waters. Groundwater redox conditions and oxidation state of dissolved uranium were studied in natural water samples from the Palmottu uranium deposit, Finland (Ahonen *et al.*, 1994). Good correlations were observed between the dissolved U(IV)/U(VI) ratio and the measured redox value. The latter, however, requires careful measurements, as recently reported (Degueldre *et al.*, 1999).

The technique of alpha and beta counting by a phoswich detector for simultaneous counting of α- and β-ray (including γ-ray) and determination of actinides is feasible by multi-interface (ZnS(Ag)/NE102A) detectors. Such systems have been developed for complementary actinide α- and β-emitter analysis (Usuda *et al.*, 1997, 1998) and are applicable for actinide identification under high background conditions.

The combination of chemical separation and radioanalysis is classical. Sequential separation combined with photon electron rejecting alpha liquid scintillation (PERALS™) is currently applied for measuring ^{228}Th, ^{230}Th, ^{232}Th, ^{234}U, and ^{238}U in soil samples without tracers (Füeg *et al.*, 1997) (see Fig. 27.18). The minimal detectable concentration ranges between 0.2 and 0.8 Bq kg^{-1} for a 1 g aliquot and 80 000 s counting time. Determination of ^{239}Pu + ^{240}Pu, and ^{241}Pu in environmental samples has been achieved (Yu-fu *et al.*, 1990). After pretreatment of the sample, the plutonium nuclides are co-precipitated with iron(III) hydroxide and calcium oxalate and isolated further from impurities by means of anion-exchange chromatography. Plutonium isotopes are extracted before spectrometric measurement with an ultra low-level liquid scintillation spectrometer. Counting efficiency of plutonium for 100 L of seawater or 40 g of soil sample was about 50%. The detection limit was 0.2 mBq (4×10^{-16} mol) for ^{239,240}Pu.

Extraction may also be used as a separation and a pre-concentration step before polarographic investigations of uranium. This protocol was applied for the determination of U(VI) (Degueldre and Taibi, 1996): the actinide was quantitatively extracted in a hydrocarbon–diethyl-2-hexyl phosphoric acid–TOPO or in hydrocarbon –tri-*n*-octylamine, the organic phase was diluted into the same volume of alcohol and spiked with H_2SO_4 (0.1 M) before electroanalytical investigation by direct current polarography and by DPP. The pulse polarographic peak allowed determination of U(VI) down to 10^{-6} M in the organic phase, which would be impossible without pre-concentration by

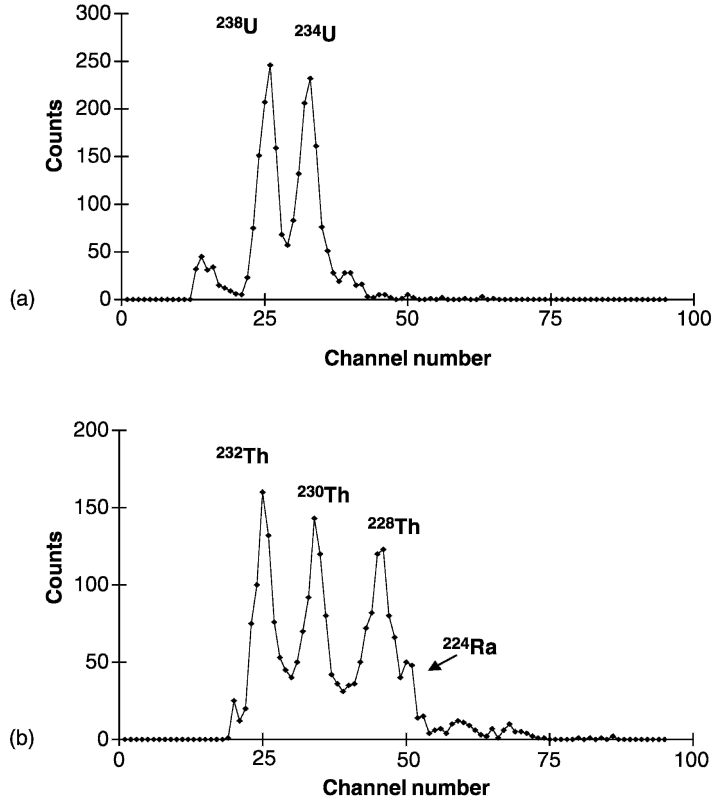

Fig. 27.18 *Typical PERALS™ spectra for the determination of uranium and thorium by extraction and counting.* (*a*) *U in reference soil IAEA*-375, (*b*) *Th in reference soil IAEA*-375*; data from* (*Füeg* et al., 1997).

extraction. This protocol of extraction and analysis is currently applied, for example, with ICPOES for the determination of uranium and thorium in apatite minerals after solvent extraction into diisobutyl ketone using 1-phenyl-3-methyl-4-trifluoroacetyl-5-pyrazolone (Fujino *et al.*, 2000).

Chromatography is basically a separation technique that needs to be completed by applying analytical sensors after the separation step. Chromatography may be performed with an ion-exchange column or by extraction with partitioning onto a liquid phase; spectroscopy and conductivity sensors are generally used for detection. Extraction chromatography was applied for the determination of plutonium and americium in soil samples from Semipalatinsk (Kazachevskij *et al.*, 1999). Ion chromatography was used to perform speciation of plutonium in natural groundwater using anion-exchange resin (Cooper *et al.*, 1995). In most cases actinides are detected using alpha spectroscopy (e.g. Morello *et al.*, 1986). Occasionally, UVS–VIS has been applied to identify actinides eluted.

The determination of actinides (U, Np, Pu, Am, and Cm) is very sensitive and accurate by combining high-performance ion chromatography and ICP quadrupole mass spectrometric detection (Garcia Alonso *et al.*, 1995; Röllin *et al.*, 1996) (see Fig. 27.19). This separation technique followed by mass spectroscopic detection allows the elimination of isobaric interferences such as from one

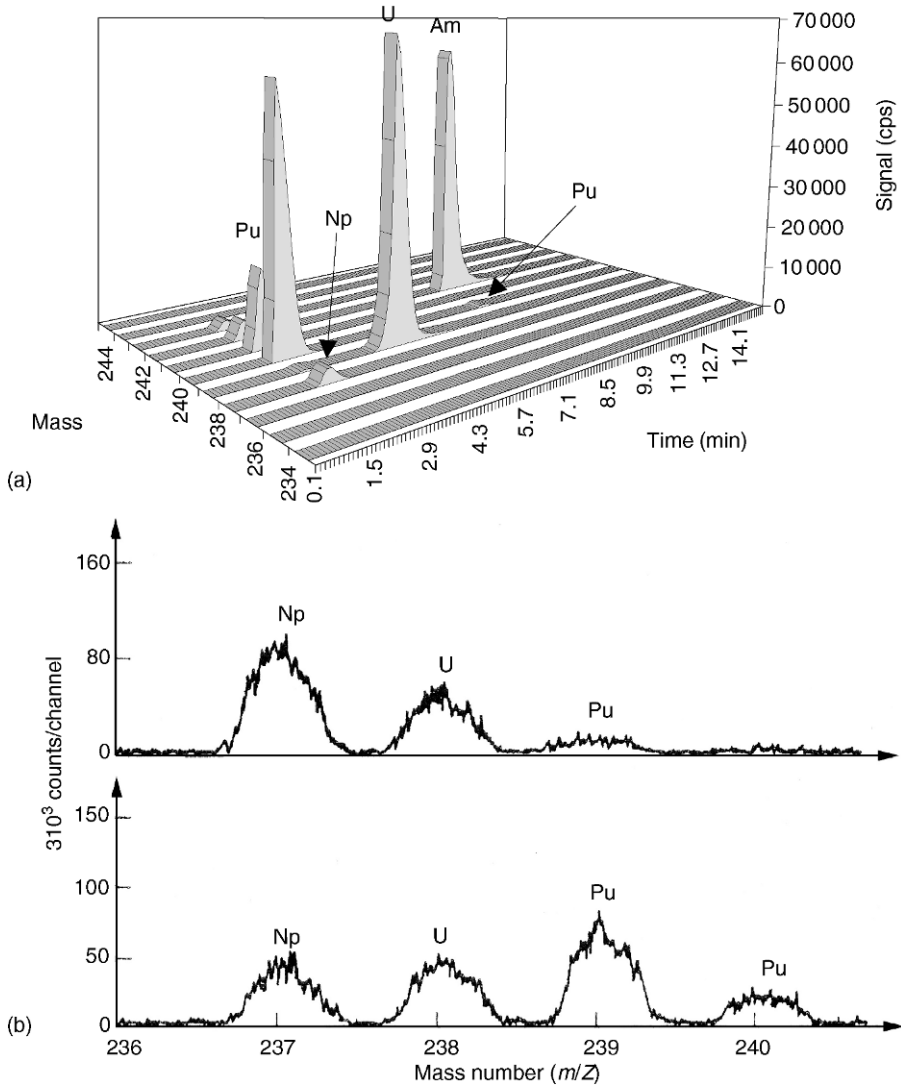

Fig. 27.19 (*a*) *Separation of U, Np, Pu, and Am in* 200 µl *of* 1% HNO_3 *solution containing* 100 ng mL^{-1} *U, Pu, and Am by HPLC-ICPMS* (*Röllin* et al., 1996). (*b*) *Result of actinide analysis by ETV-ICPMS scan of* 1 g *marine sediment collected near a nuclear discharge and subsequently chemically extracted in the laboratory* (*Kim* et al., 1989).

actinide element, e.g. ^{243}Am and ^{243}Cm, or from cluster ions, e.g. $^{155}Gd^{40}Ar_2^+$ or $^{207}Pb^{16}O^{12}C^+$ for $^{235}U^+$, $^{238}U^1H^+$ for $^{239}Pu^+$ (Moreland *et al.*, 1970), $^{232}Th^{12}C^+$ for $^{244}Cm^+$ (e.g. from ETV), or $^{232}Th^{16}O^+$ for $^{248}Cm^+$ (Becker *et al.*, 1999c).

Physical separation techniques such as filtration or ultracentrifugation may be used to enhance actinide speciation. Ultrafiltration or dialysis may be used with alpha spectroscopy for actinides associated with particles or colloids (Degueldre *et al.*, 1994). Combination of ultrafiltration and ICPMS offers also a very sensitive means for colloid analysis, as was the case for groundwater sampling around the fossil reactor of Bagombé (Pedersen, 1996).

Recently, capillary electrophoresis was coupled to ICPMS in order to combine the good performance of this separation technique with the high sensitivity of the ICPMS for the analysis of plutonium and neptunium states (Kuczewski *et al.*, 2003). It was possible to separate a model element mixture containing NpO_2^+, UO_2^{2+}, La^{3+}, and Th^{4+} in 1 M acetic acid. All separations were obtained in less than 15 min and a detection limit of 2×10^{-7} M was achieved. To verify the good speciation performances for plutonium and neptunium during the separation, capillary electrophoresis ICPMS was compared with the result of UV-VIS.

Combining XRF with micro-Raman and IR spectroscopies is a powerful experimental approach in providing information on components present in highly heterogeneous materials, which contain or have been in contact with actinides (Schoonover and Havrilla, 1999). XRF mapping allows identification of plutonium-contaminated regions, while vibrational microspectroscopy provides information on molecular species present and their spatial distribution. This approach provides insight into very complex samples and provides a technique capable of exploring the interaction of molecular components with actinides in complex environmental media. For example, XANES and XPS are combined to confirm uranium reduction from VI to IV by *Clostridium* sp. (Francis *et al.*, 1994). Speciation of uranium complexes in solutions at low ionic strength containing phosphate such as those of seepage waters from old uranium mill tailings was performed by combining data provided by potentiometric and spectroscopic investigations (Brendler *et al.*, 1996).

The feasibility of using the combination of PIXE and RBS to measure uranium and thorium in environmental and biological samples has been demonstrated for environmental studies (Paschoa *et al.*, 1987). The microdistribution of uranium-bearing particles in biological tissues was performed in order to evaluate local irradiation doses in the lungs of former and present uranium miners and millers. These particles have been localized in lungs using neutron-induced uranium FTs registered in solid-state nuclear track detectors in association with a microPIXE and RBS combination. Similarly, RBS and microPIXE have been recently used combined for the study of uranium diffusion in granitic rock matrices analyzing the effect of the presence of bentonite clay (Alonso *et al.*, 2003).

The analysis of the structure of layers on UO_2 leached in H_2O was performed by combining nuclear techniques including RBS-channeling, resonance

scattering, and ERDA using energetic He ions (Matzke, 1996). They were used for the analysis of a UO_2 single crystal leached in demineralized water with different pH values at temperatures up to 200°C. For growth of a U_3O_7 layer, the rate law for layer growth followed a $t^{1/2}$ trend for temperatures between 150 and 200°C and pH in the range 6–10.

Experiments investigating the migration behavior of Th, U, Np, Pu, and Am and the influence of smectite colloids by *in situ* tracer experiment in fractured rock have been performed in dipole mode (Möri *et al.,* 2003). The colloid determination was carried out by LIBD, PCS, and single-particle counting (SPC), while the actinides were determined by the radiochemical techniques after physical separation. Colloid recovery was comparable for these detection techniques.

A comparison of techniques for the analysis of uranium from uraniferrous coal-bearing clays has been reported (Ochsenkuehn Petropulu and Parissakis, 1993). It was carried out using separation techniques, including leaching in carbonate solution, enrichment through an ion exchanger, and elution of Mo and V with EDTA. Uranium is quantitatively eluted by HNO_3 and precipitated by NH_4OH. DPP, atomic absorption analysis (AAS), XRF, instrumental NAA, and ICPMS have been used to determine the uranium content in the raw materials and to investigate the various steps of the process.

Comparison of sensitive techniques such as ICPMS and radiometric alpha and beta spectroscopy has been systematically explored by authors (e.g. Solatie *et al.*, 2000). ICPMS remains very sensitive for the long-lived actinides while radiometric techniques are more suited for short-lived actinides. The half-lives of actinides that are appropriate for analysis by ICPMS may be estimated from Table 27.2 (DL = 10 μBq) and Table 27.7. The detection limits for ICPMS range from 4×10^{-17} to 4×10^{-19} mol in 1 mL depending on the methodology, which correspond to half-lives of 10^4 to 10^2, respectively.

Table 27.8 presents a summary of detection limits estimated for a large number of the sensitive techniques discussed in this chapter. The passive radioanalytical techniques are very sensitive to short-lived nuclides. Alpha spectroscopy has better performance than gamma spectroscopy because of the more efficient detection yield and better background conditions. NAA may improve the sensitivity but its use becomes increasingly limited. Visible spectrophotometry (VIS) is less sensitive than COL but fluorescence (TRLIFS) techniques, allowing speciation, are much more powerful. DPP and XAS provide data for actinide speciation in solution, the latter method in the solid phase also at the 10^{-9} mol level (upgraded to ~4×10^{-18} mol for microXAS, see Section 27.3.2). ICPMS, SIMS, RIMS, and AMS are all very sensitive. The latter reaches DLs better than 10^{-20} mol. Finally, EELS associated with STEM is the most sensitive identification and speciation technique. The detection limit is estimated to be of the order of 10^{-22} mol but it applies to specific small specimens in vacuum, which require extensive preparation and time-consuming analysis and interpretation. EELS has however proved its superior detection.

Table 27.8 *Comparison of detection limits for actinide isotope element or species, all data given in* mol, *normalized to* 1 mL *fluid analysis for VIS/COL, TRLIFS, DPP, and ICPMS. Note:* **bold** *figures for experimental data, and regular figures for theoretical or estimated data, γS from slim-layer source and from Table* 27.2, *αS from electroplated sources and from Table* 27.2*; VIS/COL: for* 1 mL *sample and from Table* 27.3*; TRLIFS: for* 1 mL *and from Table* 27.3*; DPP for* 1 mL *and from Table* 27.5*; EELS from Table* 27.5*; NAA from Table* 27.6*; AMS from Section* 27.3.6*; ICPMS for* 1 mL *and from Table* 27.7.

$^{A}An(Y)$	γS	αS	*VIS/COL*	*TRLIFS*	*DPP*	*EELS*	*NAA*	*AMS*	*ICPMS*
^{227}Ac(III)	4×10^{-14}	4×10^{-18}	–	–	–	1×10^{-22}	–	–	4×10^{-17}
^{230}Th(IV)	1×10^{-11}	6×10^{-17}	$\mathbf{3 \times 10^{-11}}$	$\mathbf{1 \times 10^{-17}}$	–	1×10^{-22}	–	$\sim 3 \times 10^{-20}$	$\mathbf{4 \times 10^{-17}}$
^{232}Th(IV)	5×10^{-7}	1×10^{-11}			–		$\mathbf{\sim 2 \times 10^{-15}}$		
^{231}Pa(V)	2×10^{-14}	2×10^{-17}	–	–	–	1×10^{-22}	$\mathbf{\sim 2 \times 10^{-15}}$	–	4×10^{-17}
^{234}U(VI)	2×10^{-11}	2×10^{-21}					–		
^{235}U(VI)	–	5×10^{-13}	$\mathbf{2 \times 10^{-11}}$	$\mathbf{1 \times 10^{-15}}$	$\mathbf{4 \times 10^{-12}}$	1×10^{-22}	–	$\sim 3 \times 10^{-20}$	$\mathbf{4 \times 10^{-17}}$
^{238}U(VI)	2×10^{-8}	3×10^{-11}					$\mathbf{\sim 2 \times 10^{-15}}$		
^{237}Np(V)	2×10^{-12}	2×10^{-15}	$\mathbf{1 \times 10^{-10}}$	$\mathbf{1 \times 10^{-12}}$	$\mathbf{2 \times 10^{-11}}$	1×10^{-22}	$\mathbf{\sim 2 \times 10^{-15}}$		$\mathbf{4 \times 10^{-17}}$
^{238}Pu(IV)	–	7×10^{-22}					–		
^{239}Pu(IV)	7×10^{-12}	2×10^{-17}		$\mathbf{4 \times 10^{-11}}$	$\mathbf{2 \times 10^{-11}}$	1×10^{-22}	–	$\sim 3 \times 10^{-20}$	4×10^{-17}
^{240}Pu(IV)	1×10^{-12}						–		
^{241}Am(III)	1×10^{-16}	3×10^{-19}		$\mathbf{4 \times 10^{-12}}$	–	1×10^{-22}	–	–	4×10^{-17}
^{242}Cm(III)	5×10^{-15}	3×10^{-22}	–	$\mathbf{4 \times 10^{-14}}$	–	1×10^{-22}	–	–	4×10^{-17}
^{244}Cm(III)	1×10^{-16}	1×10^{-20}			–		–	–	

27.5 CONCLUDING REMARKS

For the past 50 years, actinide identification and speciation in environmental samples has been a topic of growing interest. Techniques required to perform the characterization of actinides that will have better performance in terms of capacity, realization, precision, and detection limit are needed. This will remain a challenge for this century. Detection limits are compared in Tables 27.2–27.7 and summarized in Table 27.8.

Since most of the actinides are α emitters, development of separation techniques coupled with highly sensitive alpha spectroscopy or LSC allows their detection below the 10 mBq level. LSC allows a fast analysis while alpha spectroscopy requires more experimental efforts but permits higher resolution and more sensitive analysis (10 μBq). An alternative to conventional alpha spectrometry may be NAA for which limitations of low counting rates on the non-activated actinide-bearing samples should be improved by their activation; the background is, however, also enhanced. NAA has been found to be particularly prone to interference especially from uranium nuclides.

The trend today is to use advanced ICPMS techniques instead of separation, electroplating, and alpha spectroscopy because ICPMS uses less material and is a less time-consuming technique. ICPMS may, however, require the use of a separation technique, as discussed in Section 27.4, which may advantageously be performed on-line because ICPMS is fast enough, compared to NAA or alpha spectroscopy, to analyze the eluant on-line. Evaluation of NAA and ICPMS methods for the assay of neptunium and other long-lived actinides in environmental matrices has been discussed (Hursthouse *et al.*, 1992). ICPMS offers suitable sensitivity, precision, and accuracy compared to other techniques, with considerably faster sample throughput relative to radiometric and activation approaches. Added advantages of ICPMS include the abilities to determine concentrations of several long-lived actinides simultaneously and to quantify $^{239}Pu/^{240}Pu$ ratios.

ICPMS, NAA, and alpha spectrometry were compared (Kim *et al.*, 1989) for the determination of ^{237}Np in environmental samples. The accuracy and precision of ICPMS was assessed by comparison with that obtained by NAA and alpha spectrometry. Results are in good agreement at a relative deviation of 2–9%. The routine analysis detection limit is 0.02 mBq mL^{-1} or 4×10^{-15} mol (comparable with the estimated data in Table 27.8) calculated with the specific activity of 26 Bq per ng of ^{237}Np.

Plutonium is somewhat difficult to analyze quantitatively by γ-ray spectroscopy because all the commonly encountered isotopes ^{236}Pu, ^{238}Pu, ^{239}Pu, ^{240}Pu, ^{242}Pu, and ^{244}Pu have very low γ-ray abundance emissions, making conventional 4π α-γ coincidence counting techniques impractical. ^{241}Pu is a low-energy β emitter with low (20 keV) end point energy and no associated γ-ray. ^{241}Pu is best analyzed using LSC by calibration with ^{3}H with some corrections for differing end-point energies and beta spectrum shapes.

Several of the advanced analytical techniques described in this chapter are very powerful methods for the determination and characterization of actinides in environmental systems. Better standards and reference materials, as well as intercomparison exercises, are required. For some techniques, standards are occasionally unavailable, for example for SIMS, EMPA, LAICPMS, XRF, and some surface analyses. Other techniques such as RBS, AMS, and EELS under vacuum and XAS in solution require internal calibrations; the sensitivity of the latter is expected to improve in the future. However, the techniques presented are often complementary; in many cases they provide unique information that cannot be obtained with alternative methods. Consequently, their continued and expanded utilization is required for actinide identification and speciation in the environment. Development of analytical techniques such as MBE/AS or EPR, which is more sensitive than NMR for actinide identification and speciation, may be suggested in future research programs.

As far as the environment is concerned, one has to think the way the analyst and the environmental scientist would collaborate together to produce data that can be used by modelers or authorities. The challenge is however to understand the behavior of actinide elements in the environment. Biogeochemical pathways have to be described, quantified, and understood. The contaminated systems interact with the local environment that may modify actinide speciation by physical–chemical processes, which need to be studied. Simple processes such as actinide association with biofilm, bioaccumulation, specific co-precipitation, or sorption onto soil or rock require detailed and full quantification and speciation for the understanding of process mechanism. Transport of actinides in fluids such as air or water includes particulate or colloidal phases. These analyses must be integrated in the analytical strategy as specific species for modeling their biogeochemical affinity.

The challenge will be to find and develop direct analytical probes for actinide speciation at very low concentration to provide data that will better characterize the actinide species to predict their behavior in heterogeneous and complex natural systems.

GLOSSARY

aAFM	Acoustic AFM
AAS	Atomic absorption spectroscopy
AES	Auger electron spectroscopy
AFM	Atomic force microscope
AMS	Accelerator mass spectroscopy
COL	Colorimetry
COUL	Coulometry
DNAA	Delay neutron activation analysis
DPP	Differential pulse polarography

DPV	Differential pulse voltammetry
DRS	Diffuse reflection spectroscopy
eAFM	Electrochemical AFM
EDS	Energy-dispersive X-ray spectroscopy
EELS	Electron energy loss spectroscopy
EMPA	Electron microprobe analysis
EPR	Electron paramagnetic resonance
ERDA	Elastic recoil detection analysis
ESMS	Electrospray ionization mass spectroscopy
ETV	Electrothermal vaporization
EXAFS	Extended X-ray absorption fine structure spectroscopy
FTRAD	Fission track radiography
GRAV	Gravimetry
HPLC	High-pressure liquid chromatography
ICPOES	Inductively coupled plasma optical emission spectroscopy
ICPMS	Inductively coupled plasma mass spectroscopy
IRFT	Infrared Fourier transform spectroscopy
IRS	Infrared spectroscopy
ISE	Ion-selective electrode
LAICPMS	Laser ablation inductively coupled plasma mass spectrometry
LAICPOES	Laser ablation inductively coupled plasma optical emission spectrometry
LAMMA	Laser ablation micro mass analysis
LSC	Liquid scintillation counting
LIBD	Laser-induced breakdown detection
LIPAS	Laser-induced photoacoustic spectroscopy
LIPDS	Laser-induced photothermal displacement spectroscopy
MALDI	Matrix-assisted laser desorption ionization
MBAS	Mössbauer absorption spectroscopy
MBES	Mössbauer emission spectroscopy
MS	Mass spectroscopy
NAA	Neutron activation analysis
NIRS	Near-infrared spectroscopy
NMR	Nuclear magnetic resonance
NPHOT	Neutron photolysis
NRA	Nuclear reaction analysis
NS	Neutron spectroscopy
PAS	Photoacoustic spectroscopy
PCS	Photon correlation spectroscopy
PERALS	Photon electron-rejecting alpha liquid scintillation
PHOS	Phosphometry
PHOTA	Photoactivation
NPHOT	Neutron photoactivation
PIGE	Particle (proton)-induced gamma emission

PIXE	Proton (particle)-induced X-ray emission
RAD	Radiography, autoradiography
RAMS	Raman spectroscopy
RBS	Rutherford backscattering
RIS	Resonance ionization spectroscopy
RIMS	Resonance ionization mass spectroscopy
RMA	Raman microprobe analysis
SEAM	Scanning electron acoustic microscopy
SEM	Scanning electron microscopy
SEXAS	Secondary electron X-ray absorption spectroscopy
SIMS	Secondary ion mass spectroscopy
SNMS	Sputtered neutral mass spectroscopy
SPC	Single-particle counting
SR	Seismic reflection
SSMS	Spark source mass spectroscopy
STEM	Scanning transmission electron microscopy
TEM	Transmission electron microscopy
TFMS	Time-of-flight mass spectroscopy
TIMS	Thermal ionization mass spectroscopy
TOM	Tomography
TRLIFS	Time-resolved laser-induced fluorescence spectroscopy
VIS	Visible spectroscopy
UPS	Ultraviolet photoelectron spectroscopy
UVS	Ultraviolet spectroscopy
VOL	Volumetry
WDS	Wavelength-dispersive spectrometry
XANES	X-ray absorption near-edge spectroscopy
XAS	X-ray absorption spectroscopy
XPS	X-ray photo-electron spectroscopy
XRF	X-ray fluorescence spectroscopy
XS	X-ray conversion spectroscopy
αS	Alpha spectroscopy
βS	Beta spectroscopy
γS	Gamma spectroscopy

REFERENCES

Abuzwida, M. A., Maslennikov, A. G., and Peretrokhin, V. F. (1991) *J. Radioanal. Nucl. Chem.,* **147**, 41–50.

Agarande, M., Benzoubir, S., Bouisset, P., and Calmet, D. (2001) *Appl. Radiat. Isot.,* **55**, 161–5.

Ahonen, L., Ervanne, H., Jaakkola, T., and Blomqvist, R. (1994) *Radiochim. Acta,* **66/7**, 115–21.

Akopov, G. A., Krinitsyn, A. P., and Tikhonova, A. E. (1988) *Radiokhimiya,* **30**, 578–83.

Alfassi, Z. B. (1990) *Activation Analysis* (vol. 1), CRC Press, Boca Raton, FL, pp. 97–109.

Alonso, U., Missana, T., Patelli, A., Ravagnan, J., and Rigato, V. (2003) *Nucl. Instrum. Met. B,* **207**, 195–204.

Anczkiewicz, R., Oberli, F., Burg, J. P., Villa, I. M., Guenther, D., and Meier, M. (2001) *Earth Planet. Sci. Lett.,* **191**, 101–14.

Antonio, M. R., Soderholm, L., Williams, C. W., Blaudeau, J.-Ph., and Bursten, B. E. (2001) *Radiochim. Acta,* **89**, 17–25.

Apps, M. J., Duke, M. J. M., and Stephens-Newsham, L. G. (1988) *J. Radioanal. Nucl. Chem.,* **123**, 133–47.

Arslanov, K. A., Kuznetsov, V., Yu., Lokshin, N. V., and Pospelov, Yu. N. (1989) *Sov. Radiochem.,* **30**, 378–82.

Baechler, S., Materna, Th., Jolie, J., Cauwels, P., Crittin, M., Honkimaki, V., Johner, H. U., Masschaele, B., Mondelaers, W., Kern, J., and Piboule, M. (2001) *J. Radiochem. Nucl. Chem.,* **250**, 39–45.

Bajo, S. and Eikenberg, J. (1999) *J. Radioanal. Nucl.Chem.,* **242**, 745–51.

Balescu, S., Dumas, B., Gueremy, P., Lamothe, M., Lhenaff, R., and Raffy, J. (1997) *Paleogeogr. Paleoclimat. Paleoecol.,* **130**, 25–41.

Barrero Moreno, J., Garcia Alonso, J. I., Arbore, Ph., Nicolaou, G., and Koch, L. (1996) *J. Anal. At. Spectrom.,* **11**, 929–35.

Barth, H., Ganz, M., and Brandt, R. (1994) *Geochim. Cosmochim. Acta,* **58**, 4759–65.

Basile, L. J., Ferraro, J. R., Mitchell, M. L., and Sullivan, J. C. (1978) *Appl. Spectrosc.,* **32**, 535–7.

Baskaran, M., Santschi, P. H., Benoit, G., and Honeyman, B. D. (1992) *Geochim. Cosmochim. Acta,* **56**, 3375–88.

Baxter, M. S., Fowler, S. W., and Povinec, P. P. (1995) *Appl. Radiat. Isot.,* **46**, 1213–23.

Becerril- Vilchis, A., Meas, Y., and Rojas-Hernández, A. (1994) *Radiochim. Acta,* **64**, 99–105.

Becker, S. and Dietze, H.-J. (1999a) *Fresenius J. Anal. Chem.,* **364**, 482–8.

Becker, S. and Dietze, H.-J. (1999b) *J. Anal. At. Spectrom.,* **14**, 1493–500.

Becker, J. S., Dietze, H.-J., McLean, J. A., and Montaser, A. (1999c) *Anal. Chem.,* **71**, 3077–84.

Beitz, J. V. and Hessler, J. P. (1980) *Nucl. Technol.,* **51**, 169–77.

Beitz, J. V., Bowers, D. L., Doxater, M. M., Maroni, V. A., and Reed, D. T. (1988) *Radiochim. Acta,* **44/5**, 87–93.

Bellido, L. F., Robinson, V. J., and Sims, H. E. (1994) *Radiochim. Acta,* **64**, 11–4.

Benke, R. R. and Kearfott, K. J. (1997) *Health Phys.,* **73**, 350–61.

Bernard, G., Geipel, G., Brendler, V., and Nitsche, H. (1998) *J. Alloys Compds,* **271/3**, 201–5.

Berry, J. A., Jefferies, N. L., and Littleby, A. K. (1989) *Proc. Water – Rock Interact.*, Balkema, Rotterdam, 75–8.

Berry, J. A., Bishop, H. E., Cowper, M. M., Fozard, P. R., McMillan, J. W., and Mountfort, S. A. (1993) *Analyst,* **118**, 1241–6.

Berry, J. A., Bishop, H. E., Cowper, M. M., Fozard, P. R., McMillan, J. W., and Mountfort, S. A. (1994) *Radiochim. Acta,* **66/7**, 243–50.

Bertsch, P. M., Hunter, D. B., Sutton, S. R., Bajt, S., and Rivers, M. L. (1994) *Environ. Sci. Technol.,* **28**, 980–4.
Bhilare, N. G. and Shinde, V. M. (1994) *J. Radioanal. Nucl. Chem.,* **185**, 243–50.
Bitea, C., Müller, R., Neck, V., Walther, C., and Kim, J. I. (2003) *Coll. Surf. A,* **217**, 63–70.
Bojanowski, R., Holm, E., and Whitehead, N. E. (1987) *J. Radioanal. Nucl. Chem.,* **115**, 23–37.
Bouby, M., Ngo-Munh, Th., Geckeis, H., Scheibaum, F. J., and Kim, J. I. (2002) *Radiochim. Acta,* **90**, 727–32.
Brendler, V., Geipel, G., Bernhard, G., and Nitsche, H. (1996) *Radiochim. Acta,* **74**, 75–80.
Buck, E. C., and Fortner, J. A. (1997) *Ultramicroscopy,* **67**, 69–75.
Buckau, G., Stumpe, R., and Kim, J. I. (1986) *J. Less Common Metals,* **122**, 555–62.
Buesseler, K. O. (1989) *Development and Evaluation of Alternative Radioanalytical Methods, Including Mass Spectrocopy for Marine Material. Proc. Adv. Group Meet.,* Monaco, June 6–9 1989, TECDOC-683, IAEA, pp. 45–51.
Bundschuh, T., Knopp, R., Müller, R., Kim, J. I., Neck, V., and Fanghänel, Th. (2000) *Radiochim. Acta,* **88**, 625–9.
Bundt, M., Albrecht, A., Froidevaux, P., Blaser, P., and Flühler, H. (2000) *Environ. Sci. Technol.,* **34**, 3895–9.
Burmistenko, Yu. N. (1986) *Photonuclear analysis of substance composition*, Ehnergoatomizdat, pp. 153–7.
Burnett, W. C., Schultz, M., Inn, K. G. W., and Thomas, W. (1995) *Radioact. Radiochem.,* **6**, 46.
Butler, I. B. and Nesbitt, R. W. (1999) *Earth Planet. Sci. Lett.,* **167**, 335–45.
Byrne, A. R. (1986) *J. Environ. Radioact.,* **4**, 133–44.
Byrne, A. R. (1993) *Fresenius J. Anal. Chem.,* **345**, 144–51.
Byrne, A. R. and Benedik, L. (1999) *Czech. J. Phys.,* **49**, 263–70.
Carbol, P., Solatie, D., Erdmann, N., Betty, M., and Nylén, T. (2003) *J. Environ. Radioact.,* **68**, 27–46.
Carroll, S. A., Bruno, J., and Petit, J. C. (1992) *Radiochim. Acta,* **58/9**, 245–52.
Castillo, M. K., Santos, G. P., Ramos, A. F., and Teherani, D. K. (1996) *Nucleus,* **32**, 17–23.
Cavellec, R., Lucas, C., Simoni, E., Hubert, S., and Edelstein, N. (1998) *Radiochim. Acta,* **82**, 221–5.
Chassard-Bouchaud, C., and Galle, P. (1988) *Radiation Protection Practice,* Pergamon Press, Sydney, pp. 656–9.
Church, B. W., Shinn, J. H., Williams, G. A., Martin, L. J., O'Brien, R. S., and Adams, S. R. (2000) *Nuclear Physical Methods in Radioecological Investigations of Nuclear Test Sites.* (eds. S. S. Hecker, C. F. V. Mason, K. K. Kadyrzhanov and S. B. Kislitsin), Kluwer Academic Publishers, Dordrecht, pp. 203–19.
Civici, N. (1997) *J. Nat. Tech. Sci.,* **3**, 43–8.
Claassen, A., and Vissen, J. (1946) *Rec. Trav. Chim.,* **65**, 211–5.
Conaway, J. G., Bristow, Q., and Killeen, P. G. (1980) *Geophysics,* **45**, 292–311.
Conradson, S. (1998) *Appl. Spectrosc.,* **52**, 252A–79A.
Cooper, M. B., Burns, P. A., Tracy, B. L., Wilks, M. J., and Williams, G. A. (1994) *J. Radioanal. Nucl. Chem.,* **177**, 161–84.
Cooper, E. L., Haas, M. K., and Mattie, J. F. (1995) *Appl. Radiat. Isot.,* **46**, 1159–73.

Curran, G., Sevestre, Y., Rattray, W., Allen, P., and Czerwinski, K. R. (2003) *J. Nucl. Mater.,* **323**, 41–48.
Curtis, D. B., Cappis, J. H., Perrin, R. E., and Rokop, D. J. (1987) *Appl. Geochem.,* **2**,133.
Degueldre, C., Ulrich, H. J., and Silbi, H. (1994) *Radiochim. Acta,* **65**, 173–9.
Degueldre, C. and Taibi, K. (1996) *Anal. Chim. Acta,* **321**, 201–7.
Degueldre, C. and Paratte, J. M. (1999) *J. Nucl. Mater.,* **273**, 1–6.
Degueldre, C., Rochicoli, F., and Laube, A. (1999) *Anal. Chim. Acta,* **834**, 23–31.
Degueldre, C. and Favarger, P. Y. (2004) *Talanta,* **62**, 1051–54.
Degueldre, C., Reed, D., Kroft, A. J., and Mertz, C. (2004) *J. Synchrotron. Rad.,* **11**, 198–203.
Degueldre, C., Favarger, P.-Y., Rosser, R., and Wold, S. (2005) *Talenta*.
Della Mea, G., Dran, J.-C., Moulin, V., Petit, J.-C., Theyssier, M., and Ramsay, J. D. F. (1992) *Radiochim. Acta,* **58/9**, 219–23.
Denecke M., Dardenne, K., and Maquart, Ch. (2004) *Talanta*.
Dodge C. J., Francis, A. J., and Clayton, C. R. (1995) in *Emerging Technologies in Hazardous Waste Management*, ACS, CONF 9509139, 1352–77.
Dominik, J., Schuler, Ch., and Santschi, P. H. (1989) *Earth Planet. Sci. Lett.,* **93**, 345–57.
Dong, Z. (1990) *Uranium Geology Youkuang Dizhi China,* **6**, 291–6.
Dran, J. C., Della Mea, G., Paccagnella, A., Petit, J. C., and Menager, M.-Th. (1988) *Radiochim. Acta,* **44/5**, 299–304.
Drot, R., Simoni, E., Alnot, M., and Ehrhart, J. J. (1998) *J. Colloid Interface Sci.,* **205**, 410–6.
Dupleissis, J., Genet, M., and Guillaumont, R. (1974) *Radiochim. Acta,* **21**, 21–8.
Eikenberg, J., Zumsteg, I., Bajo, S., Vezzu, G., and Fern, M. (1999) *Radioact. Radiochem.,* **10**, 31–40.
El- Ansary, A. L., Issa, Y. M., Kandil, A. T., and Soliman, M. H. (1998) *Asian J. Chem.,* **10**, 86–98.
Eliet, V., Bidoglio, G., Omenetto, N., Parma, L., and Grenthe, I. (1995) *J. Chem. Soc. Faraday Trans.,* **91**, 2275–85.
Engkvist, I. and Albinsson, Y. (1992) *Radiochim. Acta,* **58/9**, 109–12.
Erdmann, N., Nunnemann, M., Eberhardt, K., Herrmann, G., Huber, G., Köhler, S., Kratz, J. V., Passler, G., Peterson, J. R., Trautmann, N., and Waldek, A. (1998) *J. Alloys Compds,* **271/3**, 837–40.
Fallon, S. J., McCulloch, M. T., van Woesik, R., and Sinclair, D. J. (1999) *Earth Planet. Sci. Let.,* **172**, 221–38.
Fernandez-Valverde, S., Bulbulian, S., and Segovia, N. (1988) *Nucl. Chem. Technol.,* **30**, 1–45.
Fifield, L. K., Clacher, A. P., Morris, K., King, S. J., Cresswell, R. G., Day, J. P., and Livens, F. R. (1997) *Nucl. Instrum. Methods B,* **123**, 400–4.
Fisher, R. D. (1973), in *NMR of Paramagnetic Molecules, Principes and Applications* (eds. G. D. La Mar, W. D. Horrocks, and R. H. Holm), Academics, New York, pp. 521–53.
Fortner, J. A., Buck, E. C., Ellison, A. J. G., and Bates, J. K. (1997) *Ultramicroscopy,* **67**, 77–81.
Francis, A. J., Dodge, C. J., Lu, F., Halada, G. P., and Clayton, C. R. (1994) *Environ. Sci. Technol.,* **28**, 636–9.

Francis, A. J., Gillow, J. B., Dodge, C. J., Dunn, M., Mantione, K., Strietelmeier, B. A., Pansoy-Hjelvic, M. E., and Papenguth, H. W. (1998) *Radiochim. Acta,* **82**, 347–54.
Füeg, B., Tschachtli, T., and Krähenbühl, U. (1997) *Radiochim. Acta,* **78**, 47–51.
Fujino, O., Umetani, S., Ueno, E., Shigeta, K., and Matsuda, T. (2000) *Anal. Chim. Acta,* **420**, 65–71.
Gäggeler, H., Baltensperger U., Haller P., Jost D., and Zinder, B. (1986) *Tagungsberichte Radioaktivitaetsmessungen in der Schweiz nach Tschernobyl und Ihre Wissenschafliche Interpretation*, BGW, Bern 20–22 Oct. 1986.
Garcia Alonso, J., Sena, F., Arbode, Ph., Betti, M., and Koch, L. (1995) *J. Anal. At. Spectrom.,* **10**, 381–93.
Garcia, K., Boust, D., Moulin, V., Douville, E., Fourest, B., and Guillaumont, R. (1996) *Radiochim. Acta,* **74**, 165–70.
Gatti, R. C., Carpenter, S. A., Roberts, K. E., Bescraft, K. A., Prussin, T. G., and Nitsche, H. (1994) *Proc. Fifth Conf. High Level Radioact. Waste Manage.*, 2719–29.
Gauthier, R., Ilmstädter.V., and Lieser, K. H. (1983) *Radiochim. Acta,* **33**, 35–39.
Geipel, G., Reich, T., Brendler, V., Bernard, G., and Nitsche, H. (1997) *J. Nucl. Mater.,* **248**, 408–11.
Geipel, G., Bernhard, G., Brendler, V., and Nitsche, H. (1998) *Radiochim. Acta,* **82**, 59–62.
Godbole, A. G. and Patil, S. K. (1979) *Talanta,* **26**, 330–2.
Goltz, D. M., Grégoire, D. C., Byrne, J. P., and Chakrabarti, C. L. (1995) *Spectrochim. Acta,* **50B**, 803–14.
Gonzales, E. R., Gladney, E. S., Boyd, H. A., McInroy, J. F., Muller, M., and Palmer, P. D. (1988) *Health Phys.,* **55**, 927–32.
Gouder, T. (1998) *J. Alloys Compds,* **271/3**, 841–45.
Grigoriev, M. S., Fedoseev, M., Gelis, A. V., Budantseva, N. A., Shilov, V. P., Perminov, V. P., Nikonov, M. V., and Krot, N. N. (2001) *Radiochim. Acta,* **89**, 95–100.
Groeschel, F., Bart, G., Montgomery, R., and Yagnik, S. K. (2003) *IAEA TECDOC* **1345**, 188–202.
Guillot, L. (2001) *J. Environ. Radioact.,* **53**, 381–98.
Gutmacher, R. G., Cremers, D. A., and Wachter, Z. (1987) *Trans. Am. Nucl. Soc.,* **55**, 19–20.
Hafez, M. B. and Hafez, N. (1992) *J. Radioanal. Nucl. Chem. Lett.,* **166**, 203–10.
Harduin, J. C., Peleau, B., and Piechowski, J. (1993) *Radioprot. Bull. Soc. Radioprot. Fr.,* **28**, 291–301.
Hartman, M. J. and Dresel, P. E. (1998) Report PNNL-11793.
Harvey, B. R., Lovett, M. B., and Boggis, S. J. (1987) *J. Radioanal. Nucl. Chem.,* **115**, 357–68.
Hecht, F. and Reich-Rohrwig, W. (1929) *Monatsh. Chem.,* **53/4**, 596.
Heier, K. S., and Rogers, J. J. W. (1963) *Geochim. Cosmochim. Acta,* **27**, 137–54.
Henge Napoli, M. H., Ansoborlo, E., Claraz, M., Berry, J. P., and Cheynet, M. C. (1996) *Cell. Mol. Biol.,* **42**, 413–20.
Hess, N. J., Felmy, A. R., Rai, D., and Conradson, S. D. (1997) *Mat. Res. Soc. Symp. Proc.,* **465**, 729–34.
Hirose, K. (1994) *J. Radioanal. Nucl. Chem.,* **181**, 11–24.
Hoffman, D. C., Lawrence, F. O., Merwerter, J. L., and Rourke, F. M. (1971) *Nature,* **234**, 132–34.

Holm, E. and Fukai, R. (1986) *J. Less Common Metals,* **122**, 487–97.
Holm, E., Rioseco, J., and Pettersson, H. (1992) *J. Radioanal. Nucl. Chem.,* **156**, 183–200.
Horn, I., Rudnick, R. L., and McDonough, W. F. (2000) *Chem. Geol.,* **164**, 281–301.
Huff, E. A. and Bowers, D. L. (1990) *Appl. Spectrosc.,* **44**, 728–29.
Hunter, D. B. and Bertsch, P. M. (1998) *J. Radioanal. Nucl. Chem.,* **234**, 237–42.
Hursthouse, A. S., Baxter, M. S., McKay, K., and Livens, F. R. (1992) *J. Radiochem. Nucl. Chem.,* **157**, 281–94.
Igarashi, Y., Shiraishi, K., Kim, Ch. K., Takaku, Y., Yamamoto, M., and Ikeda, N. (1990) *Anal. Sci.,* **6**, 157–64.
Itagaki, H., Tanaka, S., and Yamawaki, M. (1991) *Radiochim. Acta,* **52/3**, 91–4.
Ivanov, V. M., Morozko, S. A., and Massud, S. (1995) *J. Anal. Chem.,* **50**, 1171–8.
Ivanovich, M. (1994) *Radiochim. Acta,* **64**, 81–94.
Iwatschenko-Borho, M., Frenzel, E., and Kreiner, H. J. (1992) *Am. Chem. Soc.,* **49**, 507–14.
Jaiswal, D. D., Dang, H. S., Pullat, V. R., and Sharma, R. C. (1994) *Bull. Radiat. Prot.,* **17**, 44–7.
Jensen, M. P. and Choppin, G. R. (1998) *Radiochim. Acta,* **82**, 83–8.
Johansson, L. and Holm, E. (1996) *Nucl. Instrum. Methods A,* **376**, 242–7.
Johnson, S. G. and Feary, B. L. (1993) *Spectrochim. Acta,* **48B**, 1065–77.
Johnson S. G., Giglio J. J., Goodall P. S., and Cummings D. G. (1998) ANL report 95703, 11 p.
Jones, D. G. (2001) *J. Environ. Radioact.,* **53**, 313–33.
Kadyrzhanov, K. K. *et al*., (2000) in *Nuclear Physical Methods in Radioecological Investigations of Nuclear Test Sites* (eds. S. S. Hecker, C. F. V. Mason, K. K. Kadyrzhanov and S. B. Kislitsin), Kluwer Academics Publishers, Dordrecht, 17–42.
Karelin, A. I., Semenov, E. N., and Mikhailova, N. A. (1991) *J. Radioanal. Nucl. Chem.,* **147**, 33–40.
Kasar, U. M., Joshi, A. R., and Patil, S. K. (1991) *J. Radioanal. Nucl. Chem.,* **150**, 369–76.
Kazachevskiy, I. V., Solodukhin, V. P., Khajekber, S., Smirin, L. N., Chumikov, G. N., and Lukashenko, S. N. (1998) *J. Radioanal. Nucl. Chem.,* **235**, 145–9.
Kazachevskij, I. V., Lukashenko, S. N., Chumikov, G. N., Chakroya, E. T., Smirin, L. N., Solodukhin, V. P., Khaekber, S., Berdinova, N. M., Ryazanova, L. A. Bannyh, V. I., and Muratova, V. M. (1999) *Czech. J. Phys.,* **49**, 445–60.
Keil, R. (1978) *Fresenius Z. Anal. Chem.,* **292**, 13–9.
Keil, R. (1979) *Fresenius Z. Anal. Chem.,* **297**, 384–7.
Keil, R. (1981) *Fresenius Z. Anal. Chem.,* **305**, 374–8.
Kerbelov, L. M., and Rangelov, R. (1997) *Uranium Exploration Data and Techniques Applied to the Preparation of Radioelement Maps, IAEA TECDOC* **980**, 299–304.
Khater, A. E., Higgy, R. H., and Pimpl, M. (2001) *J. Environ. Radioact.,* **55**, 255–67.
Khokhrin, V. M. and Denisov, A. F. (1995) *Zadodskaya Laboratoriya,* **61**, 15–7.
Kim, Ch. K., Takaku, A., Yamamoto, M., Kawamura, H., Shiraishi, K., Igarashi, Y., Igarashi, S., Takayama, H., and Ikeda, N. (1989) *J. Radioanal. Nucl. Chem.,* **132**, 131–7.
Kim, Ch. K., Morita, S., Seki, R., Takaku, Y., Ikeda, N., and Assinder, D. J. (1992) *J. Radioanal. Nucl. Chem.,* **156**, 201–3.

Kim, J. I., Buckau, G., and Klenze, R. (1987) Natural Colloids and Generation of Actinide Pseudocolloids in Groundwater, in *Natural Analogues in Radioactive Waste Disposal* (eds. B. Come and N. Chapman), Graham and Trottman, London.
Kim, J. I., Rhee, D. S., Buckau, G., and Morgenstern, A. (1997) *Radiochim. Acta,* **79**, 173–81.
Kimura, T., Serrano, J., Nakayama, S., Takahashi, K., and Takeishi, H. (1992) *Radiochim. Acta,* **58/9**, 173–8.
Kimura, T., Kato, Y., and Yoshida, Z. (1998) *Radiochim. Acta,* **82**, 141–5.
Klenze, R. and Kim, J. I. (1988) *Radiochim. Acta,* **44/5**, 77–85.
Klenze, R., Kim, J. L., and Wimmer, H. (1991) *Radiochim. Acta,* **52/3**, 97–103.
Klett, A. (1999) *IEEE Trans. Nucl. Sci.,* **46**, 877–9.
Kobashi, A., Choppin, G. R., and Morse, J. W. (1988) *Radiochim. Acta* **43**, 211–5.
Kosyakov, V. N., Yakovlev, N. G., Vlasov, M. M., and Piskarev, P. E. (1994) *Radiokhimiya,* **36**, 175–8.
Kuczewski, B., Marquardt, Ch., Seibert, A., Geckeis, H., Kratz, J. V., and Trautmann, N. (2003) *Anal. Chem.,* **75**, 6769–6774.
Kudo, A. (1998) *Radiochim. Acta,* **82**, 159–66.
Kuperman, A., Ya., Smirnov, Yu. A., Fedotov, S. N., Nikol'skaya, T. L., and Efimova, N. S. (1989) *Sov. Radiochem.,* **30**, 750–5.
Kuvik, V., Lecouteux, N., Doubek, N., Ronesch, K., Jammet, G., Bagliano, G., and Deron, S. (1992) *Anal. Chim. Acta,* **256**, 163–76.
La Breque, J. J. (1994) *J. Radioanal. Nucl. Chem.,* **178**, 327–36.
Legin, A. V., Seleznev, B. L., Rudnitskaya, A. M., Vlasov, Yu. G., Tverdokhlebov, S. V., Mack, B., Abraham, A., Arnold, T., Baraniak, L., and Nitsche, H. (1999) *Czech. J. Phys.,* **49**, 679–85.
Lierse, G., Pomar, C., and Rugel, G. (2000) *Nucl. Instrum. Methods B* **172**, 333–37.
Li, B., Wang, M., Lu, B., and Wu, J. (1991) *At. Energy. Sci. Technol.,* **25**, 66–70.
Li, R. and Li, Yu. (1997) *Uranium Geology Youkuang Dizhi,* **13**, 359–63.
Liu, Ch. Yu., Ngian, F. H. M., Kuo, Sh. Y., Northrup, D. R., and Huffman, A. C. (1985) *Soc. Exploration Geophys.,* **1**, 163–5.
Lin, J. C., Broecker, W. S., Anderson, R. F., Hemming, S., Rubenstone, J. L., and Bonani, G. (1996) *Geochim. Cosmochim. Acta,* **60**, 2817–32.
Linauskas, S. H., Szostak, F., and Trivedi, A. (1996) *Health Phys.,* **70**, 85–6.
Livens, F. (2001) *J. Environ. Radioact.,* **55**, 1–3.
Livingston, H. D. and Cochran, J. K. (1987) *J. Radioanal. Nucl. Chem.,* **115**, 299–308.
Lujaniene, G., Lujanas, V., Jankunaite, D., Ogorodnikov, B., Mastauskas, A., and Ladygiene, R. (1999) *Czech. J. Phys.,* **49**, 107–14.
Lumpkin, G. R. (1999) *J. Nucl. Mater.* **274**, 206–17.
Lyons, P. C., Hercules, D. M., Morelli, J. J., Sellers, G. A., Mattern, D., Thomson Rizer, C. L., Brown, F. W., and Millay, M. A. (1987) *Intern. J. Coal Geol.* **7**, 185–94.
Marx, G., Esser, V., Bischoff, H., and Xi, R. H. (1992) *Radiochim. Acta,* **58–9**, 199–204.
Mátel, L., Mikulaj, V., and Rajec, P. (1993) *J. Radioanal. Nucl. Chem.,* **175**, 41–6.
Matthews, R., Koch, R., and Leppin, M. (1997) in *Proc. Exploration* 97 (ed. A. Gubins), pp. 993–1024.
Matzke, H. and Turos, A. (1991) *Solid State Ionics,* **49**, 189–94.
Matzke, H., Della-Mea, G., Freire, F. L., Jr., and Rigato, V. (1990) *Nucl. Instrum. Method B,* **45**, 194–8.

Matzke, H. (1996) *J. Nucl. Mater.,* **238**, 58–63.
May, S., Engelmann, Ch., and Pinte, G. (1987) *J. Radioanal. Nucl. Chem.,* **113**, 343–50.
Maya, L. and Begun, G. M. (1981) *J. Inorg. Nucl. Chem.,* **43**, 2827–32.
Michel, H., Gasparro, J., Barci-Funel, G., Dalmasso, J., Ardisson, G., and Sharovarov, G. (1999) *Talanta,* **48**, 821–5.
Mietelski, J. W., LaRosa, J., and Ghods, A. (1993) *J. Radioanal. Nucl. Chem.,* **170**, 243–58.
Miller, K. M. (1994) *Trans. Am. Nucl. Soc.,* **70**, 47–8.
Miller, K. M., Shebell, P., and Klemic, G. A. (1994) *Health. Phys.,* **67**, 140–50.
Misaelides, P., Godelitsas, A., Charistos, D., Filippidis, A., and Anousis, I. (1995) *Sci. Total Environ.,* **173**, 237–46.
Mitchell, P. I., Vinto, L. L., Dahlgaard, H., Gasco, C., and Sanchez Cabeza, J. A. (1995a) *Environmental Radioactivity in the Artic* (eds. P. Strand and A. Cooke), pp. 339–45.
Mitchell, P. I., Batlle, J. V., Downes, A. B., Condren, O. M., León Vintró, L. L., and Sánchez Cabeza, J. A. (1995b) *Appl. Radiat. Isot.,* **46**, 1175–90.
Mohan, M. S., Ilger, J. D., and Zingaro, R. A. (1991) *Energy and fuels U.S.,* **5**, 568–573.
Moody, G. J., Slater, J. M., and Thomas, J. D. R. (1988) *Analyst,* **113**, 699–703.
Moreland, P. E., Rokop, D. J., and Stevens, C. M. (1970) *Int. J. Mass Spectrom. Ion Phys.,* **5**, 127–36.
Morello, M., Colle, C., and Bernard, J. (1986) *J. Less Common Metals,* **122**, 569–76.
Möri, A., Alexander, W. R., Geckeis, H., Hauser, W., Schäfer, T., Eikenberger, J., Fierz, Th., Degueldre, C., and Missana, T. (2003) *Coll. Surf. A,* **217**, 33–47.
Morris, D. E., Chilsholm-Brause, C. J., Barr, M. E., Conradson, S. G., and Eller, P. G. (1994) *Geochim. Cosmochim. Acta,* **58**, 3613–23.
Moss, J. H. (1960) AERE report 3214.
Moulin, C., Decambox, P., Mauchien, P., Moulin, V., and Theyssier, M. (1991) *Radiochim. Acta,* **52/3**, 119–25.
Moulin, C., Decambox, P., Moulin, V., and Decaillon, J. G. (1995) *Anal. Chem.,* **67**, 348–53.
Moulin, C., Charron, N., Plancque, G., and Virelizier, H. (2000) *Appl. Spectrosc.,* **54**, 843–8.
Moulin, C., Amekraz, B., Hubert, S., and Moulin, V. (2001) *Anal. Chim. Acta,* **21**, 1–11.
Mount, M. E., Sheaffer, M. K., and Abbott, D. T. (1995) *J. Environ. Radioact.,* **25**, 11–9.
Murray, A. S., Marten, R., Johnston, A., and Martin, P. (1987) *J. Radioanal. Nucl. Chem.,* **115**, 263–88.
Mwenifumbo, C. J. and Kjarsgaard, B. A. (1999) *Exploration Mining Geol.,* **8**, 137–147.
Myers, W. A., and Lindner, M. (1971) *J. Inorg. Nucl. Chem.,* **33**, 3233–8.
Nagao, S., Matsunaga, T., and Muraoka, S. (1999) *J. Radioanal. Nucl. Chem.,* **239**, 555–59.
Nagasaki, S., Tanaka, S., and Takahashi, Y. (1988) *J. Radioanal. Nucl. Chem.,* **124**, 383–95.
NAGRA (1991) *Sondierbohrung Leuggern*, Technischer Bericht 88–10, Beilage Band 5.16, Wettingen, Switzerland.
Nair, G. M. and Kumar, P. C. (1986) *J. Radioanal. Nucl. Chem.,* **107**, 297–22.
Nakada, M., Saeki, M., Masaki, N. M., and Tsutsui, S. (1998) *J. Radioanal. Nucl. Chem.,* **232**, 201–7.

Nakashima, S. (1992) *Sci. Total Environ.,* **117/8**, 425–37.
Neck, V., Runde, W., Kim, J. I., and Kanellakopulos, B., (1994) *Radiochim. Acta,* **65**, 29–37.
Negi, R. S. and Malhotra, R. K. (1980) *Proc. Symp. Chem. Anal. Geol. Mater.*, **1**, 33–5.
Nelson, D. M. and Metta, D. N. (1983) *Radiol. Environ. Res. Div. Ann. Rep.* 42–7.
Nelson, D. M. and Lovett, M. B. (1978) *Nature,* **276**, 599–601.
Neu, M., Hoffman, D., Roberts, K. E., Nitsche, H., and Silva, R. J. (1994) *Radiochim. Acta,* **66/7**, 251–8.
Niese, S. (1994) *Zhurn. Analit. Khim.,* **49**, 132–4.
Nitsche, H. (1995) *J. Alloys Compds,* **223**, 274–9.
Noller, B. N. and Hart, B. T. (1993) *Environm. Technol.,* **14**, 649–56.
Ochsenkuehn Petropulu, M. and Parissakis, G. (1993) *J. Anal. Chem.,* **345**, 43–7.
Ohnuki, T., Isobe, H., and Hidaka, H. (1996) *Hoshasei Haikibutsu Kenkyu,* **2**, 145–51.
Okajima, S., Reed, D. T., Beitz, J. V., Sabau, C. A., and Bowers, D. L. (1991) *Radiochim. Acta,* **52/3**, 111–7.
Orlandi, K. A., Penrose, W. R., Harvey, B. R., Lovett, M. B., and Findlay, M. W. (1990) *Environ. Sci. Technol.,* **24**, 706–12.
Oughton, D. H., Fifield, L. K., Day, J. P., Cresswell, R. G., Skipperud, L., Di Tada, M. L., Salbu, B., Strand, P., Drozcho, E., and Morrov, Y. (2000) *Environ. Sci. Technol.,* **34**, 1938–45.
Papadopulos, N. N. and Tsagas, N. F. (1994) *J. Radioanal. Nucl. Chem.,* **179**, 35–43.
Paschoa, A. S., Cholewa, M., Jones, K. W., Singh, N. P., and Wrenn, M. E. (1987) *J. Radioanal. Nucl. Chem.,* **115**, 231–40.
Pedersen, K. (ed.) (1996) *Bacteria, Colloids and Organic Carbon in Groundwater at the Bagombé Site in the Oklo Area*. SKB Technical report 96–01, Stockholm, Sweden.
Penrose, W., Polzer, W., Essington, E., Nelson, D., and Orlandi, K. (1990) *Environ. Sci. Technol.,* **24**, 228–34.
Peppard, D. F., Studier, M. H., Gergel, M. V., Mason, G. W., Sullivan, J. C., and Mech, J. F. (1951) *J. Am. Chem. Soc.,* **73**, 2529–31.
Perkins, W. T., Pearce, N. J. G., and Jefferies, T. E. (1993) *Geochim.Cosmochim. Acta,* **57**, 475–82.
Phelps, W. T., Jr. and Davis, T. L. (1981) *Soc. Exploration Geophys.,* **1**, 89.
Pollard, P. M., Liezers, M., McMillan, J. W., Phillips, G., Thomason, H. P., and Ewart, F. T. (1988) *Radiochim. Acta,* **44/5**, 95–101.
Poty, B. and Roux, J. (1998) *Uranium Ores*, EDF Publisher, Paris, p. 610.
Price, G. R., Ferretti, R. J., and Schwartz, S. (1953) *Anal. Chem.* **25**, 322–31.
Probst, T., Zeh, P., and Kim, J. I. (1995) *Fresenius. J. Anal. Chem.,* **351**, 745–51.
Purser, K. H., Litherland, A. E., and Zhao, X. (1996) *Nucl. Instrum. Methods B,* **113**, 445–52.
Qu, H., Stuit, D., Glover, S. E., Love, S. F., and Filby, R. H. (1998) *J. Radioanal. Nucl. Chem.,* **234**, 175–81.
Quigley, M. S., Santschi, P. H., and Hung, C. C. (2002) *Limnol. Oceanogr.,* **47**, 367–77.
Rastogi, R. C. and Sjoeblom, K. L. (1999) *Inventory of Radioactive Waste Disposal at SeaI,* IAEA-TECDOC–1105.
Rink, W. J., and Odom, A. L. (1991) *Nucl. Track Rad. Meas. Inter., J. Rad. Appl. Inst.,* **18**, 163–73.

Robertson, D. E. (1985) *Speciation of Fission and Activation Products in the Environment*, Elsevier Science, New York, pp. 47–57.
Röllin, S., Kopajtic, Z., Wernli, B., and Magyar, B. (1996) *J. Chromatogr. A,* **739**, 139–49.
Römer, J., Plaschke, M., Beuchle, G., and Kim, J. I. (2003) *J. Nucl. Mater.,* **322**, 80–6.
Rozenberg, G. and Hoektra, P. (1982) *Soc. Exploration Geophys.,* **1**, 376–8.
Rubio Montero, M. P. and Martin Sánchez, A. (2001a) *J. Environ. Radioact.,* **55**, 157–65.
Rubio Montero, M. P. and Martin Sánchez, A. (2001b) *Appl. Radiat. Isot.,* **55**, 99–102.
Runde, W., Neu, M. P., Conradson, S. D., Clark, D. L., Palmer, P. D., Reilly, S. D., Scott, B. L., and Tait, C. D. (1997) *Mat. Res. Soc. Symp. Proc.,* **465**, 693–703.
Rykov, A. G., Piskunov, E. M., and Timofeev, G. A. (1975) *J. Anal. Chem. USSR,* **30**, 598–601
Salbu, B. (2000) in *Speciation of radionuclides in the environment. Encyclopedia of analytical chemistry,* (ed. R. A. Meyers, John Wiley, Chichester, pp. 12993–3016.
Salbu, B. (2001) *J. Environ. Radioact.,* **53**, 267–8.
Sampson, K. E., Scott, R. D., Baxter, M. S., and Hutton, R. C. (1991) in *Proc. Radionuclide in the Study of Marine process*, Elsevier, London, pp. 177–86.
Sawant, L. R., Kalsi, P. K., Kulkarni, A. V., and Vaidyanathan, S. (1996) *J. Radioanal. Nucl. Chem.,* **207**, 39–43.
Schimmack, W., Auerswald, K., and Bunzl, K. (2001) *J. Environ. Radioact.,* **53**, 41–57.
Schoonover, J. R. and Havrilla, G. L. (1999) *Appl. Spectrosc.,* **53**, 257–65.
Sheng, Z., Zhao, Y., and Gu, D. (1985) *Ti Ch'iu Hua Hsueh,* **2**, 188–95.
Skwarzec, B., Struminska, D., and Borylo, A. (2001) *J. Environ. Radioact.,* **55**, 167–78.
Smyth, J. R., Thomson, J., and Wolfberg, K. (1980) *Radioact. Waste Manage.,* **1**, 13–24.
Solatie, D., Carbol, P., Betti, M., Bocci, F., Hiernaut, T., Rondinella, V., and Cobos, J. (2000) *Fresenius J. Anal. Chem.,* **368**, 88–94.
Soto-Guerrero, J., Gajdosova, D., and Havel, J. (2001) *J. Radioanal. Nucl. Chem.,* **249**, 139–43.
Sreenivasan, N. L. and Srinivasan, T. G. (1995) *J. Radioanal. Nucl. Chem.,* **201**, 391–9.
Stepanov, A. V., Aleksandruk, V. M., Babaev, A. S., Demyanova, T. A., Nikitina, S.-A., and Preobrazhenskaya, E. B. (1990) *Radioisot. Czech.,* **31**, 267.
Strelow, F. W. (1961) *Anal. Chem.,* **33**, 1648–50.
Swift, D. J. and Nicholson, M. D. (2001) *J. Environ. Radioact.,* **54**, 311–26.
Szabó, G., Guczi, J., and Nisbet, A. (1997) *J. Radioanal. Nucl. Chem.,* **226**, 255–9.
Taylor, D. M. and Farrow, L. C. (1987) *Nucl. Med. Biol. Inter. J. Rad. Appl. Instrum.,* **14**, 27–31.
Testa, C., Desideri, D., Guerra, F., Meli, M. A., Roselli, C., and Degetto, S. (1999) *Czech. J. Phys.,* **49**, 649–56.
Teterin, Yu. A., Ivanov, K. E., Teterin, A. Yu., Lebedev, A. M., and Vukcevic, L. (1997) *Yugoslav Nucl. Soc.*, CONF 961055, pp. 449–52.
Timerbaev, A. (2001) *Anal. Chim. Acta,* **433**, 165–80.
Trautmann, N., Peuser, P., Rimke, H., Sattelberger, P., Herrmann, G., Ames, F., Krönert, U., Ruster, W., Bonn, J., Kluge, H.-J., and Otten, E.-W. (1986) *J. Less-Common Metals,* **122**, 533–8.
Trautmann, N. (1992) in *Proc. of Transuranium Elements. A Half Century*, Washington, DC, pp. 159–67.

Triay, I. R., Hobart, D. E., Mitchell, A. J., Newton, T. W., Ott, M. A., Palmer, P. D., Rundberg, R. S., and Thompson, J. L. (1991) *Radiochim. Acta,* **52/3**, 127–31.
Usuda, S., Sakurai, S., and Yasuda, K. (1997) *Nucl. Instrum. Methods A,* **388**, 193–8.
Usuda, S., Yasuda, K., and Sakurai, S. (1998) *Appl. Radiat. Isot.,* **49**, 1131–7.
Van Britsom, G., Slowikowski, B., and Bickel, M. (1995) *Sci. Total Environ.,* **173**, 83–9.
Veselsky, J. C. and Ratsimandresey, Y. (1979) *Anal. Chim. Acta,* **104**, 345.
Veselsky, J. C. and Degueldre, C. (1986) *Analyst,* **111**, 535–8.
Virk, H. S. (1997) *Bull. Radiat. Prot.,* **20**, 139–42.
Virk, H. S., Sharma, A. K., and Naresh, K. (1998) *J. Geol. Soc. India,* **52**, 523–8.
Vogler, S., Scholten, J., Rutger, van-der-Loeff, M., and Mangini, A. (1998) *Earth Planet. Sci. Lett.,* **156**, 61–74.
Wahlberg, J., Skinner, D. L., and Rader, L. F., Jr. (1957) *Anal. Chem.,* **29**, 954–7.
Wallenius, M., Tamborini, G., and Koch, L. (2001) *Radiochim. Acta,* **89**, 55–8.
Wallner, C., Faestermann, T., Gerstmann, U., Hillebrandt, W., Knie, K., Korshinek, G., Lierse, C., Pomar, C., and Rugel, G. (2000) *Nucl. Instrum. Methods B,* **172**, 333–37.
Walther, C. (2003) *Coll. Surf. A,* **217**, 81–92.
Waqar, F., Jan, S., Mohammad, B., and Ahmed, M. (1995) in *Spectroscopy for Material Analysis*, PINSTECH, Islamabad, pp. 189–93.
Ward, W. C., Martinez, H. E., Abeyta, C. L., Morgan, A. N., and Nelson, T. O. (1998) *J. Radioanal. Nucl. Chem.,* **235**, 5–10.
Wasserburg, G. T., McDonald, G. J. F., Hoyle, F., and Fowler, W. A. (1964) *Science,* **143**, 465–7.
Wimmer, H., Kim, J. I., and Klenze, R. (1992) *Radiochim. Acta,* **58–9**, 165–71.
Winkelmann, I., Thomas, M., and Vogl, K. (2001) *J. Environ. Radioact.,* **53**, 301–11.
Wolf, S. F., Bates, J. K., Buck, E. C., Dietz, N. L., Fortner, J. A., and Brown, N. R. (1997) *Environ. Sci. Technol.,* **31**, 467–71.
Wong, K. (1971) *Anal. Chim. Acta,* **56**, 355
Xu, H. and Wang, Y. (1999) *J. Nucl. Mater.,* **265**, 117–123.
Yu-fu, Y., Salbu, B.Bjørnstad, H. E., and Lien, H. (1990) *J. Radioanal. Nucl. Chem.,* **145**, 345–53.
Yu-fu, Y., Bjørnstad, H. E., and Salbu, B. (1992) *Analyst,* **117**, 439–42.
Yukawa, M., Watanabe, Y., Nishimura, Y., Guo, L., Yongru, Z., Lu, H., Zhang, W., Wei, L., and Tao, Z. (1999) *Fresenius J. Anal. Chem.,* **363**, 760–6.
Zamzow, D., Baldwin, D., Weeks, S., Bajic, S., and D'Silva, A. (1994) *Environ. Sci. Technol.,* **28**, 352–8.
Zarki, R., Elyahyaoui, A., and Chiadli, A. (2001) *Appl. Radiat. Isot.,* **55**, 164–74.
Zhao, X., Nadeau, M. J., Garwan, M. A., Kilius, L. R., and Litherland, A. E. (1994) *Nucl. Instrum. Methods B,* **92**, 258–64.
Zhao, X. L., Nadeau, M. J., Kilius, L. R., and Litherland, A. E. (1994) *Earth Planet. Sci. Lett.,* **124**, 241–4.
Zhao, X., Kilius, L. R., Litherland, A. E., and Beasley, T. (1997) *Nucl. Instrum. Methods B,* **126**, 297–300.